ARL 65-185

THE MAGNETIC STABILIZATION OF AN ELECTRIC ARC IN TRANSVERSE SUPERSONIC FLOW

CHARLES E. BOND

THE UNIVERSITY OF MICHIGAN
ANN ARBOR, MICHIGAN

OCTOBER 1965

Contract No. 33(657)-8819
Project No. 7063
Task No. 7063-03

AEROSPACE RESEARCH LABORATORIES
OFFICE OF AEROSPACE RESEARCH
UNITED STATES AIR FORCE
WRIGHT-PATTERSON AIR FORCE BASE, OHIO

FOREWORD

This report is essentially identical with the dissertation submitted in May, 1964, by the author to the University of Michigan in partial fulfillment of the requirements for the degree of Doctor of Philosophy in Aeronautical and Astronautical Engineering. Portions of this dissertation have been published elsewhere. A note by the author -- "Magnetic Confinement of an Electric Arc in Transverse Supersonic Flow," AIAA Journal, Vol. 3, No. 1, p. 142, January, 1965 -- summarizes observations related to the confinement mechanism. A paper co-authored with A. M. Kuethe -- "Some Observations of an Electric Arc Magnetically Confined in a Transverse Supersonic Flow", Proceedings of the AGARD Specialists' Meeting on "Arc Heaters and MHD Accelerators for Aerodynamic Purposes", Rhode-Saint-Genese, Belgium, AGARDograph 84, part 2, September, 1964\--includes further observations and quantitative data on the confined arc. The present report contains a general review of convective arc phenomena, a more extensive presentation and analysis of results, and a discussion of the experimental approach and techniques involved in arc establishment and stabilization.

The investigation reported herein was sponsored by the Aerospace Research Laboratories, Office of Aerospace Research, United States Air Force, Contract No. AF 33(657)-8819, under the technical cognizance of Charles A. Davies and Ward C. Roman.

The author wishes to express his deep appreciation to the chairman of his doctoral committee, Professor A. M. Kuethe, for guidance and encouragement, and for many helpful and well-timed suggestions.

He is also indebted to the members of the doctoral committee and others, who contributed many useful suggestions during the course of the investigation: J. L. Amick, Director of the Aerodynamics Laboratory; H. C. Early, Director of the Plasma Engineering Laboratory; Professors A. F. Messiter and J. A. Nicholls of the Department of Aeronautical and Astronautical Engineering; P. H. Rose of the AVCO-Everett Research Laboratory; and Professor R. A. Wolfe of the Physics Department.

He wishes to thank Mr. Eric Soehngen of the Aerospace Research Laboratories, Wright Field, Ohio, for his support and encouragement, and Mr. Ward C. Roman for his helpful suggestions.

The excellent laboratory assistance of the following students is gratefully acknowledged: Claus Beneker, Kurt Richter, John Ducmanis, and especially James Bennett.

Finally, the author wishes to acknowledge the untiring editorial assistance of his wife, Fran.

ABSTRACT

A method is presented for the magnetic confinement and stabilization of a d-c electric arc in an unheated supersonic airstream directed normal to the electric field. It is shown that stable confinement is governed by dynamic processes in the positive column, and is independent of material and flow conditions at the surface of the cathode.

The positive column exhibited remarkable spatial stability when allowed to slant across the electric field, parallel to a freestream Mach line. Under conditions where the column could not follow the Mach angle, a very unstable discharge was observed.

The direction of column slanting was the Hall direction, cathode-root downstream; but the magnitude of the slant angle was not affected by changes in the Hall parameter, $\omega_e \tau_e$, corresponding to changes in ambient pressure, arc current, and local magnetic induction by factors of 2.

At the Mach numbers investigated, 2.0 and 2.5, the stable column invariably followed the Mach angle -- which happens to be very nearly the angle corresponding to a maximum in the discharge parameter E_{11}/P_s, the ratio of parallel component of electric field to pressure at the upstream boundary of the arc.

The experimental results demonstrate the possibility of stable conduction of electricity through transverse supersonic flow, and suggest that such conduction is governed by a convective interaction mechanism which is not entirely Hall-effect.

A general review of the convective arc is given, and results of the present investigation are compared with those of previous investigations.

TABLE OF CONTENTS

TABLE OF CONTENTS CONT'D

LIST OF ILLUSTRATIONS

LIST OF ILLUSTRATIONS CONT'D.

LIST OF ILLUSTRATIONS CONT'D.

LIST OF ILLUSTRATIONS CONT'D.

LIST OF SYMBOLS

A'	=	tunnel area at point where uniform heat addition is assumed to occur
A/A^*	=	tunnel area ratio, referred to sonic throat area
$\underline{B}$	=	magnetic induction
B_{av}	=	average between values of transverse induction at anode and cathode roots
B_c	=	transverse magnetic induction at cathode root
B_x	=	streamwise component of magnetic induction
B_y	=	transverse component of magnetic induction
C_p	=	specific heat at constant pressure
d_e	=	effective arc width
d_L	=	arc luminosity width
$\underline{E}$	=	electric intensity
E_o	=	open circuit voltage
E_{ll}	=	component parallel to arc axis, of external electric field
E'_{ll}	=	E_{ll}/E
e	=	electron charge
g	=	inter-electrode gap
h	=	gas enthalpy
I	=	current
I_c	=	current through field coils
$\underline{j}$	=	current density
K	=	thermal conductivity
k	=	Boltzmann constant
L	=	circuit inductance
M	=	Mach number
m	=	particle mass
m_a	=	mass of gas molecule

m_e	=	mass of electron
$\dot{m}$	=	mass flow rate
n	=	particle number density
n_e	=	electron density
n_i	=	ion density
P	=	gas pressure
P_s	=	pressure at leading edge of solid cylinder
P'_s	=	P_s/P_{t_1}
P_{t_1}	=	free-stream stagnation pressure
P_1^*	=	static pressure at sonic velocity
P	=	free-stream static pressure
Q	=	heat added to flow
q	=	electric charge of particle
R_B	=	ballast resistance
Re	=	Reynolds number
S	=	radiation energy
s	=	heat-flow function
T	=	temperature
t	=	time
T_a	=	gas temperature
T_e	=	electron temperature
T_{o1}	=	initial stagnation temperature
T_{o2}	=	final stagnation temperature
T_o^{*H}	=	stagnation temperature where M = 1 due to heat addition
V	=	voltage
V_a	=	arc voltage

$\underline{v}_\infty$	=	free-stream velocity
$\underline{v}$	=	gas velocity
$\underline{v}_d$	=	electron drift velocity
W	=	arc power
x	=	distance along tunnel exis, positive upstream
y	=	distance normal to vertical plane through tunnel axis, positive East
z	=	distance normal to horizontal plane, positive down
δ	=	elastic-collision energy-loss parameter
η	=	perturbation in current
θ_E	=	slant angle for maximum $\frac{E_{11}}{P_s}$
θ_s	=	arc slant angle; angle between arc axis and impressed electric field
λ	=	electron mean free path
μ	=	Mach angle
ρ	=	gas density
ρ_o	=	gas density at standard conditions
σ	=	electrical conductivity
σ_{11}	=	electrical conductivity parallel to current
τ_e	=	electron mean free time
ω_e	=	electron cyclotron frequency

CHAPTER I

INTRODUCTION

During the past decade there has been a crescendo in the intensity and diversity of electric arc research. Much of this increased activity is directed toward a scientific understanding of arc behavior under conditions dictated by new applications of the electric arc in the aerospace sciences. The application to deep space propulsion, where the arc-jet engine can best perform some missions requiring thrust devices with specific impulse on the order of 1500 to 15,000 sec., is one example.[1] The simulation of the high enthalpy gas flows experienced on ballistic-missile and satellite-re-entry trajectories is another important area where the electric arc finds new application.[2]

In most new applications of the electric arc to space propulsion, plasma generation, and re-entry simulation, the arc is used as a mechanism for the volume-addition of energy to a gas. Efficient energy addition generally requires some form of forced convection. Very little is known about arc behavior under the new conditions and particularly under the influence of forced convection. It has been noted,[3] for example, that no theory and no experimental data exist predicting even the voltage required to sustain an arc of 100 amps or more under given conditions of transverse forced convection. There has been, in fact, no assurance that an arc can be sustained at all under arbitrary conditions of forced convection.

In many devices the convective arc is sustained and controlled with the help of external magnetic fields which move the arc column in a direction normal to its axis. At present, it is not possible to calculate the velocity of motion of a given arc due to a given magnetic field; generally, it is not even possible to estimate the order-of-magnitude of the velocity.

Physically, a magnetically-controlled electric arc can be described as an interaction among a thermal-energy field, an electric field, a velocity field, a pressure field, and a magnetic field. The laws governing the interaction are well-known, but the equations expressing these laws have not been solved.[4]

Most studies of the convective arc have had as their objective the formulation of a physical model which expresses those mechanisms most essential to arc behavior under the existing conditions, leading hopefully to a simpler mathematical model. The means for determining the essential mechanisms has been through experimental observation of arc behavior under differing conditions.

One way to observe the effects of transverse convection is to move the arc through still air in a direction normal to the axis of the arc by means of a magnetic field. Most of the meaningful observations of convective-arc behavior have been made in this way, using the rail accelerator. As the name suggests, a balance between aerodynamic and magnetic forces is here achieved through the mechanism of acceleration of the arc to an equilibrium velocity.

With this experimental set-up, the conducting column and the points of contact, or roots of the arc, must move with respect to the rails. In view of the relative motion, it is not surprising that experiments have shown that the velocity at which the arc moves along the rails varies with root conditions[5-20] (such as cathode material)

by factors of up to four, and with conditions which affect the "flexibility" of the column (such as rail spacing and circuit inductance[12,13,21]) by factors up to five.

A surprising result of the rail-accelerator experiments has been the observation that the arc column does not necessarily remain in the electrode plane, but fluctuates from side to side, forming loops and spirals.[14,21-23] Because of these erratic fluctuations in column length and shape, it has generally not been possible with the rail accelerator to measure such important characteristics as column voltage-gradient, electrode fall voltages, and electrical conductivity of the column.

Another way to observe the effects of convection on the column is to constrain or confine the arc within a transverse stream of moving air by use of magnetic fields. To accomplish this constraint, it is necessary to provide precisely the magnetic field which will result in stable equilibrium for the given flow conditions. Because of the difficulties of achieving a stable equilibrium, very few observations of the convective arc have been made in this way - though a significant step in this direction was made by Smith and Early[24] at the University of Michigan in 1954.

This dissertation presents a method for the magnetic stabilization of a high current d-c electric arc in a transverse supersonic air flow. It is shown that the arc can be successfully held in the flow by this method in such a way that spatial and temporal fluctuations in the positive column are not in evidence. The time available for observations is of the order of seconds, compared to the milliseconds typical of the rail-accelerator setup. Significant observations of arc behavior under this mode of confinement include the observation that the stable supersonic arc is characterized by a positive column which is slanted with respect to the electric field and that forced departures from the slanted configuration result in column instability.

The experimental setup consists of two rail electrodes mounted in a supersonic wind tunnel and oriented parallel to the tunnel free-stream. External coils provide a transverse magnetic field which is mutually perpendicular with the electric field and free-stream. The coils are placed such that there is a monotonic increase in magnetic flux density from the upstream to the downstream end of the rails. The arc is initiated by means of an exploding wire between the upstream ends of the rails. The plasma column generated then moves under the action of aerodynamic and electromagnetic forces until a location and orientation are reached where these forces come into balance. The stable arc column remains locked in at this location until the current is shut off.

Stabilization is achieved primarily through dynamic processes in the positive column; and for a given current and magnetic field, arc location is determined by the location of the external field coils and by free-stream conditions - independent of whether the electrode material is copper, carbon, or brass and of disturbances to the flow near the cathode surface upstream of the cathode root. Stability in the streamwise direction results from the increase in Lorentz force with downstream displacement.

The stable positive column assumes a slanted orientation with respect to the electric field. At a Mach number, M, of 2.5, only one angle of slant is observed, independent of arc current from 150 to 700 amperes, of free-stream stagnation pressure, P_{t_1}, from 10 to 25 in. Hg, and of inter-electrode gap from 0.6 to 1.1 inches.

The angle of slant is that of a free-stream Mach line, which is roughly the angle for maximum ratio of the parallel component of the electric field to the pressure at the upstream boundary of the arc. The direction of slant is the Hall direction for free-electron conduction (cathode root downstream), but the angle of slant does not appear to vary with the Hall parameter $\omega_e \tau_e$, the product of the electron cyclotron frequency and the electron mean free time. Spatial fluctuations of the column occur when the relative location of the electrodes and field coils is such that the column must depart from the correct angle of slant. However, when conditions allow the arc to assume the stable slanted configuration at locations along the rails sufficiently remote from the rail ends, the column exhibits extreme spatial stability.

The high spatial stability of the column when confined by the method presented allows meaningful measurement of the voltage gradient for the convective arc. At $M = 2.5$ and $P_{t_1} = 20$ inches Hg, the gradient is found to be about 14 volts/cm for currents between 300 and 700 amperes.

The average magnetic induction required to balance the aerodynamic forces on the stable column is independent of current between 150 and 700 amperes, and increases from about 2000 gauss at a P_{t_1} of 10 in. Hg to about 3500 gauss at 25 in. Hg.

The next four chapters of this dissertation comprise a general review of convective arc phenomena. The remaining chapters contain a fairly comprehensive discussion of the present investigation. The reader interested primarily in the experimental results of the present investigation should refer directly to chapters VIII, IX, and X.

CHAPTER II

DEFINITION OF THE ARC

The electric arc can be defined[25,26] as a gaseous discharge capable of passing large electric currents (over about 1 amp) at relatively low voltage. The electric discharges discussed herein fall well within this definition, since the currents are of the order of hundreds of amperes and the total voltage (column plus electrode fall voltages) is of the order of 90-150 volts. The arc discharge is distinguished from the glow discharge by its relatively low fall in voltage at the cathode root, compared to a voltage fall for the glow discharge roughly equal to the Paschen minimum* (about 300 v). Arc discharges have been established under an amazingly wide range of conditions: 1) from extremely low pressures (the so-called vacuum arcs) to hundreds of atmospheres; 2) in almost every gas; 3) in vaporized solids and liquids; 4) with currents from 1 amp to hundreds of thousands of amps; 5) with lengths ranging from millimeters to meters; 6) with total power dissipation from hundreds of watts to millions of watts; 7) confined and free-burning; 8) with forced convection parallel to the axis, normal to the axis, or circling the axis.

The conducting column or positive column of the arc is essentially a mechanism for energy conversion. The energy of the electric field is converted to directed kinetic energy in the highly mobile electrons. This directed energy is converted through collisions into random thermal energy. Because of the energy continually absorbed from the electric field, the electron kinetic temperature is somewhat higher than the temperature of the heavy particles. There is a transfer of thermal energy from the electrons to the heavy particles, both through the cumulative effects of large numbers of elastic collisions and through inelastic collisions.[27] There results a very high gas temperature in the column. The column voltage-gradient is low. The collision frequency for a free-burning arc at atmospheric pressure is great enough to maintain quasi-equilibrium,[25] so that the ionization fraction is given by the Saha equation. The ionization is balanced by volume recombination in the column and by some loss of the ion pairs which diffuse to the cooler outer regions of the column, where they recombine and release their energy of ionization. The ambipolar diffusion and recombination of ion pairs, together with the recombination of dissociated molecules, constitute an important mechanism for the transfer of thermal energy from the column to the surrounding gas. Other mechanisms for this transfer are thermal conduction, convection, and radiation - though the total energy lost through radiation is usually negligible.[25] Thus the column provides mechanisms for the ultimate conversion of energy in the electric field to thermal energy in the gas.

In a given configuration, the mechanisms available for energy transfer to the environment are essentially properties of the arc-interaction and, as such, their effectiveness dominates the overall behavior of the arc.

An arc subjected to the effects of forced convection will be referred to herein

---

*With a uniform electric field, the breakdown voltage V_s of a spark gap of width d in a gas of density ρ at constant temperature, varies with ρd only.[28] When the mean free path in the gas is of order d, V_s decreases with ρd; when the mean free path is much less than d, V_s increases with ρd. Thus, the Paschen curve of V_s vs ρd has a minimum which is a characteristic of the gas.

as a convective arc; thus, a convective arc is here defined to be one for which there is relative motion between the arc and the gas. An arc which moves along electrodes in a still gas will be termed a moving arc. An arc which is held at, or confined to, a fixed position between the electrodes, and is blown-against by a gas flow, will be termed a blown arc. As defined here, both the moving arc and the blown arc are convective arcs, since for both there is relative motion between the column and the gas. The difference between them is that for the moving arc there is relative motion between the arc and the electrodes; whereas for the blown arc, there is not.

An arc which is held within a given region of space for the required time will be herein termed a confined arc. A confined arc for the present investigation would be one which is held (by a magnetic field) on the electrodes within the region of uniform flow in the tunnel test-section.

A stable arc can be defined as one which exhibits only predictable or desired time-variation in such significant characteristics as current, voltage, and location. A stable arc can thus be stationary or moving. For example, the arc in a plasma generator can be referred to as magnetically stabilized, even though the column may be moving very rapidly around the annulus between electrodes; in this example, if the arc for some reason stopped moving, it could be considered unstable and in fact would probably melt the electrodes. For the present investigation, a stable arc is one which exhibits no appreciable time-variation in current, voltage, or column geometry. An arc which remains on the electrodes but which exhibits column fluctuations, is in this context a confined arc but not a stable arc.

The term arc characteristic is used herein and in the literature to refer to the relationship between the arc voltage and the arc current. Where the voltage decreases with current, the arc is said to have a negative characteristic.

CHAPTER III

THEORY OF THE POSITIVE COLUMN

3.1 INTRODUCTION

Although the first experimental observation of an electric arc moving through a gas under the impetus of a magnetic field was made at least 140 years ago,* there is still no general theory for the structure of the convective arc column.

The magnetically-stabilized arc with convection can be physically described as an interaction between a thermal energy field, an electric field, a velocity field, a pressure field, and a magnetic field. The mathematical formulations of the physical laws governing this interaction must vary with the arc conditions at hand, and in every case result in extremely complex sets of equations.

Since the arc column contains a number of gaseous species, mathematical treatment can be based on the equations governing the various species, on the equations governing suitably-defined total or average quantities, or on both sets of equations. The laws generally expressed by these equations include the conservation of mass, the conservation of momentum, the conservation of energy, and the conservation of charge. Also needed are an equation expressing the relation between current density and the field variables along with Maxwell's field equations, and the constitutive relations. Full presentations of governing equations can be found in references 25, 29, and 30.

The theoretical work discussed in this section is almost all based on the approximate solution of a simplified version of only one of these equations. The analyses apply only to very specialized cases, and assume thermal equilibrium as well as stationarity. The theory of the non-convective arc will first be discussed, after which the further difficulties involved in the analytical treatment of the convective arc will be considered.

3.2 THE NON-CONVECTIVE ARC

Even when convection can be ignored, the energy equation which then governs cannot be solved in closed analytical form--chiefly because of the non-linearity introduced by the highly irregular variations of thermal conductivity with temperature (see Figure 1). Theoretical treatments of the non-convective arc have consisted primarily of approximate solution of the form of this equation known as the Elenbaas-Heller equation:[31-38]

$$\sigma E^2 = -\nabla\cdot(K\nabla T) + S(T) \qquad (1)$$

where

σ = electrical conductivity E = electric intensity

K = Thermal conductivity T = temperature

S = radiation energy

---

*For an excellent bibliography (through 1956) of the moving arc, see reference 12.

Neglecting radiation, and given E, $\sigma(T)$, and $K(T)$, this equation determines the single unknown, T.

The use of only the above equation for the description of the arc column is already a severe limitation on the physical phenomena covered. For even in the absence of forced convection, there will be few cases where energy transfer from natural convection can be ruled out a priori. But since the detailed calculation of the internal velocity-field resulting from buoyancy forces is extremely difficult, only cases where the effects of gravity are negligible have been considered.

The case which has been most successfully treated in this way is the wall-stabilized or tube arc, where the tube diameter is small enough to maintain a dominance of conduction over convection. The boundary conditions placed on the Elenbaas-Heller equation for the wall-stabilized arc are a prescribed temperature at the wall and a zero temperature gradient at the axis of the arc.[25] It has been found easier[39] to express the Elenbaas-Heller equation in terms of the heat-flow function.

$$s(T) \equiv \int_0^T K(T)\,dT \tag{2}$$

The equation then becomes:

$$\sigma(s)E^2 = -\nabla^2 s \tag{3}$$

Several investigators[33-35,38] have solved this equation by approximate means, including piece-wise linearization of the electrical conductivity function. The results usually agree well with experiment, provided great care is taken in the design of the experiment[33] to assure that the effects of convection will be negligible as assumed in the theory.

3.3 THE CONVECTIVE COLUMN

The radial energy loss to the walls of a confining tube has a great effect in stabilizing the arc.* [25] If, however, the tube is large enough for convection currents to play a significant role, the arc is observed to break away from the wall and to swing back and forth in the interior.[30] If the walls are displaced farther, an increasing portion of the energy from the arc is transferred to the environment by convection currents.[29,30] But, while free convection assumes this energy-transfer function of the wall, it does not provide the stabilizing influence of the wall. The horizontal freely-burning arc is often observed to fluctuate in spatial location due to the natural convection currents. Thus, Weitzel[30] refers to the tube-arc as wall-stabilized, but to the freely-burning arc as convection-determined, since the latter is not necessarily stable. The spatial fluctuations of the freely-burning arc

---

*The wall is near enough to the axis to be in a region of large temperature gradient where thermal conduction predominates. The thermal conduction to the wall will thus dominate the temperature distribution and the arc size and shape.[30]

have a counterpart in the more violent fluctuations observed in arcs with forced convection, as discussed in section 4.1.3.2.

The introduction of convection complicates the theoretical treatment by necessitating the consideration of fluid dynamics as well as thermodyamics. For the non-convective arc, the temperature distribution can be considered the solution sought. Given the temperature, one can calculate the electrical conductivity, and from this the current density can be calculated from Ohm's Law, provided that the electric field is considered an independent variable of the problem. With convection, however, the energy balance is materially affected by convective heat transfer, and the temperature distribution must be considered as a function of the fluid velocity distribution. Convection distorts the isotherms and provides a mechanism for possible charge separation. The steady-state energy equation, neglecting radiation and viscosity, becomes:

$$\sigma E^2 = -\nabla\cdot(K\nabla T) + P\underline{v}\cdot\nabla\left(h + \frac{v^2}{2}\right) \qquad (4)$$

where the velocity and density introduce a strong coupling between the non-linear energy equation and the non-linear equations of motion. The obstacles to solution are immense. Rother,[40] considering the case of an arc between co-linear electrodes, has artificially de-coupled these equations by assuming a uniform velocity field which is not disturbed by the presence of the arc (see Figure 2a). This assumption represents an overestimation of the mass flux through the conduction zone, of course, but it results in an approximate energy equation which allows in a simple way for convective heat losses. Assuming constant conductivities, Rother solves the energy equation by finding the appropriate Green's function in two dimensions. From this he obtains information on arc curvature which he finds is in good agreement with experiment.

Rother's analysis is concerned with the electric arc between co-linear pointed electrodes which are located in a transverse uniform gas flow, Figure 3. The electric field is similar to that of a dipole in the region of the arc and is non-uniform across the diameter of the arc. Rother's model follows that of Weitzel, according to which the arc bends to the point where the unsymmetrical cooling of the column due to convection is just compensated by the unsymmetrical heating due to curvature and to the non-uniform electric field (see Figure 3). Thus, the non-uniformity of the electric field and the curvature of the arc column provide the mechanism for maintaining arc integrity in this model.

Another analysis along the lines followed by Rother has recently been published by Thiene.[41] For simplicity it is assumed that the curved arc will follow the electric field lines. Thiene justifies this assumption by noting that since, under steady conditions, Ohm's Law and charge conservation require that

$$\nabla\cdot\underline{j} = \underline{E}\cdot\nabla\sigma + \sigma\nabla\cdot\underline{E} = 0 \qquad (5)$$

the assumption of charge neutrality along with Poisson's equation

$$\nabla\cdot\underline{E} = 4\pi e(n_i - n_e) = 0 \qquad (6)$$

yields

$$\underline{E} \cdot \nabla \sigma = 0 \tag{7}$$

This last equation indicates that lines of constant conductivity, and thus isotherms, are parallel to the electric field lines. Edels[29] has earlier commented that this simple orthogonal relation between $\nabla\sigma$ and $\underline{E}$ can be destroyed by small net space charges. It has been pointed out[25] that only negligible separation of the charge carriers in the quasi-neutral column is necessary to counteract the effects of even very strong external electric fields. It would appear from this that the column can cross external electric field lines.

In view of the experimental observations which indicate a flame-like behavior of the convected arc column,[30] there seems little reason to doubt that forced convection can support the net charge separation necessary to disturb the parallelism indicated by equation (7). It is difficult to imagine, for example, a column following the electric field lines if subjected to a gas flow which contains a velocity gradient, or perhaps flows in one direction against part of the column and in another direction against the rest of the column.* But in any case, the analyses of Rother and Thiene do represent models which serve as steps in the direction of full analytical treatment of the convective arc between co-linear electrodes with no magnetic field.

It can be shown[25] by integration of the energy equation over a disk containing a section of the free-burning arc column, that the energy input to the column is ultimately carried off by convection, disregarding radiation. It is therefore possible to estimate the overall electrical characteristic of the arc from empirical knowledge of the magnitude of convective heat transfer from solids.[42]

Champion[43] has found it possible to use an experimental temperature distribution with the momentum and energy equations to calculate an axial velocity distribution which agrees with experimental measurements for the vertical free-burning arc.

The introduction of an external magnetic field complicates the theoretical problem not only because it usually implies higher convection velocities, but also because of the additional coupling between the energy equation and the momentum equation, imposed by the Lorentz body force. The energy and momentum equations are as follows:

$$\sigma E^2 = -\nabla \cdot (k \nabla T) + \rho \underline{v} \cdot \nabla \left(h + v^2/2 \right) \tag{8}$$

$$\rho \underline{v} \cdot \nabla \underline{v} = -\nabla p + \sigma \underline{E} \times \underline{B} \tag{9}$$

---

*After this dissertation had been submitted, a note was published by Fay (Physics of Fluids, Vol. 7, No. 4, p. 621, April, 1964) which questioned this same assumption (Eq. (7)) in the Thiene analysis. The results of the present investigation, of course, afford a striking proof that the (supersonic) convective arc need not follow the electric field lines.

Here the viscous terms have been omitted because they are generally assumed to be negligible. The omission of time derivatives is much less justifiable, since it is not known under what conditions a steady-state treatment might be applicable. Ohm's Law has been used in the above. Under some conditions the presence of a magnetic field results in tensor transport coefficients. This results from the so-called "transverse effects" of which the Hall effect is the one of most interest to the present investigation (see Appendix B and section 9.3.3).

It can be seen from the above equations that for the magnetically stabilized arc, the energy equation is strongly coupled to the momentum equation explicitly through the mass density, convective velocity, and electrical conductivity. Thus, a treatment based purely on energy transfer or purely on column dynamics appears unjustified for the convective arc. Nevertheless, some observations of a general nature can be made.

Two of the simplest conceivable fluid flow patterns for the convective arc are shown in Figure 2. The first of these, 2a, illustrates the undeflected uniform flow-field assumed by Rother.

It seems likely, however, that the flow approaching the arc column will behave somewhat as though approaching a solid obstacle (see Figure 2b). The great increase in temperature (about 30 to 1) due to the energy addition from the column must, at least in the equilibrium case, result in a large expansion ratio for the small stream of gas which passes through the column; and the main part of the stream must deflect to allow for this expansion.

The flow pattern in the wake of the arc will, of course, be quite different from that following a solid cylinder. The temperature and pressure may be higher and the wake contraction less. Since it is known that, at least for one-dimensional flow, a magnetic body force[44] as well as heat addition tends to force the flow Mach number toward unity, it is conceivable that the flow just downstream of the arc will be moving at sonic velocity. Rough calculations indicate that if this were the case, there would, in addition to the Lorentz force, be an appreciable thrust on the arc control-volume due to net momentum flux. The mechanism for acceleration would be flow from the high pressure region near the leading boundary of the arc to the lower pressure region of the wake. The Lorentz force would balance out the difference between the pressure integral and the momentum thrust.

Of course, the body force must have a profound effect on the flow pattern as must the energy addition; and it is probably futile to attempt the formulation of a flow pattern for an interaction of such complexity--involving the flow of a real gas, body forces, and volume energy addition--until the formulation can contain at least the elements of this complexity.

The discussion given here of the difficulties of theoretical treatment of the convective arc is based on the one-fluid equations of magnetogasdynamics because of their relative simplicity. However, even if solutions to these equations were available, it is not clear that they would be applicable to the high-speed convective arc, since it is not known whether equilibrium exists in the high-speed arc, even at atmospheric pressure (see section 3.4). Without thermal equilibrium the variables involved in the one-fluid continuum equations are not well defined, and multi-fluid equations or the statistical methods of kinetic theory must be resorted to, with the Boltzmann collision equation serving in the mathematical formulation of the governing physical laws.[4]

3.4 THE QUESTION OF EQUILIBRIUM

In thermodynamic equilibrium, the population of all energy states is given by the Boltzmann formula. This means that the kinetic temperature of all species must be equal, and from the principal of detailed balancing,[45] the rate at which a given energy state is de-populated by a given process must equal the rate at which the state is re-populated by the inverse process. Since the electric arc is an optically thin radiator, generally, and since there is an irreversible flow of energy from the electric field, the gas in the positive column can never be in true thermodynamic equilibrium.[25] In particular, the electron temperature must always exceed the gas temperature to some degree.

The detailed diagnostics of the convective plasma column and field interactions are beyond the scope of this dissertation. But it is shown herein that a convective plasma column of sufficient spatial stability and duration for the application of both probe and spectroscopic diagnostic techniques can be achieved. It is therefore of interest to consider briefly some of the questions which will ultimately be answered by the application of such techniques.

Diagnostic observations will be essential not only for evaluation of the processes active under specific experimental conditions, but also for the determination of the physical regimes which prevail and the mathematical form of the applicable physical laws. Thus, the field equations of continuum magnetogasdynamics provide the proper starting point for theoretical analyses where it has been shown that the macroscopic quantities which these equations govern are well-defined for the dimensions of space and time of interest. But for phenomena where characteristic times, or distances, are too short to permit the definitions implied by the continuum equations, the statistical equations of kinetic theory give the proper foundation for analysis.[4,45]

Precise knowledge of the equilibrium state of the plasma can be obtained only through diagnostic measurements. These should give the gas and electron temperature or their difference[27] directly, or indicate the column voltage-gradient, collision frequency, and other variables from which the equality of these temperatures can be deduced.[25] Equality of electron and gas temperatures does not, of course, imply complete thermodynamic equilibrium. Finkelnburg and Maecker[25] have given a detailed discussion of the question of ionization and excitation equilibrium, and have shown that at atmospheric pressure or above, the excitation temperature and ionization temperature are essentially equal to the electron (and gas) temperature. Thus, the gas temperature or electron temperature can be used in the Saha equation to give the correct ionization fraction (provided the effective ionization energy can be determined), or in the Boltzmann formula to give the correct fraction of particles in a given excited state. Under these conditions, there is one locally well-defined temperature which determines the kinetic reaction equilibria for all species in the gas. This situation is particularly useful for analytical work, since the spatial temperature distribution is the principal dependent variable for most arc problems. Many important arc characteristics such as electrical conductivity, thermal conductivity, and current density distribution can be determined from a knowledge of the equilibrium temperature distribution.

The difference between the electron temperature T_e and the gas temperature T_a can be estimated from simple considerations. It can be assumed[25,46,47] that the mean

energy lost by the collision of an electron is a fraction $\delta m_e/m_a$ of the excess electron energy which has been acquired from the field. The loss is then given by $\delta \frac{m_e}{m_a} \frac{3}{2} k(T_e - T_a)$ and the rate of energy loss is

$$3k\delta m_e(T_e - T_a)/2m_a\tau_e \qquad (10)$$

A value of 2 is taken for the elastic-collision energy-loss parameter, by Finkelnburg and Maecker. Kerrebrock uses δ as an adjustable parameter of the problem, which for the noble gases is reasonably near the value of 2. For diatomic gases, δ is much higher (36 for N_2)[48] than 2. Kerrebrock suggests, and the calculations in reference 27 tend to confirm, that the higher values of δ for diatomic gases denote an increased efficiency of energy transfer due to inelastic collisions, which excite rotational and vibrational degrees of freedom in the molecule. The rate of energy absorption accompanying the average drift in the direction of the field is $eE\upsilon_d$ where υ_d is the electron drift velocity. For steady conditions, this energy must be given up at the same rate to the gas by collisions:

$$e\underline{E}\cdot\underline{\upsilon}_d = (T_e - T_a)\,3k\delta m_e/2\tau_e m_a \qquad (11)$$

now

$$\underline{\upsilon}_d \approx e\underline{E}\tau_e/m_e \qquad (12)$$

so that

$$(T_e - T_a)/T_e = 2m_a e^2(E\tau_e)^2/3\delta k m_e^2 T_e \qquad (13)$$

It is not possible to apply this simple equation directly to a mixture of gases, such as air, since δ is not known and since an effective m_a is difficult to assign. But this equation does serve to indicate the important variables involved in determining the approach to equilibrium electron-temperature. In particular, it will be noticed that increased electric field strength, E, or increased mean free time $\tau_e (\sim \frac{1}{p})$ tends to increase the temperature difference.

Experimental work with mercury arcs indicates that the electron temperature and mercury vapor temperature are equal for pressures over about 2 cm Hg.[48] For air there is little experimental information available, but one recent measurement[49] indicates that equilibrium exists for pressures above 300 mm Hg. This measurement was made with a 10-amp arc 4 mm in length, under highly unfavorable conditions for equilibrium, since the high field strength in the cathode region can be expected to dominate such a short arc at low pressures. The field strength, in fact, was about 100 v/cm, which is several times the value one might expect in the positive column of an arc under similar conditions. From the preceding equation one would expect that for the longer arc, thermal equilibrium might exist at considerably lower air pressures. Another recent measurement[27] indicates that for a low-current arc in still air at 100 mm Hg, the electron temperature is four per cent higher than the gas temperature, and that the temperature difference rises rapidly as the pressure is decreased below 100 mm Hg.

The theory of non-equilibrium conductivity has been recently treated by Kerrebrock, who assumes that the ionization level is determined by the electron temperature rather

than the gas temperature, and derives a two-temperature conduction law therefrom. This assumption, at least under some conditions, is borne out by experimental measurements of conductivity.[47] Kerrebrock points out the practical advantages for certain magnetogasdynamic devices of the high conductivity and low gas temperature associated with non-equilibrium conduction.

Demetriades[50] has given a rough equation for the threshold values of electric field and pressure separating the equilibrium from the non-equilibrium case in the absence of inelastic collisions.

The existence of equilibrium depends also on the arc current. Kitaeva[51] discusses a case where for an argon arc the plasma is in a non-equilibrium state when the current is 4 amps, but is in equilibrium when the current is 10 amps.

The above remarks apply to the arc column with little convection. The introduction of high-speed forced convection provides additional conditions unfavorable to thermal equilibrium. First, it is to be expected that high-speed convection will cause a considerable steepening of the temperature gradient at the leading edge and sides of the arc column. If this gradient becomes so great that there is a significant relative change in temperature over a distance of one mean free path for the process in question, then there will be a perturbation in the temperature equilibrium.[25] Second, although it seems likely that the gas near the leading edge of the column will be moving at low velocity relative to the column, there may be regions or conditions where the gas velocity is great. With high gas velocity, the transit time required for the gas particles to pass through the column could become less than the relaxation time required for the establishment of thermal equilibrium. The relaxation time will vary with collision frequency, and for air at atmospheric pressure, is estimated[25,52,53] to be betweem 10^{-3} and 10^{-7} seconds; thus, if the arc internal gas velocities reached the order of 10^{3} feet per second, the gas might not come to equilibrium temperature before passing out of the column. There would be a resulting imbalance between the temperature of the gas and electrons in the column.

For the present experiments, the pressure in the positive column can be estimated to be no greater than that which would exist on the leading edge of a solid cyclinder yawed at the Mach angle for M = 2.5. This pressure is simply the free stream static pressure, P_1, divided by the sonic pressure ratio, (P_1^*/P_{t_1}), or about 50 mm of mercury. This pressure lies below the lowest pressure where thermal equilibrium has been demonstrated for the arc column in still air; reference 27 indicates an electron temperature about 10 per cent above the gas temperature at 50 mm Hg.

On the basis of the above considerations, it seems likely that under the conditions of the present investigation the electron temperature in the column will be of the order of 10 per cent greater than the gas temperature.

CHAPTER IV

BEHAVIOR OF THE CONVECTIVE ARC

4.1 THE MOVING ARC

4.1.1 Introduction. In the past, the primary application for convective-arc data has been to the design of circuit breakers. In such applications, the arc must move with respect to the electrodes. There must be a mechanism for the motion of the electron emission and absorption sites at the electrode surfaces, as well as a mechanism for the motion of the conducting path formed by the positive column. Since it is not to be expected that the motion of the arc roots will be affected by an external magnetic field in the same manner as is the column motion, it can be expected that the velocity of the roots will in general be different from the velocity of the column. This difference between the velocities of the arc roots and the column can be manifest in two ways: either the arc must sever, or there must be some mechanism of accommodation which brings about an intermediate equilibrium velocity of the whole arc. It is primarily the latter circumstance that is of interest here. In this case, the measured arc velocity is necessarily determined by root phenomena as well as column phenomena.

Most experimental observations of moving arcs have been made using the rail accelerator.[5-16,19,20,21-23,54-59] The simplest form of this device (see Figure 4) consists of two parallel rail electrodes with an external magnetic field normal to the electrode plane. The current is fed to the two rails in any one of several possible ways,[13,15] chosen to give the desired configuration of the magnetic field resulting from the current in the electrodes.

The velocity of arc motion has been found with the rail accelerator to vary with cathode root conditions such as surface oxidation,[11,17,19] surface polish,[8,9,12,13,15,20] cathode material,[5-10,13-16,18,19] and magnetic permeability;[5-7,9,10,13-15,19,54] with conditions which affect the flexibility of the positive column, such as circuit inductance[13] and electrode gap;[12,13,21,57,62] and with conditions which might be expected to affect both root and column phenomena, such as arc current[5,6,8,12-14,18,21-23,62] and magnetic flux density.[5-19,21-23,54-58,62-64] Changes in conditions at the anode root appear to have little effect on arc velocity.[9,16]

4.1.2 Motion of the Cathode Root

4.1.2.1 Introduction. In general it has been found that in the low speed range from 0 to about 200 ft/sec, the moving arc is greatly affected by conditions at the cathode root (material, surface polish, oxidation, magnetic permeabilitiy). The cathode root has been found to move over the cathode surface in any one of several modes of motion.[5,6,8,9,12-16,21,58] These modes will be grouped here in only two categories: the continuous mode and the discontinuous mode.[9,13]

Continuous arc motion is apparently dominated by conditions at the cathode root. Discontinuous motion is more susceptible to processes active in the arc column, and at high speeds is probably dominated by these processes.

4.1.2.2 Motion of the Spot in the Continuous Mode. In the continuous mode, the cathode root leaves a continuous track of surface discoloration and oxidation or

melting along the cathode surface. The fact that the velocity in this mode is almost solely determined by conditions at the cathode root is illustrated by the observation that there is no effect on continuous velocity, of changing electrode orientation from horizontal to vertical.[9] Movement of the center of the arc column produces no effect on continuous movement, but can influence discontinuous movement.[9] To discuss movement of the cathode spot, it is first necessary to consider the nature of the stationary cathode root.

In the absence of a magnetic field and without convection, three mechanisms for the cathode root have been observed experimentally:[25] without burning spots, with burning spots, and with non-stationary burning spots. The arc without burning spots is characterized by significant thermal electron emission from the cathode. The arc with a burning spot, or spots, is one in which there is a considerable contraction of the root at the cathode surface, terminating in a brilliant high-temperature spot which may supply positive ions to the cathode, and electrons to the other parts of the plasma.[25] The arc with a non-stationary burning spot is characterized by very rapid and unsteady motion and short lifetimes of the burning spots. With the burning spot mechanism, it is possible for several spots to exist at the same time.

As might be expected, refractory electrode materials generally result in an arc with a site of significant thermionic electron emission, and therefore without cathode burning spots. But burning spots can occur on refractory cathodes, such as carbon, immediately after ignition while the cathode is still cold.[25] Evidence of the burning spot is clearly visible, for example, in Figure 52, where the arc immediately after initiation has played over the surface of the carbon until the establishment of the thermionic site, which is also visible in Figure 52. "Cold cathode" materials, such as copper and mercury, generally result in an arc with burning spots at the cathode root.

There is no generally-accepted physical theory for the continuous motion of the cathode spot under the impetus of a magnetic field. Such a theory must of course explain retrograde motion[63-77] as well as continuous motion in the amperian direction. The absence of an accepted theory for spot motion is not surprising, since the emission mechanism for the stationary spot has not yet been fully explained.[25]

It is beyond the scope of the present discussion to deal with the many theories which have been proposed for cathode spot motion,[12] but it does seem appropriate to mention one mechanism[67] which has received some support and extension.[17,19]

Even though the mechanism of electron emission for the moving arc is admittedly not known, it is hypothesized that motion of the site of emission is effected through the conditioning of new sites by ion bombardment which gives rise to localized thermionic points, or which charges an oxide layer to a point where field emission is caused by large electric fields across the layer.* It is also assumed that while this new site is being so prepared, the existing site is losing its effectiveness because of a reduction in ion bombardment. Thus the cathode spot motion is seen to be a process of the growth of new emission sites prepared by ion bombardment and the loss in effectiveness of existing sites. The rate at which this process can take place determines the spot velocity. Thus, the process of ion bombardment and the location of the bombardment zone assume a dominant role in root motion.

---

*Lewis and Secker[17] have demonstrated that the presence of insulating layers--usually the oxides of the cathode metal--is vital in determining the velocity of cathode root motion.

It has been suggested[17,19,56] that Ecker's[67,68] theory for the cathode zone of the arc can be applied to motion of the cathode spot in the amperian mode, as well as to motion of the spot in the retrograde mode. In this model the arc cross-section contracts as the cathode root is approached, ending in a space-charge zone very near (10^{-5} cm) the surface.[6] The space-charge zone is maintained thin through the back-diffusion of electrons. Ions move toward the cathode through the voltage fall in a stream (see Figure 5). Most of the electric field lines leave this stream in radial directions and terminate at nearby electrons, causing a trough of low potential, or a potential tube, surrounding the path of the ions. Low energy electrons emitted at the cathode surface are forced to travel in this tube unless their energy is sufficient to break through the radial potential wall. The electrons emitted from the surface eventually gain sufficient kinetic energy from the electric field to produce new ions. The new ions in turn travel back to the surface. The zone of impingement of these ions governs the new location of electron emission sites. The shape of the ion tube determines the location of the zone by guiding the electrons.

The ion tube is subject to the effects of the magnetic field and always deflects or bends in the amperian direction, (see Figure 5).

In Ecker's model for the retrograde motion of the spot at low pressures, the electrons are not impeded by collision from gaining sufficient kinetic energy to break through the ion tube on the retrograde side. Thus, new ions are created on the retrograde side. The ion bombardment zone, the new emission sites, and a new ion tube will in turn also form on the retrograde side.

In their extension of this model to the higher pressures characteristic of amperian spot motion, Guile, Lewis and Secker, and others, suggest that due to frequent electron collisions with heavier particles in the ion tube, the electrons follow the ion tube very closely. But due to the Lorentz force in the amperian direction and their higher drift velocity, they tend to break out of the tube and create new ions on the amperian side. Thus, the model agrees with the observed amperian motion at higher pressures. For a fuller discussion of this model for cathode spot motion in the continuous mode, see references 17, 19, and 26.

4.1.2.3 Motion of the Spot in the Discontinuous Mode. It has been seen that continuous motion of the cathode spot can be explained in terms of the preparation, through ion bombardment, of new emission sites on the amperian side of the cathode spot and through decline of the effectiveness of old sites. These same ideas can be used to describe the discontinuous motion of a cathode root in which the track consists of an irregular series of spots with no connecting marks.[58]

It has been observed[9,12,14] that in the discontinuous mode the arc moves by a stepping mechanism (see Figure 6). The positive column deflects in the amperian direction until it very nearly touches the cathode surface ahead of the cathode root. Positive ions from the column bombard the cathode surface and prepare it for the formation of a new cathode spot.[58] Eventually electrons are emitted from this new spot and electrical breakdown occurs because of the potential difference between the new spot and the nearby column. There are then two cathode roots in parallel. The new root grows at the expense of the old one until a transfer of emission sites is completed. Here too, ion bombardment of the cathode surface is believed to have a dominant role in the formation of new emission sites.

Although there has been at least one contrary report,[14] it seems logical that the

arc velocity should be greater for discontinuous motion than for continuous, as is reported in reference 19. The onset of the stepping mechanism indicates that the column velocity is greater than the continuous cathode-root velocity. The velocity of the arc as a whole should then be somewhere between these two velocities and therefore greater than the continuous velocity.

With the stepping mechanism, the positive column plays a more important role in determining the velocity of the arc as a whole.[13] One would expect the positive column to dominate the arc motion for high fields, high current, and high velocity, since it is likely that under these circumstances the motion of both roots is accomplished by the stepping mechanism[13,14] or what might be termed a "running mode." It has been seen that with this mechanism there are two essential features: 1) the flexing of the column to the point where an interchange with the cathode surface can be established, and 2) the growth of a new cathode spot or spots to the stage where a significant portion of the arc current can be taken over from the old spot configuration. The period of time required for the growth of new spots (which varies with cathode surface conditions) can be expected to have less and less effect at high arc velocities. At high speeds, any increased delay in the formation of new spots will merely allow the column to flex farther and begin pre-conditioning of the new spots earlier. Changing the cathode conditions might thus result in no change in arc velocity for a given arc current, though changes in arc voltage would be expected.

Since many of the new applications of the moving arc require high currents, high external induction, and resulting high velocities of arc motion, it is to be expected that the cathode root will move in these devices by the stepping mode, and that their performance will be determined to a large degree by processes in the positive column. In some applications, of course, the dynamics of the positive column will dominate completely the arc behavior due to the geometry of the device. For example, the plasma generator with a central thermionic cathode and a surrounding coaxial anode is a device where the positive column may travel at very high velocities,[8] while the cathode root need not move at all (and in any case can move very easily over the white-hot thermionic cathode).

It has been shown[13] that with increasing inter-electrode gap, the velocity of discontinuous motion increases. With increased column length, a given voltage fluctuation permitted by given circuit parameters corresponds to an increased absolute fluctuation in arc length. Thus, the longer arc is more "flexible" and can execute the stepping motion more readily.

The same reasoning has been used to explain the increase (by as much as five times) in arc velocity with increase in circuit inductance, or rather, time constant, L/R. With a greater time constant, greater fluctuations in voltage are possible, greater fluctuations in column length are possible, and therefore increased arc velocity in the discontinuous mode results.

4.1.2.4 The Effects of Magnetic Permeability. It has been found[5-7,9,10,13-15, 19,54] that when the motion is caused by the self-magnetic field, the velocity of continuous motion of the cathode spot increases (by factors up to about five) with increased magnetic permeability of the cathode material. When the motion is caused by an external field, arc velocity decreases with permeability. It has been deduced from this that root velocity for low-speed continuous motion depends on the magnetic field in the immediate neighborhood of the cathode.[19]

Two factors[10] are believed to account for the increase with permeability of velocity in the self-magnetic field. First, the magnetic field in the region very near or "in" the cathode surface, where the cathode fall in voltage occurs, is greater for a magnetic material--due to the effect of microscopic surface asperities obliterating the mathematical discontinuity in magnetic induction at the cathode surface. Second, the magnetic induction at the cathode surface is greater for a magnetic material due to the occurrence of a significant skin effect which results in an increased current concentration beneath the cathode surface near the spot.

4.1.2.5 The Effects of Axial Induction. If in addition to the external transverse magnetic field, an external longitudinal field parallel to the rails is applied to the arc, there will be a tendency for the cathode root to move around the circular rail in a spiral path.[6-7,15] The longitudinal field exerts a circumferential force on the cathode root in the same manner that the transverse field exerts an axial force. The cathode root has been observed[6] to complete three turns around the cathode without a shorting of the column to the surface. No explanation for this absence of column shorting has been given, but it seems reasonable to assume that the longitudinal magnetic field plays a decisive role. The Lorentz force on the column from this field will be directed away from the cathode in all cases, tending to hold the column at some distance from the cathode surface. The bombardment of the cathode surface by ions from the column, which presumably is necessary for establishing electron emission at a potential shorting point, would thus be impaired by the longitudinal field.

An unexpected result of experiments with longitudinal magnetic fields is the observation[6] that whether the axial field is due to a permanently magnetized cathode or to an electromagnet, the cathode spot moves in a direction determined by the longitudinal field beneath the cathode surface. For the permanent magnet the longitudinal field just outside the surface is in the reverse direction from that within the surface. At the surface itself then, the magnetic induction is indeterminate. The above observation, obtained at arc velocities under about 10 ft/sec, indicates that the essential cathode spot phenomena occur at points between the surface irregularities where the magnetic field is in the same direction as beneath the surface.[6] It thus appears that for spot velocities up to at least 10 ft/sec, there is a motive force in the cathode spot which is stronger than any tendency to motion which might exist in the column just above the cathode surface.

4.1.2.6 The Effect of Oxide Layers. The effect of an insulating oxide layer on the cathode spot motion is dramatically illustrated by the difficulties encountered[12] in initiating a stable arc discharge from polished electrodes in an oxygen-free gas, or from electrodes made of non-oxide-forming material, such as platinum. Systematic studies of the effect of oxidation on continuous spot motion[20] show that with increasing time for oxidation, the continuous spot velocity increases to a peak beyond which further oxidation results in diminished spot velocity.

With polished copper electrodes it has been found impossible at a pressure of 25 mm Hg to establish an arc.[17] Even when the copper cathode was allowed to oxidize for several days, the arc which could then be established at 25 mm was short-lived. This is believed to be due to the fact that when copper oxidizes, the bulk of the oxide layer is made up of cuprous oxide, a semiconductor which is apparently not satisfactory for stable arc formation.[17] Unfortunately, reference 17 does not specify

the type of copper used. During the present investigation, for example, despite some trouble with "plain" copper electrodes, there was no special difficulty involved in establishing the arc on OFHC (oxygen-free, high-conductivity) copper, a form in common use for plasma-generator electrodes.

4.1.2.7 The Effects of Surface Polish. The degree of surface roughness has a pronounced effect on spot velocity in the continuous mode. Increased roughness results in increased arc velocity.[20] This effect is believed due to localized points of high electric field intensity at the microscopic asperities of the roughened surface.[20]

4.1.2.8 The Effects of Current. The effect of current on cathode spot velocity can be simply stated: in air at atmospheric pressure, the spot velocity increases with current for currents under about 45 amps, and is independent of current between 45 amps and 700 amps.[13-15,19,54] It has been suggested that for given gas conditions a definite limit exists on the current possible from a single spot, and that under the influence of a magnetic field the motion of each burning spot is essentially independent of the motion of the other spots. This suggestion has been offered to explain the above-mentioned observation that for given magnetic field strength (including self-field), the velocity of motion of the arc root is independent of total arc current above 45 amps at atmospheric pressure. With a limit on the current to a given spot, increases in total current merely result in the formation of additional spots, each of which moves at the same velocity.

4.1.2.9 The Effects of Pressure. Experiments with the rail accelerator to determine the effects of pressure on arc velocity have been generally conducted with very low arc currents (under 10 amps) with below-atmospheric pressure,[19] and the primary emphasis has been the study of retrograde motion. (For discussion and references, see references 12, 19, 67, and 69.)

The effects of pressure can be expected to be exerted through changes in the mean free path and collision frequencies in the gas.[56] It has already been mentioned that these changes can result in a reversal of the direction of spot motion in the continuous mode. This transition from amperian to retrograde motion occurs at a critical pressure which varies with gas properties, magnetic induction, and current. Although there have been many experiments on retrograde motion, there appears to be for air no data on the critical pressure for arc currents of several hundred amperes and magnetic induction of several thousand gauss. This could indicate that continuous spot motion is not possible under these conditions, in which case retrograde tendencies could not be observed. In the discontinuous mode, column processes become important, and the preferred direction of column motion is invariably amperian.[12] For the low current ($\sim$ 10 amp), low speed ($<$ 40 ft/sec) arc in air above the critical pressure, decreases in pressure can cause decreases in velocity[19] or increases in velocity[17] for continuous spot motion, depending apparently on cathode surface conditions.

4.1.3 Motion of the Positive Column

4.1.3.1 Column Velocity. There has been one deduction, based on measurements of the effect of variations in circuit inductance, cathode material, and arc current, that the rate of column movement must be independent of arc current.[13] However, with the rail accelerator there is little opportunity to observe the inherent tendencies of the positive column because of root effects and because of the fluctuations which the column executes.[14,21-23]

4.1.3.2 Column Fluctuations. One of the interesting results of the rail-accelerator experiments has been the observation that the moving column does not remain in the electrode plane, but shows a strong tendency to bow out to the side, forming fluctuating loops and spirals[21,23,55] as it moves along. Two inferences to be drawn from this observation are: 1) that some factor militates against steady-state translatory motion of the column, and 2) that it is possible for the column to follow paths which coincide neither with lines of the external electric field, nor with lines of constant external induction.

The results of the present investigation indicate that there is a "preferred" steady-state column velocity and orientation, and that when root conditions are such as to interfere with the preferred configuration, the column assumes an unsteady, spatially-fluctuating nature (see section 9.1). If this be the case for the moving arc, then one could reason that the characteristic or preferred velocity of the positive column is not, in general equal to the preferred velocity of the arc roots. The mechanism for the accommodation of this difference in velocities is apparently the unsteady fluctuation of the positive column. This fluctuation apparently can carry the column outside the electrode plane, as well as account for the stepping mechanism with which the high-speed arc moves along the rails (see section 4.1.2.3 above).

As mentioned in section 3.3, it seems reasonable that the positive column can cross the external electric field lines. It has been found that a very slight charge separation is sufficient to cancel the effects of a very strong external electric field.[25] The dynamic processes in the column under the influence of forced convection and magnetic induction evidently determine the column shape, while microscopic charge-separation molds an electric field configuration which follows isotherms inside the column and thus provides the volume addition of energy required to sustain the arc. Outside the column, the electric field can have components normal to the arc axis terminating in a region of charge separation at the column boundary.

4.1.3.3 Column Guide Walls. Some investigators have made use of guide walls to eliminate the sidewise fluctuations of the arc,[21-23,57] but it has been shown that the effects of these guide walls on the arc behavior are great. This is especially demonstrated by the observation that a slit in the wall causes a considerable change, depending on current, in arc velocity.[21,57] If the arc is confined with insulated guide walls which are sealed at the rails and on one end, thus forming a channel open only at one end, the very high-current arc (300 K amp) will move at very high velocities (up to 4,000 m/sec). In such a configuration, a shock wave precedes the arc and can cause sufficient ionization of the gas to affect materially the arc characteristics.[22] The results obtained using guide walls will not be discussed further, since the flow field is so different from the freely convected arc.

4.2 THE BLOWN ARC

There have been very few experimental studies of the electric arc held stationary in a stream of flowing gas. Guile and Mehta[9] mounted rail electrodes in a wind which passed through a 16-inch-square working section. They investigated the behavior of high current a-c arcs under the effects of the self-magnetic fields of the current in the rails. By adjusting the wind speed to a value which kept the a-c arc oscillating between fixed points on the rails, they were able to determine that this "equilibrium

wind speed" was roughly equal to the a-c arc velocity in still air. The arc was observed to move upstream during each half-cycle at about the same speed as in still air, but to reestablish after current zero at roughly the same downstream station each time. However, at higher currents and wind speeds the cathode root did not move as rapidly over the cathode surface as in still air.

Guile and Mehta concluded that the study of a-c arc motion is complicated by the fact that the magnitude of the force on the arc varies periodically and by the fact that the anode and cathode spots must transfer to the opposite electrode during the re-strike of the arc at current zero. They proceeded to study the movement of the d-c arc in still air, but apparently did not attempt to use the opposing-wind technique for the d-c arc.

Rother[40] and Thiene[41] report some results of measurements of the deflection of small electric arcs between co-linear electrodes with a wind normal to the arc axis. Each presents a mathematical model (see section 3.3) which he finds in agreement with his experimental results. Very little experimental data is included in these reports. Rother gives no description of his experimental conditions. Thiene[41,78] indicates that his studies were conducted for arc currents from 2-6 amps and arc lengths around 0.6 cm. He finds that arc blowout occurs for gas velocities around 200 cm/sec. As mentioned in Chapter III, both Thiene and Rother feel that the non-uniformity of the dipole electric field between the electode tips contributes to the "flexural rigidity" necessary for the column to withstand the bowing effect of the wind. No consideration was given to magnetic field effects.

Smith and Early,[24] in a study of electrical methods for adding heat to a supersonic air stream, performed feasibility tests in which a low current (under 15 amps) d-c arc was held in a 1" x 1" Mach 4 wind tunnel by means of a strong external magnetic field. In reference 24 they give a qualitative description of the arc appearance and behavior.

For all the arc tests conducted by Smith and Early, the electrodes were in direct contact with the tunnel boundary-layer. Thus a path through the boundary-layer existed along which the arc could pass without traversing the higher velocity, higher density tunnel free-stream. Smith and Early report that the arc showed a strong preference for this path through the tunnel boundary-layer, and they therefore proposed alternative methods for attaining a more uniform heat addition to the gas stream. (For later work, see reference 79.) But even though the arc for their experiments passed through the tunnel boundary-layer, some of their qualitative observations of arc behavior agree with the results of the present investigation, where the arc passed through the free-stream.

The electromagnet used by Smith and Early was capable of 6,000 gauss. For most of the experiment the contoured metal blocks of the two-dimensional tunnel were used as electrodes. The parallel side walls were made of insulating material. Smith and Early report that with the contour-electrode tunnel, the discharge showed a strong tendency to assume a skewed orientation, with the cathode end always downstream of the anode end. They report a slant-angle of from 20 to 70 degrees. This observation is understandable in view of the results of the present investigation, which indicate that an arc in a supersonic free-stream tends to follow a Mach angle. Smith and Early observed that it was possible to add more energy to the flow than theory predicts, without choking the tunnel. The results of the present investigation confirm this, and the explanation in both cases is probably the same: that the energy addition is non-uniform, and that substantial energy goes into heating the electrodes and tunnel walls.

Smith and Early performed several experiments designed to eliminate the skewed orientation of the arc. The most interesting of these was an experiment in which slots and fins were used to provide a sheltered place in which the cathode spot could exist directly across from the anode spot. They found that arc slanting could not be eliminated in this way. This finding is also confirmed by the results of the present investigation, where Teflon flow-baffles had little effect on cathode root location.

High-speed motion pictures obtained by Smith and Early indicated rapid fluctuations in arc location. These fluctuations also characterized arcs in the present investigation in cases where the possible root locations did not allow the arc to assume the stable slanted orientation, and in cases where the tunnel flow was separated due to the presence of the arc. They report that some pictures indicated cathode spot movement by the stepping mechanism.

Finally, Smith and Early conducted some experiments in which insulated rod electrodes normal to the flow were used. In these experiments too, the arc passed through the tunnel boundary-layer. The arc also assumed an S-shape indicating a slanting tendency even though the electrodes were directly across from each other. An important conclusion drawn by Smith and Early from their feasibility study was that the slanting of the arc did not necessarily depend upon the processes at the anode or cathode, but was a consequence of the momentum transfer mechanism in the arc column itself.

In summary, although the flow conditions in the boundary-layer through which the arc column passed were non-uniform and unknown, and the arc exhibited spatial fluctuations, the slanting tendency and root independence qualitatively reported by Smith and Early are in agreement with the results of the present investigation; the fluctuations observed by them could have been caused by the fact that the arc passed through the tunnel boundary-layer, or by root interference or flow separation, two factors shown in the present investigation to be major causes of arc fluctuations (see section 9.1).

CHAPTER V

ARC STABILIZATION

5.1 INTRODUCTION

The crucial problem in developing the experimental approach for the present investigation was the problem of arc stabilization.

There appear to be no reports in the literature of a convective arc without column fluctuations. On the contrary, there are reports emphasizing the erratic behavior of the moving arc.[21,23,55] Nevertheless, for the present investigation it was decided to attempt the achievement of as high a degree of column stability as possible to allow meaningful measurements of the important arc properties and to facilitate later diagnostic studies of the column structure.

It will be seen below that for the convective arc, stabilization involves circuit considerations which have been known for some time, as well as considerations dictated by the peculiar environment of the arc - by the convection velocity, pressure, and magnetic induction. These latter considerations are related to the problem of arc confinement.

The requirements for circuit stability and the requirements for arc confinement are coupled, and both together determine arc stabilization. The confinement mechanism will affect the V-I characteristic and thus stability for the external circuit; similarly, the external circuit will affect the requirements for confinement, since the circuit parameters help determine the arc current and column flexibility. Arc confinement will be discussed in section 5.3 and in Chapter VI; the classical aspects of arc stabilization will be discussed in section 5.2 below.

5.2 THE KAUFMANN CRITERION

The electric arc as a conductor of electricity must be considered as something apart from other conductors. In the first place, there is a non-linear dependence between the voltage across it and the current through it. In the second place, it shows great variations in static voltage-current characteristic depending on ambient conditions.* In fact the voltage across it can be a multi-valued function of the current (see, for example, Figure 31).

For constant ambient conditions over a fairly wide range, the electric arc has a voltage-current characteristic similar to that shown in Figure 7. Since the characteristic is negative** for these cases, i.e. decreasing applied voltage can result in increasing arc current, instability can result in the circuit of which the arc is an element. Kaufmann[80] first gave a formal treatment of this stability problem for the fixed-characteristic electric arc.

---

*Conditions within the column, as well as in the vicinity of the column.
**That is, the slope is negative (see Chapter II).

The steady-state circuit equation is given by

$$E_o - IR_B - V_a - L\frac{dI}{d\tau} = 0 \tag{14}$$

where

E_o = open circuit voltage

I = current

V_a = arc voltage

L = circuit inductance

R_B = ballast resistance

Assuming a perturbation η in current, Kaufmann writes

$$E_o - (I+\eta)R_B - \left(V_a + \frac{dV_a}{dI}\eta\right) = L\frac{d}{d\tau}(I+\eta) \tag{15}$$

Subtracting the steady-state equation gives

$$L\frac{d\eta}{d\tau} = -\eta\left[R_B + \frac{dV_a}{dI}\right] \tag{16}$$

for which the solution is

$$\eta = \eta_o e^{-\frac{1}{L}\left(R_B + \frac{dV_a}{dI}\right)\tau} \tag{17}$$

The circuit is thus stable provided

$$R_B + \frac{dV_a}{dI} > 0 \tag{18}$$

This is the Kaufmann stability criterion for the arc.

It is interesting to note that the square of the coil voltage can serve as a Lyapunov V-function for this stability problem.* First we note that

$$\left(L\,dI/d\tau\right)^2$$

---

*For a treatment of the Lyapunov "direct approach" to the stability of non-linear systems, see reference 81.

is positive. The derivative

$$-2L\left(\frac{dI}{dt}\right)^2\left(R_B + \frac{dV_a}{dI}\right)$$

is negative provided

$$R_B + \frac{dV_a}{dI} > 0$$

This equation thus serves as a stability condition and is in fact the Kaufmann condition.

Figure 7 shows the typical case where the external-circuit characteristic intersects the arc characteristic at two points, A and B. Each of these points represents a possible static operating condition. From the above stability criterion it is seen that point A is a point of unstable equilibrium, and point B is one of stable equilibrium.

It is seen that the arc static characteristic $V_a(I)$ and its behavior determine circuit stability. The static characteristic is a reflection of the steady-state energy transfer processes in the arc, since it can be considered a description of the power input IV_a as a function of arc current. Therefore, all factors which affect the energy transfer in the arc column affect the current-voltage characteristic and the arc-circuit stability. Among these factors are those involved in arc confinement, such as magnetic induction,* convection velocity, and ambient pressure.

Figure 8 gives an example of the change in static characteristic which can be expected with changes in arc length[25] (similar changes occur due to changes in ambient pressure). Arc convection changes the energy transfer processes in the positive column and thereby also changes the arc characteristic. Increased convection, like increased pressure, shifts the characteristic toward higher[25] voltage.

5.3 ARC CONFINEMENT

The classical considerations in arc stabilization are directed primarily toward the control of the temporal behavior of the external circuit; considerations of the problem of arc confinement are directed primarily toward the control of the spatial behavior of the arc. Arc confinement for the present investigation is based on the concept of controlling the interaction by application of an external magnetic field. The details of this approach to confinement are discussed in Chapter VI.

Among the possible difficulties which can be encountered in arc confinement are the following:

---

*The magnetic field can play no direct role in energy transfer, of course, since the Lorentz force is always normal to the particle velocity; but indirectly it can have a decisive effect through changing the arc length, location, orientation, etc.

1. Electrode burnout--the catastrophic melting of a metal electrode. This problem was encountered during early tests in this investigation with arc currents over about 1,000 amps.

2. Electrode attrition and gas contamination--excessive erosion of electrodes. There was no trouble from attrition in this investigation since all runs were less than three seconds long. Color photography indicated that, at least for copper electrodes, any small amount of vaporized electrode material there might have been was carried away with the free-stream without entering the column.

3. Electrode fracture--cracking of refractory electrodes. This difficulty was experienced for runs at high current or long run times (see Figure 11).

4. Arc mislocation--this problem is discussed in section 8.1.4. Figure 12 illustrates a case where the arc struck to the electrode support struts, Figure 13 to a cable, and Figure 14 to the lower tunnel wall.

5. Arc collapse--extinguishment of arc due to displacement of the arc characteristic beyond power supply capability (see section 8.1.2).

6. Excessive column fluctuation--this problem is discussed in section 8.2.

These phenomena are strongly influenced by experimental conditions such as electrode geometry, free-stream pressure, arc current and voltage, and magnetic field strength. In order to avoid these difficulties, it was first necessary to conduct exploratory tests to locate the envelope of satisfactory experimental conditions. These exploratory tests will be mentioned from time to time herein, but will not be discussed in detail.

CHAPTER VI

APPROACH TO ARC CONFINEMENT

Although confinement is only one factor in arc stabilization, it was the added instrumentality essential to making arc research in the wind tunnel possible.[82]

The experimental approach used to confine the arc for the present investigation is based on the use of rail electrodes and a non-uniform magnetic field. The magnetic field is perpendicular to the electrode plane and the free-stream. The field coils are placed such that there is a monotonic increase in magnetic flux density from the upstream end of the rails. With this scheme of confinement the hope was that the plasma column generated by the exploding wire between the upstream ends of the electrodes, where the magnetic field is weakest, would be convected downstream to a point where the magnetic induction would be sufficient to provide a condition of stable equilibrium between the aerodynamic force and the Lorentz force.

Smith and Early (see section 4.2) observed a dominant tendency for a low-current arc to follow the low density, low velocity boundary-layer around a supersonic mainstream, in some cases forming a column of length many times the distance between electrodes. In addition to the boundary-layer question, there is also the problem of avoiding excessive lateral fluctuation of the column relative to the flow direction. Some investigators using the rail-accelerator approach have made use of guide walls which prevent sidewise bulges in the column. The effects of these guide walls on arc behavior have been shown to be profound (see section 4.1.3.3). Fréchant[21] showed that the use of guide walls with slits open to the atmosphere results in more regular arc movement than guide walls without slits. Fréchant also showed that even with slits, changes in the distance between guide walls result in changes in arc velocity.

Magnetic fields have been employed in a variety of cases for the stabilization of moving arcs.[83-85] Moreover, for a high-current electric arc, even without magnetic stabilization, there can be large magnetic effects due to the field from the input power cables.[2]

In principle the use of magnetic fields for wind-tunnel confinement of an electric arc requires merely the provision of a magnetic field directed such that $\underline{B}$, $\underline{j}$, $\underline{v}$ form a positive orthogonal triple. The magnetic Lorentz force on the column can then balance the aerodynamic resistance force. There are two basic difficulties in the application of this principle.

First, unlike the rail-accelerator approach, where a balance between aerodynamic and magnetic forces is achieved through the mechanism of column acceleration, the wind tunnel approach requires that the balance of forces be achieved through provision of the correct flux density. The required flux density, however, cannot be calculated, and is in fact one of the items under investigation.

Second, as with all forms of confinement, there must be more than a balance of forces, there must be a stable balance.

The approach which was taken here to the solution of the confinement problems mentioned above can be itemized as follows:

1. To prevent arcing through the tunnel boundary-layer, the electrodes were completely within the uniform supersonic free-stream, the electrodes were insulated from the supporting struts (Figure 11), and the supporting struts were mounted on opposite tunnel walls (Figure 12).

2. It was decided to take no special steps to prevent excessive lateral bowing and fluctuation of the positive column until the nature of the problem could be determined experimentally. The electric field from the electrodes will appear, looking downstream, similar to that of an electric dipole, with greatest intensity between the electrodes. Since the arc column tends to follow lines of maximum intensity, this field should exert a restraining influence on sidewise excursions of the positive column. It had been shown[14,15,55] that this restraining influence does <u>not</u> prevent sidewise bowing, bulging, and looping of the column in the rail-accelerator experiments; but the causes of this behavior had not been found, and there was no certainty that bowing would be observed in the wind tunnel experiment.

3. To discourage arcing to the wind tunnel walls, the external arc circuit was kept electrically ungrounded.

4. Rather than mount the electrodes in a region of uniform magnetic induction and attempt a precisely correct choice for the magnitude of B_y necessary for dynamic equilibrium, it was decided to mount the electrodes in a region of continuous variation in B_y (Figure 14). In this way, a given field-coil configuration and current correspond to a range in B_y, and the likelihood of correct choice for the coil current is greatly increased.

5. To provide a balance of forces stable to streamwise perturbations in arc location, the rail electrodes were placed relative to the external field coils such that there was a monotonic <u>increase</u> in B_y in the downstream direction.

CHAPTER VII

EXPERIMENTAL SET-UP

7.1 INTRODUCTION

The experimental set-up consists of two rail electrodes mounted in a supersonic wind tunnel, oriented in a vertical plane parallel to the free-stream (Figures 12, 16, and 17).

External coils provide a transverse magnetic field essentially perpendicular to the plane of the electrodes (Figure 13). The arc is initiated by means of an exploding wire (see Figure 16) between the upstream ends of the rails. Energy is supplied through the electrodes to the resultant plasma by an external circuit consisting of a large d-c generator connected in series with a ballast resistor (Figure 18). The same generator supplies power to external field coils which are energized about three seconds prior to arc ignition.

7.2 ELECTRODES

Each electrode is a cone-cylinder about six inches long, with a $7\frac{1}{2}^{o}$ half-angle cone and $\frac{1}{2}$"-diameter cylinder (Figure 11). The electrodes are connected electrically to insulated stranded cables which extend downstream from the electrodes and out through Plexiglas ports in opposite sides of the tunnel (Figure 16).

The cone angle of $7\frac{1}{2}^{o}$ was chosen to limit the disturbance to the flow. It produces a very weak conical shock at M = 2.5, the shock angle being within about 1^{o} of the Mach angle (see Figure 19 a, b and c). Figure 20 shows a pressure distribution which typifies cone-cylinders. Figure 19 includes a Schlieren photograph (through Plexiglas), showing the flow at M = 2.5 and a schematic drawing taken from the photograph.

The length of the electrodes was made roughly equal to the test rhombus length. The electrodes are uncooled, and the electrode diameter was, consistent with structural considerations, minimized to allow tunnel starting at low Mach numbers.

Photographs of the electrode assembly and installation are shown in Figures 21 and 22 respectively.

7.3 ELECTRODE SLEEVES

A one-inch brass sleeve separates the base of the electrode from the support strut (Figure 21). This sleeve is insulated with Teflon, and serves to prevent damage to the struts caused by multiple arcing.

7.4 ELECTRODE SUPPORT STRUTS

The support struts (Figures 11 and 21) have leading-edge half-angles of 5^{o}, and will therefore maintain shock attachment down to $M \sim 1.3$. The struts are mounted from Plexiglas windows and are thus insulated from the tunnel structure and the electrodes.

7.5 WIND TUNNEL

The 4" x 7" supersonic wind tunnel is a blow-down type with Mach number variable between 1.4 and 4.0 and with run times around two minutes.[86] It has a 4" x 4" test section which exhausts into the top portion of a 4" x 7" channel (Figure 12).

This wind tunnel has been used for studies of supersonic jet mixing,[87] for which a second supersonic stream exhausts into the lower portion of the 4" x 7" channel. For the present investigation this lower channel has been plugged (Figure 12).

The expansion fan from the channel enlargement crosses the flow downstream of the electrodes, which are mounted in the uniform supersonic flow of the test rhomboid (Figure 12). The uniformity of the flow is shown in Figure 23.

The side walls of the tunnel consist of large 3/4"-thick windows which extend from the throat downstream past the test rhomboid, allowing optical observations of the flow in any part of the nozzle not obscured by external apparatus (Figures 16, 17, and 23).

For the present investigation, the walls (or windows) are made of Plexiglas to allow simple installation of pressure orifices when needed, to facilitate installation of electrode support struts, and to avoid problems which might result from thermal stresses if the walls were of glass. The Plexiglas windows reduce the effectiveness of Schlieren photography, especially in areas which ablated slightly due to heating during early high-current runs.

For normal photography, the Plexiglas is quite satisfactory, and high-speed motion pictures (Fastax) of the arc over a fairly wide angle are made possible by the large windows (Figure 17).

The tunnel is so constructed that it is possible to mount the 13"-diameter field coils flush with the outside surfaces of the windows (Figure 17).

For the present investigation, parallel controls for the downstream quick-opening valve of the wind tunnel were installed in the arc control panel (Figure 24).

7.6 FIELD COILS

The electromagnet consists of two coaxial coils, located on opposite sides of the tunnel, Figures 16b, 17, and 25. Each coil contains eleven pancake segments. Each pancake is one inch thick, about 12 inches in diameter, with a three-inch hole through the center. The pancakes are connected in series electrically, but are connected to the cooling-water supply in parallel. Each consists of twenty turns of 3/8" x .065" copper tubing, and is capable of carrying at least 2400 amps of continuous current without overheating. The copper tubing is insulated with plastic tubing, and each pancake is held in shape by epoxy resin.

The distance between the two external field coils, including end plates, is about six inches. The maximum flux density on the tunnel centerline is about 6400 gauss with 2000 amps flowing through the coil. The flux density was found to be proportional to the coil current over a wide range of current and at several points in the test section; a sample curve is given in Figure 26.

The calculated variation of B_y, the transverse component of magnetic induction, is given in Figure 14. Measured values of B_y are given in Figure 15.

The field coils are so mounted that they can be placed in various streamwise locations. Thus the location of the peak induction can be moved relative to the electrodes and/or test rhomboid.

The electrodes are mounted upstream of the coil centerline (Figures 14 and 17) to provide a variation in B_y along the rails (see Chapter VI).

7.7 GENERATOR

The arc power supply is a d-c generator, Figure 27a, rated at 600 v and 1600 amp. For the present investigation it is connected for self-excitation. Its characteristic is quite flat out to 2400 amp at 600 v terminal.[82] The generator field rheostat provides fine control on terminal voltage in the arc circuit.

A double-pole, double-throw knife switch (Figures 27a and 27b) was installed in the generator armature circuit, to allow switching of the generator from the Ward-Leonard circuit of the low-speed wind tunnel, for which the generator was originally installed, to the arc circuit, Figure 28. A four-pole, double-throw switch, Figure 27b, is used to switch the generator field windings to series connection and self-excitation, for use with the arc circuit, Figure 28.

Power from the generator house is brought to the tunnel room through 1500 MCM cables which connect directly to knife switches just inside the tunnel room, Figure 29a.

7.8 BALLAST RESISTORS

The ballast resistors for the arc and coil are identical (see Figure 29b). Their grids are cooled by radiation and convection. Possible values of resistance are from about .01 ohm to about 1.3 ohm. These resistors provide a simple means for changing arc current and coil current independently.

7.9 ARC POWER CIRCUIT

The arc power circuit is shown schematically in Figures 18 and 28. Since the wind tunnel is grounded, the power circuit is left ungrounded to lessen the likelihood of arcing to the upper and lower tunnel walls. Safety features incorporated into the power circuit are discussed in section 7.10 below.

It should be noted that the choice of sizes for the cables of the power circuit was based on intermittent operation. There is a definite limit on the time a given branch of the circuit can be operated. This limit depends on the current, but was in no instance restrictive.

7.10 CONTROL CIRCUIT

The control circuit designed and developed during this investigation is shown in Figure 28.* Safety features incorporated in the main circuit include the following:

1. Two circuit breakers, Figures 18, 27b, and 28.

2. A double-pole, double-throw armature switch which makes it impossible to supply power to low speed tunnel (for which the generator was originally intended) and the arc at the same time, Figure 28. Interlocks are installed to make it impossible to energize either branch of the power circuit from the wrong control panel.

3. Two knife switches, mounted overhead in the supersonic tunnel room, provide visible assurance of safety during coil, ballast, or electrode changes, Figure 29a. These switches are not intended for breaking the circuit current, of course.

In addition to providing control for the circuit-breakers and indicating circuit current and voltages, the control panel, Figure 24, provides for operation of the supersonic tunnel. It also provides that the Fastax camera, the recording oscillograph, the manometer pressure-switch or guillotine, and the Schlieren camera can all be operated automatically at the appropriate times during the run. Safety features of the control system include the following:

1. Three stages of shutdown switching. The first makes use of the circuit breakers. But since the circuit breakers operate on d-c voltage from the generator itself, situations can be envisaged where they would be inoperable. The other two stages enable the operator to interrupt the generator field circuit or to shut down the synchronous motor.

2. When the knife switches in the tunnel room are closed in preparation for a run, appropriate signals automatically warn personnel in the tunnel area and the power house.

3. An interlock with indicator light prevents operation of the main breaker when the cooling-water-flow to the electromagnet is insufficient.

4. The principle components of the arc firing circuit, Figure 28, are:

   a. a key-operated switch;

   b. a timer switch which can be set for run-times of from zero to 60 seconds;

   c. a "dead-man" arc-operate switch;

   d. a time-delay relay to provide about a one-second delay before the main breaker closes.

---

*This circuit diagram is included here in the interest of completeness and should not, of course, be used as a working diagram during further phases of the investigation, since circuit modifications are rather frequent for an investigation of this nature.

7.11 SEQUENCE OF OPERATION

The sequence of operation using the parallel power circuit was as follows:

1. Establishment of supersonic flow in the tunnel test section and settling of mercury manometer columns.

2. Energizing of external magnetic-field coils through closing of main breaker (see Figures 18 and 28).

3. Energizing of arc circuit through closing of arc breaker (see Figures 18 and 28). With the proper field coil location, field coil current and tunnel stagnation pressure for the given Mach number, arc current, and arc length, these three steps result in explosion of the firing wire (Figures 16a, 16b, and 23), the formation of a plasma, and the movement of this plasma down the rails to the point of dynamic equilibrium, where a stable arc configuration is established and maintained until the arc current is shut off with the arc circuit breaker.

7.12 OSCILLOGRAPH

Measurements of current and voltages were made using a modified light-beam oscillograph, Visicorder Model 1508 (Figure 24). The standard galvanometer block for this instrument has insufficient insulation to withstand the voltage surges associated with the use of rotating machinery. For this reason a special mounting block was fabricated from cloth-phenolic, and galvanometers manufactured by Hathaway Instrument Company were mounted thereon (Figure 30a). These galvanometers are rated for 2500 volts channel-to-channel and channel-to-ground, compared to the 500-volt rating on the standard Visicorder galvanometer-block.

Initial tests with Hathaway galvanometers resulted in a gradual decrease of the intensity of the trace made on the oscillograph paper (Figure 56, for example). It was determined that this was due to a yellowing of the light reflected from the galvanometer mirror, and that this yellowing was caused by the ultra-violet light used as a light source in the Visicorder but for which the Hathaway galvanometers were not designed. The manufacturers were ultimately successful in modifying these galvanometers so that they could be used with ultra-violet light without any significant loss in intensity.

With this modification, the Hathaway galvanometers gave very satisfactory results. These galvanometers are, however, considerably more dangerous to use, since the terminals are exposed (Figure 30a). For this reason the galvanometer input-plug was chained to the Visicorder chassis in such a way as to make it impossible to open the instrument (for setting zeroes, for example) without unplugging the galvanometers (Figure 30b).

The frequency response for the galvanometers used for voltage measurements was 1200 cycles/second, and for the current measurement was 800 cycles/second. The internal resistance of the current galvanometer was about 1 ohm, and the use of this galvanometer with an 80-millivolt shunt for current measurement resulted in more variation of calibration constant than would be desirable; this variation was probably due to the fact that the total circuit resistance was so low that minor variations therein could have an appreciable effect on the calibration constant. Much of the scatter

observed in the measurements of arc current and coil current (and therefore of magnetic induction) is believed due to these considerations. A higher resistance galvanometer would appear more suitable to the measurement of current, although the frequency response is somewhat lower.

The paper speed of this instrument is variable from .1 to 80 in/sec. Most of the data taken during the initial attempts to establish the arc were taken at 80 in/sec. Later runs were generally made at 10-20 in/sec.

7.13 GAUSSMETER

The measurements of the magnetic induction from the external field coils were made using a Bell Model 120 gaussmeter (Figure 24). The probe was mounted on a simple traversing mechanism designed for this purpose.

7.14 HIGH SPEED CAMERA

The camera used to obtain high-speed motion pictures of arc behavior was a 16 mm Fastax, Model W163269. The aperture generally employed was f/16. For most runs the camera was synchronized to begin about .4 seconds before arc initiation, and to stop about .4 seconds after arc initiation. The camera speed at the beginning of most runs was about 4000 frames per second, and at the end about 7000 frames per second. No filters were used for the photographs included herein. The film type was usually DuPont 931A. Some good results were obtained using Kodochrome II KR430 with f/5.6 at speeds of from 4000 to 7000 frames/sec.

CHAPTER VIII

EXPERIMENTAL RESULTS

8.1 ARC ESTABLISHMENT

8.1.1 Introduction. The conditions, if any, under which the planned approach to arc confinement would be efficacious could not be predicted a priori because they depend upon the unknown column mechanisms which were under investigation. Initial tests, therefore, were concerned with experimental study of the transient processes which occur during the establishment of an arc.

These initial tests of arc establishment were made with the arc electrodes connected in series with the external field coils. For series operation, the starting fuse-wire must be sufficiently large to allow the current to build up before arc initiation to a point where the external field is sufficient to prevent convective extinguishment of the nascent arc. Three problems in arc establishment are described in the following sections. Confinement of the established arc is discussed in section 8.2. Observations of the stably-confined arc are presented in section 8.3.

8.1.2 Arc Collapse or Blowout. For many runs arc collapse occurred at the beginning of the run--that is, the arc was never fully established. For a few runs the arc was extinguished after seemingly stable conditions had been attained. Arc collapse in almost all cases could be obviated by lowering the free-stream stagnation pressure, or strengthening the external magnetic field. (It was later found that arc collapse can result from the use of an insufficiently large fuse-wire, even when the external field is completely established by a parallel circuit before arc initiation.)

Figure 31a shows the voltage-current time history for arc collapse. The current through the field coils is seen to be only about 500 amps when the voltage buildup signals arc initiation. The external field is too weak to prevent arc blowout. The arc current goes to zero while the electrode voltage goes to the terminal value.

Figure 32 shows Fastax photographs of the first part of a run which resulted in arc collapse. It can be seen that the arc is blown off the downstream end of the rails. Figure 33 shows a similar run where the arc reestablished between the power cables at points where they pass out the tunnel through Plexiglas portholes (see Figure 17). In this case the arc passes through the lower tunnel boundary-layer in much the same way as the arc observed by Smith and Early.

The arc length is much greater than the shortest distance between the electrode cables, and the column shows considerable fluctuation. The electrodes used for this and other early feasibility runs were of rectangular cross-section (see Figure 34).

8.1.3 Excessive Arc Power. For the proper conditions the arc will be established and confined. Figure 31b shows a voltage-current time history for this case. It is seen in this figure that there is an initial buildup of arc (and coil) current to about 1000 amps with little increase in electrode voltage. During this buildup the firing wire remains intact while the magnetic induction increases with the current. Next there is a rapid buildup in arc voltage, signaling arc initiation. The arc voltage increases to a value very near the characteristic of the external circuit. After this the arc evidently traces out a portion of its static voltage-current characteristic until it intersects the characteristic of the external circuit at the point of Kaufmann stability.

For this run the arc power input was great enough to cause flow-reversal in the boundary-layer on the lower tunnel wall. In such cases, the arc shows considerable fluctuation in column and root location and in voltage and current.

The limits on test conditions imposed by thermal blocking are discussed in Appendix A. Figure 35 shows Fastax photographs of an arc where the value of W/P_{t_1} was about 60 per cent over the separation limit. The column instability is clearly evident in these pictures.

8.1.4 Arc Mislocation. Figure 31c shows the time history of a run where the arc power was so great that flow-separation apparently occurred far enough upstream for the lower electrode to be immersed in reversed flow. This reversed flow caused the arc to strike momentarily from the electrode tip to the lower tunnel wall (Figure 9b).

In this case it can be seen from Figure 31a that the arc at first traced out a voltage-current path similar to that for arc blowout. But here the arc is blown in the upstream direction, finally striking to the lower tunnel wall. It then begins to trace out a portion of the characteristic for a new arc configuration. This new configuration, however, adds less energy to the flow and results in changes in the velocity field which extinguish it, causing the time history to follow a trace which is again similar to that for arc blowout. Before final blowout occurs the arc power again rises to a point where some new arc configuration begins to establish itself, so that the voltage dips downward slightly. But this new configuration is not sustained either, and the time history then traces a final blowout trajectory. Fortunately it was found that the tunnel-flow extinguished this arc before significant damage could be done to the tunnel wall (Figure 9b).

8.2 MODES OF CONFINEMENT

8.2.1 Introduction. Initial test runs with the arc and field coils in series established that currents over about 1200 amps result in levels of arc energy-addition too high for undisturbed tunnel-flow (see Appendix A). In order to operate at lower arc currents and yet maintain high currents through the external field coils, the arc power circuit was revised to allow operation of the arc in parallel with its field coils. This revised circuit has been described in section 7.9, and is shown in Figure 18. With the parallel circuit the external field is established a few seconds before the arc breaker is closed, so that firing-wire size is not as critical as with the series circuit. Initial tests also led to several changes in the design of the electrodes, electrode mounts, and windows. The design described in Chapter VII incorporates these changes.

Figure 31d gives the voltage-current history of an arc with a steady-state current around 300 amps between electrodes of the latest design. Here the power is low enough so that there is no disturbance to the supersonic free-stream ahead of the arc. Current to the field coils is about 2000 amps. Runs such as this, which resulted in arc confinement in undisturbed supersonic flow, can be divided into three categories according to root location.

8.2.2 Root Strikes to Anode Tip. Fastax film shows these runs are characterized by lateral fluctuations in column location which are accompanied by large fluctuations in arc voltage ($\pm$ 15%) and by acoustical noise which can be heard above the wind tunnel noise. Figure 36 illustrates the appearance of the anode tip after such a run.

Figure 37 includes a corresponding cathode mark. Figure 38 is a high-speed film sequence of a tip-strike run. In Figure 38 the upper electrode is the cathode. The anode root strikes to the tip of the anode, while the cathode root strikes somewhat downstream. It can be seen that the arc column is highly unstable and diffuse.

For an anode-tip strike with carbon electrodes, the thermionic site at the cathode moves slowly upstream (during the first half-second of the run) to a point where it remains for the rest of the run. If a flow-baffle is placed on the cathode for an anode-tip-strike run, the cathode site is established at its ultimate location and does not move upstream.

It is found that if the field coils are moved downstream sufficiently, or if the free-stream stagnation pressure is increased sufficiently, the anode root will strike downstream of the shoulder of the electrode cone tip.

8.2.3 Root Strikes to the Cathode Base. These runs are also characterized by fluctuations in the column location and arc voltage ($\pm$ 10%), and by acoustical noise. Figures 39-42 illustrate the appearance of the cathode after base-strike runs. Figure 39 includes the corresponding anode. Figure 43 is a typical oscillograph record, and Figure 44 is a typical Fastax sequence for a base-strike run. In Figure 44 the cathode is the top electrode. The column fluctuations are obvious. If Teflon washers are placed around the cathode (Figure 42), the root location remains at the base. This behavior indicates that root convection is not the cause of the downstream root location. If a knife-edged cathode is used, the root will remain at the base (Figure 40); if saw-tooth ridges are cut in the cathode (Figure 41), the root still remains at the base. These runs indicate that electric field concentration at the base is not the cause of the downstream root location. The magnetic flux density can be varied over a wide range--for example, from about 700 to about 3000 gauss--without causing either the roots to move upstream or the arc to extinguish. If the flux density is zero, the arc cannot be established. But if the flux density is raised enough, or the pressure lowered enough, the roots will strike upstream of the electrode base.

These observations indicate that arc confinement in this mode is based on dynamic processes in the positive column. The (unsteady) mechanism is probably related to arc curvature and dependent upon the "fringing" electric field in the base region in a manner similar to that suggested by Rother[40] and Thiene.[41] In the present case, however, an external magnetic field is also present and exerts a stabilizing influence on the column.

From measurements in this mode of arc confinement, no inference can be made of the relation between magnetic induction and the velocity of an arc column moving through a two-dimensional electric field.

8.2.4 Root Strikes Along Electrode Cylinders, Upstream of Base and Downstream of Cone. In this case the arc column shows little or no lateral fluctuation, little voltage fluctuation ($\pm$ 4%), little current fluctuation, and no audible noise. Teflon flow-baffles have no effect on ultimate cathode root location, indicating that confinement is due to column processes. If the external coils are moved in the streamwise direction, the arc roots will follow that motion, provided they can do so without striking to the electrode tip or base. Thus the confinement in this mode is based purely on the external magnetic field.

Changes in electrode material among OFHC copper, carbon, and brass, have no measurable effect on stable arc location. For the run with steel electrodes there was more instability in root location, indicating a marginal base-strike due to local decrease in the magnetic induction (see Figure 55). For plain copper (not OFHC) it appears to be impossible to establish the arc on the rails, though this point was not investigated thoroughly.

Figures 45-55 show typical marks left by the arc root in this pure-magnetic mode. Figure 56 shows a typical oscillograph trace, and Figures 57-60 show typical Fastax sequences taken from runs of this type. The high stability of the arc column when stabilized in the pure-magnetic mode is discussed in more detail in section 8.3.

For OFHC copper electrodes the cathode root usually occurs at spots (points B and C, Figure 61) near the far side of the cathode, away from the anode. Figures 46 and 48-51 show the cathode appearance after such runs. A tendency for the cathode root to strike on the far side is also noticeable for other electrode materials. For carbon cathodes, the root can be seen occasionally to dart around to the far side, only to be re-established immediately at a thermionic site on the near side (point A, Figure 61).

It is believed that the tendency to strike to the far side of the cathode is due to the slight streamwise component of the magnetic induction which exists at points to the side of the center plane (Figure 13). When the cathode root makes an excursion to either side of this plane, it moves into a region where the streamwise component is finite. There is then a force on the root tending to move it farther toward the far side of the cathode (Figure 61). This same induction component also exerts a force on the column, tending to hold it away from the electrode (Figure 61).

In the case of carbon, the near proximity of the column eventually results in sufficient heating of the near side of the cathode (point A, Figure 61) to establish a thermionic site there. For copper, there seems to be a similar tendency though it is seldom manifest. In this case the new root moves, perhaps aided by an oxide layer, from B past A to an opposite far-side point, C. Motion of the root around the cathode is accompanied by fluctuations in the column. Figure 58 gives a Fastax sequence which shows a case where the cathode root moved from point B to point C. For this run the transfer occurred about half-way through the run.

Results of the measurement of arc properties in this pure-magnetic mode of confinement are discussed in section 8.3 below.

8.3 THE STABLE ARC

8.3.1 Introduction. The subjective sensation of firing an arc of high stability is similar to that of switching on a bright light. There is no sound above the usual sound of the wind tunnel, and there is no flicker in the light. It is immediately obvious that this was a stable arc.

Confinement in the stable mode is discussed in section 8.2.4 above. Figure 60 is a sequence from the Fastax motion picture of a stable arc. The conditions for the run are as follows:

I = 132 amps

Arc voltage = 147 volts

Interelectrode spacing = 1.1 inches

Electrode material: OFHC (oxygen-free high-conductivity) copper

Firing wires: Two AWG 26 bare copper

Run time: 0.8 seconds

Mach no. = 2.5

Dewpoint of air supply = -60°F.

Free-stream stagnation pressure = 20.2 in. Hg

Cathode root location = 0.6" upstream of electrode base

Cathode root induction = 4300 gauss

Anode root location = 0.3" downstream of cone shoulder

Anode root induction = 1380 gauss

Figure 48 shows the cathode root mark for this run. It can be seen that the cathode root struck to the far side and remained there throughout the run, as shown by the complete Fastax film, of which Figure 60 shows the first part. Figure 56 is the oscillograph trace from this run. It is seen that the voltage fluctuations are about three per cent. The outstanding characteristic of these data is the extremely stable nature of the arc positive column. The flutuation in voltage is very small for a convective arc. The spatial fluctuation of the column is so slight that if it were not for the obvious slant, it would be difficult to determine from the motion picture alone that the column is immersed in (supersonic) flow. From the motion picture there are no observable sidewise fluctuations in the column, and it appears certain that what fluctuations exist must be less than a few per cent of the diameter. The fluctuating loops which were observed by Angelopoulos[23] to form "in all directions," or the spirals which were reported by Féchant,[21] are properties of the convective arc which do not necessarily carry over to the wind-tunnel experiment.

Figure 62a is a single frame from the Fastax film. The anode root (bottom) is seen to be contracted for a distance of perhaps $\frac{1}{4}$-inch above the anode surface. The cathode root (top) is also contracted, and is striking to the far side. The photographs indicate there are occasional vapor-jets which appear to spew out normal to the cathode surface from the cathode root, Figure 60; but the appearance of the cathode after the run, Figure 48, indicates that the amount of material involved must be quite small.

8.3.2 Column Slanting. One of the most noticeable characteristics of the stable arc is the slanting of the positive column. Figure 52 shows root locations of a run where the cathode was the top electrode, and Figure 53 shows root locations of a

similar run where the cathode was the bottom electrode. In both cases, the cathode root is downstream of the anode root.*

Measurements of root location indicate a well-defined angle of arc slant repeatable within about 5°. The Fastax photographs (see Figures 60 and 62a, for example) confirm the fact that the column is slanted and is approximately straight. The apparent angle of slant, of course, is foreshortened in the photographs by the fact that the photographs are made from a position almost directly upstream of the arc.

Figure 62b is a photograph made with a SpeedGraphic camera (with Polaroid back) of the reflection from the glossy surface of an opaque black Plexiglas window, which shows the arc from a position almost directly to the side. This photograph also demonstrates that the column is definitely slanted and is approximately straight, despite variations by a factor of 2 in B_y and presumably $\omega_e \tau_e$ along the straight portion (see section 9.3.3). The slant angle from this photograph is foreshortened somewhat, but not as much as for the Fastax photographs.** Figure 63 shows a plot of measured slant angle θ_s versus arc current, and Figure 64 shows θ_s versus free-stream stagnation pressure for M = 2.5. It can be seen that there is no variation in slant angle with either current or pressure.

Figure 65 shows the range of slant angles measured at M = 2.5 and M = 2.0. It is seen that the arc follows a path very nearly parallel to a free-stream Mach line.

A discussion of some possible causes of slanting is given in section 9.3.

8.3.3 Column Geometry. It can be seen from Figures 62a and 62b that the positive column of the arc appears to be approximately straight and to have no tendency to extend in the downstream direction through its own heated wake. This observation is confirmed by the concentrated nature of the electrode markings generally left by the stable arc root (see Figures 45 and 46, for example).

The arc width and its variation with the interaction parameters is discussed in section 8.3.8.

8.3.4 Stabilizing Induction. Figures 45 through 54 show examples of the markings left by the arc roots on the electrodes. It is clear from these photographs that root location can in most cases be positively determined after the run. The magnetic induction at the arc roots can then be determined from measurements made of the external induction without the arc (see Figure 15), since the induction at the cathode surface due to the current in the electrodes is in all cases not more than five per cent of the external induction. From this the induction required for dynamic equilibrium in the arc column can be determined.

Since the column is slanted across lines of equal magnetic induction, the induction measured at the anode root is less than that at the cathode root. The average between anode root and cathode root induction appeared to be more significant to the equilibrium than either alone.

---

*With the cathode located below the anode, a longer time was required for the root to come to its ultimate location. This delay is probably due to slight asymmetries in the magnetic field and electrode location.

**Although the photographs of Figures 62a and 62b were taken from the same side of the tunnel, the arcs appear slanted in opposite senses due to the prism used on the Fastax camera.

For two comparable runs, one with a 0.6" inter-electrode gap located in the upper half of the test section and the other with a 0.6" gap in the lower half of the test section, the arc column did not follow along a single line as it would be expected to do if fixed to the magnetic field. For the low gap run and the high gap run the arc struck at about the same streamwise location, indicating that the value of the column induction is more important to the equilibrium than any particular location in the magnetic field.

8.3.5 Effects of Electrode Material. Figure 66 is a plot showing the cathode root induction B_c required for column confinement as a function of the free-stream stagnation pressure, P_{t_1}. It will be noted that this figure contains data obtained using cathodes made from copper, carbon, steel, and brass--materials which for the rail accelerator set-up would cause variations in velocity by factors$^{5-20}$ of up to five. Yet the points in Figure 66 define a single curve. The equilibrium location for the thermionic site for carbon agrees very well with that for the cold OFHC copper, for example, despite the great difference in cathode mechanism. These data indicate that confinement in the pure magnetic, or stable,mode is independent of root phenomena.

This does not mean that root effects can be completely ignored, of course. It is clear, for example, that if the cathode were coated with a thick insulator, the arc could not be established regardless of the magnetic induction. Thus, in this extreme case, root effects would be dominant. It is also true that with "plain" copper electrodes it seemed impossible to confine the arc in the pure magnetic mode, though no concerted attempt was made to prove this. For the one run with steel electrodes, the electrode markings (Figure 55) indicate that the roots oscillated between the base of the electrode and the position for pure magnetic confinement. This behavior indicated a marginal (unstable) base-strike, perhaps caused by the weakening of the magnetic field due to the presence of the steel. Thus it is only for the stably-confined arc that root location is independent of electrode material.

Figure 47 shows the electrode markings from three runs which were made to determine if the downstream cathode-root location (column slanting) is caused by convective forces near the cathode surface. It is clear from this figure that the downstream location is not due to surface convection. Figure 47a shows the root location with no flow-baffles. Figure 47b shows the root location with a single baffle at the cathode cone. The root location for the two runs is the same, within the accuracy of electrode positioning. Figure 47c shows the root location for a run where three flow-baffles were placed on the cathode. For this run, the field coil (and arc) current was somewhat higher than expected, and the arc location was upstream of the planned location; rather than just downstream of the third Teflon baffle, the cathode root struck almost exactly at the baffle and destroyed it. It must be concluded from Figures 47a, b, and c, that flow conditions at the cathode surface have little to do with cathode root location. This, along with the fact that root location is independent of electrode material, lead to the conclusion that the confinement mechanism is dominated by processes in the positive column.

8.3.6 The Effect of Pressure. Figure 67 gives a plot of average induction versus free-stream stagnation pressure for constant current at M = 2.5, and shows, as does Figure 66, that the induction required increases with the pressure. This result seems logical since the aerodynamic forces on the column would be expected to increase with free-stream pressure. However, it should be kept in mind that, unlike solid bodies, the electric arc can change its structure with ambient conditions so that logic based on conventional aerodynamic configurations is not directly applicable.

8.3.7 The Effects of Current. Figure 68 shows the magnetic induction required for pure magnetic confinement as a function of arc current.

Dashed lines of constant BI are shown. Since the data points indicate conditions where the aerodynamic force equals the Lorentz force, it is seen that the aerodynamic force decreases with decreasing current throughout the given range of current.

Secker and Guile observed[13] that the magnetic induction for a given velocity of motion was apparently independent of current for the column as well as for the roots. Although this observation was made for low speeds, it is interesting to note that it agrees qualitatively with the data of Figure 68.

8.3.8 Arc Width. Since from Figure 68 the aerodynamic force on the arc increases with arc current, it seems reasonable to expect that the arc diameter must also increase with current. Although no accurate measurements could be made of the actual width of the conduction zone, it was possible to obtain very rough estimates of the arc width from Fastax photographs. Figure 69 shows the variation of this rough luminosity width, d_L, with arc current. Within the accuracy of the measurement, the width is proportional to the arc current. It will be seen below that arc current is proportional to the power density in the column, and thus a plausible proportionality between column width and power density exists (see section 8.3.9).

Figure 70 shows that the arc luminosity width decreases with free-stream pressure, as might be expected.

Figure 71 gives a plot of luminosity width versus $\frac{B_{av} I}{p_{t_2}}$ for a range of pressure and current. It is seen that this relationship appears experimentally to be a linear one.

8.3.9 Voltage-current Characteristics. Due to the stability of the column in the pure-magnetic mode of confinement it is possible to make meaningful measurements of the column voltage gradient. Figure 72 gives the voltage-current characteristics for the stable arc on carbon electrodes at M = 2.5 and P_{t_1} = 20" Hg. After correction for column slant, these data indicate, for P_{t_1} = 20" Hg and M = 2.5, a column gradient of 14 volts/cm, independent of arc current. A total fall voltage (anode and cathode) of 30v is indicated. The electrical conductivity of the column is difficult to determine, because of uncertainties in determining column cross-section photographically; but from the data at hand, it appears that the conductivity is around 10 mhos/cm.

CHAPTER IX

CONCLUDING REMARKS

9.1 ARC STABILITY

The extremely stable arc column observed in the present investigation stands in sharp contrast to the wildly fluctuating columns observed in other investigations using the rail accelerator.[21,23,55] It appears likely that this increased stability results from the fact that for the present investigation the arc column was free to seek a stable configuration without constraints imposed by requirements for root motion, whereas for the rail accelerator, the requirements for cathode-root motion are possibly incompatible with stable column movement. Any explanation for the stability observed in the present investigation based on the lower pressure and higher Mach number (compared with the rail-accelerator experiments), would not be satisfactory, since column fluctuations can occur under these same conditions when the arc roots strike at the ends of the electrodes. The evidence that root constraints cause column fluctuations can be cast in terms of the following hypothetical experiment (see Figure 73), which is based on the results of many different experiments of the present investigation: A stable column is established with the arc roots away from the ends of the electrodes (Figure 73b), and with the cathode root remaining on one side of the electrode plane (Figure 60, for example). The column is slanted, the cathode root being nearer the electrode base in streamwise location, and the anode root being nearer the electrode tip. There are no spatial fluctuations. The field coils are now moved slowly in the upstream direction. The column follows this motion. Ultimately, the column location is such that the anode root strikes the anode tip-cone. If the coil is moved farther forward, the cathode root will move forward not quite as much as the coil, the anode root will move hardly at all, and the column will begin to fluctuate (Figure 38, for example). This fluctuation is apparently due to the fact that the column is prevented from assuming its stable (slanted) configuration -- by the requirement of continuity at the anode (Figure 73a). If the field coils are brought back to the original location and then moved downstream, the column follows that motion. When the column location is such that the cathode root strikes at the cathode base (Figure 73c), further motion downstream results in no further motion of the cathode root, little motion of the anode root (after perhaps an initial slip), and fluctuations of the positive column (Figure 44, for example). These fluctuations also appear to result from the fact that the column can not assume the stable configuration and still maintain continuity at the electrodes (Figure 73c).

The indication is strong that the column has a single stable configuration, and that fluctuations result when root constraints prevent it from assuming that configuration. Applied to the rail accelerator, this would mean that column fluctuations could result from root conditions which interfere with the stable column configuration, and not from the lack of a possible stable configuration. This interference might result, for example, from an inequality in the equilibrium velocities of the anode root, cathode root, and column; under this condition, the integrity of the arc would be maintained principally through the ability of the positive column to change in length and geometry readily, and it would be expected that the column would be forced into the unpredictable and complicated fluctuations which characterize rail-accelerator experiments.

In this reasoning, it has been tacitly assumed that for the present investigation there is no effect of root phenomena on the location of the arc when confined in the pure-magnetic mode. This assumption is supported by the experimental evidence (see section 8.3).

9.2 THE SEAT OF ARC MOTION

The present investigation is concerned with the positive column of the arc. The experimental results indicate, within certain fairly loose qualifications, that arc behavior is dominated by processes in the column and that root phenomena play no role. Nevertheless, rail-accelerator experiments have indicated that root phenomena influence strongly the behavior of the low-speed moving arc. These results are not necessarily contradictory. If the cathode root dominates the moving arc through the resistance it offers to the motion of the column, the cathode root would have little effect on column behavior for the present investigation, since no root (or column) motion with respect to the electrodes is necessary. With the rail accelerator, a certain time is required for the transfer of electron emission sites regardless of column tendencies (in the continuous mode); with the present set-up, there is no need for transfer of emission sites.

There appears to be little evidence for the existence of a significant amperian motive force in the root apart from the passive resistance it offers to motion of the column. The experiments of Guile, Lewis and Mehta,[6] where the cathode spot was observed to move in the amperian direction determined by the magnetic field beneath the cathode surface, do indicate a motive force since in some cases the field above the surface was in the opposite direction; but these observations were made for velocities under 10 ft/sec, compared with the 1800 ft/sec of the present investigation. The present results indicate that if a motive force in the cathode root does exist, it is far overshadowed by the requirements for continuity with the positive column.

In summary, in the present investigation the results of variation of cathode root conditions (cathode material and surface flow) and column conditions (free-stream pressure, location of peak induction, and inter-electrode gap), indicate that for pure-magnetic confinement under the conditions investigated, root location and overall arc behavior are dominated by processes in the column. This result does not contradict the results from the low-speed rail-accelerator experiments.

The root independence observed in the present experiment indicates that analysis of arc behavior under these conditions can be based on considerations of the column processes alone. Moreover, the column stability observed indicates that time derivatives can be ignored.

The relation

$$BI/P_t = f(M, Re)d_e \qquad (19)$$

where:

B = magnetic induction

d_e = effective column width

I = arc current

M = Mach number

P_{t_1} = stagnation pressure

R_e = Reynolds number

can be derived from more than one model for the column. The simple solid-cylinder model[21] gives this relation. A column model where the flow pattern just upstream of the column is assumed to be essentially the same as that for a solid cylinder, but where the flow just downstream of the column is assumed sonic, also leads to the above relation. Whether or not one of these, or some other model for the column mechanism is nearest reality, the experimental data of Figure 71 tend to bear out this simple formula, and at least indicate that an important scaling parameter for the convective arc is the dimensionless combination of $BI/P_t d$.

9.3 POSSIBLE CAUSES OF SLANTING

9.3.1 Introduction. Although the determination of the causes for arc slanting must await more detailed measurement of the structure of the stable column, there are several conceivable mechanisms which might affect slanting, and these will be discussed here. It might be well first to itemize some of the fairly certain results or concomitants of slanting:

1. A reduction in the velocity component normal to the arc.
2. The existence of a velocity component tangential to the arc.
3. A reduced pressure near the upstream boundary of the arc.
4. A reduced component of electric field along the column axis.
5. The existence of a component of electric field normal to the column axis.

Four principal observations bearing on the question are the following:

1. The slant angle is equal to the Mach angle at $M = 2.0$ and 2.5.
2. The slant angle is independent of pressure.
3. The slant angle is independent of current.
4. The slant angle changes sign with reversal of polarity.

It is not the purpose of this section to propose a conclusive explanation for slanting. It is, rather, to point out that there are several phenomena which may be involved, and that further observations will be necessary to isolate the cause or combination of causes active.

9.3.2 Fluid-mechanical Effects. It is not clear what fluid-mechanical effect might cause the arc column to slant at the Mach angle, and it probably can not be clear until more is known of the flow pattern. The Mach angle is the angle of lines along which infinitesimal pressure distrubances must propagate. It is also the minimum yaw angle for an infinite solid cylinder without a bow shock. The fact that the slanted arc follows a path parallel to a free-stream Mach line (see Figure 65) strongly suggests that the cause for slanting may be fluid-mechanical in nature (see also section 9.3.5 below).

9.3.3 Hall Effect. The Hall effect is another possible cause for arc slanting. The Hall effect becomes significant when $\omega_e \tau_e$ is comparable to unity (see Appendix B). Since an analysis of Hall effects for a cylindrical plasma geometry is not available, it is not possible to state precisely the functional relationship which might exist between $\omega_e \tau_e$ and the macroscopic behavior resulting from the Hall effect. It is certain, however, that such a relationship must exist, since the macroscopic behavior ultimately derives from microscopic particle trajectories (Figure 78), which are strongly influenced by $\omega_e \tau_e$.

The experimental observations indicate that the Hall effect is probably not the dominant factor in arc slanting: the slant angle does not appear to vary with $\omega_e \tau_e$. For example, the side-view photograph of Figure 62b indicates that the column in the central region, away from the root portions of the arc (see Figure 62a), is straight. Yet this straight portion of the column exists in a region where B_y and presumably $\omega_e \tau_e$ almost double (see Figure 15). This evidence appears to indicate that either the slant angle θ_s is not related to $\omega_e \tau_e$, in which case the Hall effect would be not active at all, or that there must be an additional mechanism which causes τ_e to go down as ω_e goes up, keeping $\omega_e \tau_e$ and θ_s constant along the straight column, in which case the Hall effect could not be considered the sole active factor.

Another indication that the slant angle, θ_s, does not vary when $\omega_e \tau_e$ should vary, is given by the fact that θ_s does not vary with current. The gas temperature varies with arc current[90] and this temperature variation results in direct changes in collision frequency for high temperatures,[89] as well as indirect changes due to the variation in density for a given pressure. Thus, with a Hall effect one would expect variation in slant angle with arc current. But the experimental data of Figure 63 show the angle to be independent of arc current. Figure 68 shows that the arc does not compensate for changes in current (and τ_e) by moving to regions of differing values of B_y (and ω_e).

The fact that θ_s does not vary with P_{t_1} (see Figure 64) is not as significant as might first appear. Even though τ_e should be inversely proportional to the gas density, which might in turn be expected to vary roughly as the free-stream pressure varies, the decrease in τ_e with pressure could well be cancelled by a roughly proportional increase in B and ω_e, which accompanies the downstream displacement of the arc with pressure (see Figure 67).

Finally, it should be mentioned that the observed reversal of slant direction with electrode polarity would be expected if the slanting were related to the Hall effect. As discussed in Appendix B (see equation 29 and Figure 78), the Hall angle is independent of the direction of the electric field; but due to the change in the sense of $\underline{B}$ necessary to maintain an upstream Lorentz force, the Hall angle will change sign with reversal of electrode polarity.

9.3.4 Differential Root Forces. Minorsky,[65] in an early investigation of retrograde motion at very low pressures* in mercury, observed a slanted arc column with the cathode root preceding the anode root. It is well known that the arc column experiences a force in the amperian direction by a magnetic field, even when the cathode root is forced in the opposite or retrograde direction.[12,15,69,75] It might be supposed that in the present investigation a similar phenomenon occurs. This supposition does not appear to be borne out by the experimental evidence. In the first place, if conditions exist for retrograde motion of the cathode spot, then it is very difficult to explain the amperian direction of spot-motion shown by the far-side strikes (far-side relative to the anode, see section 8.2.2); with retrograde spot-motion, the axial magnetic field would tend to cause not far-side, but near-side cathode-root location. It would be even more difficult to explain the arc column slanting observed with carbon electrodes, where the cathode spot was clearly thermionic, since retrograde motion of the cathode spot is not observed with carbon electrodes,[91] and apparently requires a burning-spot mechanism.[72]

Finally, since the retrograde tendency is a strong function of pressure and current, one would expect a variation in slant angle with pressure and current for this mechanism, contrary to observation.

It appears that the only observation with which the retrograde-cathode-root supposition agrees is the direction of slant and its change with polarity.

9.3.5 Leading Edge Ignition. The "ignition" mechanism at the leading boundary of the high velocity arc column is not known. This region cannot be ignored in the consideration of possible causes for arc slanting. To show that this is so, a hypothetical ignition mechanism will be considered. Assume that the ions farthest upstream of the column are created in the gas through photo-ionization due to the absorption of radiation from the column. These ions can exist upstream of the arc even though the flow is supersonic, since they are created by photons which travel at the speed of light.** With electrons upstream, there exists a new possible mechanism for the transport of energy upstream in the supersonic gas flow, namely, electron thermal-conduction.*** The increase in temperature of the precursor electrons could result in additional ionization and increased electrical conductivity in the upstream region, since for at least some conditions the ionization fraction takes on a value corresponding to ionization equilibrium at the electron temperature.[46] As the ion pairs move downstream, the electrons will also take up energy from the electric field.

---

*Minorsky gives little quantitative data in his paper, but for the stated equilibrium temperature of 150° C. for the liquid mercury cathode, the vapor pressure of mercury is about 3mm Hg. From the dimensions of his apparatus and the one oscillogram he gives, it appears that the velocity of motion was around 50 ft/sec.

**Such photo-ionization in air plays a very important role in the streamer mechanism for electric spark formation,[92] which was first hypothesized to explain the extremely rapid spark propagation velocities observed experimentally.

***It has been shown,[93] for example, that in the supersonic flow of an ionized gas, an increase in electron temperature precedes aerodynamic shock waves. A discussion of possible causes for precursor electrons in shock tubes is given in reference 94.

With this assumed mechanism, the conduction zone of the moving arc column would progress by increasing the electrical conductivity of the gas just ahead of the column through photo-ionization and subsequent elevation of the electron temperature through absorption of energy from the electric field and through electron thermal-conduction. Two of the concomitants to arc slanting are the decrease in P_S, the pressure expected at the leading boundary, and the decrease in $E_{//}$, the component of the electric field parallel to the arc column. Now E/P is a well-known similarity parameter for electric discharges. Its importance derives from the fact that it is proportional to the average energy acquired by an electron between collisions:

$$E/P \sim E\lambda \sim eV$$

Since both $E_{//}$ and P_S vary (decrease) with increasing slant angle, θ_S, it becomes of interest to calculate how $E_{//}/P_S$ varies with θ_S. Figure 74 shows the results of a calculation for M = 2.5. P_S was evaluated as that pressure which would exist at the stagnation point of an infinite solid cylinder in frictionless flow. It is seen from Figure 74 that there is an angle θ_E for which $E_{//}/P_S$ is a maximum. This angle is very near that of a free-stream Mach line.

In Figure 65, θ_E is plotted versus Mach number. Two things of interest about this figure stand out: first, θ_E is very nearly equal to the Mach slant $90 - \mu$; and second, the experimentally observed column slant angles, θ_S, at M = 2.0 and M = 2.5, fall near θ_E (though nearer to $90 - \mu$).

The near agreement between θ_E and θ_S may well be coincidental, as may the agreement between $90 - \mu$ and θ_S. Note that though $E_{//}/P_S$ will vary with Pt_1, θ_E (like $90 - \mu$) will not--as θ_S does not.

There are, of course, two angles, equal with opposite signs, for maximum $E_{//}/P_S$. The one observed experimentally happens to be the one for which the parallel component of free-stream velocity is in a direction such that the low-mobility positive ions are forced "downstream" by the parallel component of the electric field, and the high-mobility electrons are forced "upstream," though hardly noticing the counter-movement of the heavy particles.

Determination of the manner in which $E_{//}/P_S$ in the upstream zone determines arc slanting, if it does, must ultimately be based on some knowledge of the flow field and relative importance of competing processes at the leading boundary of the arc.

9.3.6 Concluding Remark. The above discussion of possible causes of arc slanting is of necessity vague in nature. The actual cause could be a combination of these, or it could be completely different, deriving perhaps from the internal structure of the column. Fortunately, a means now exists for the detailed study of the structure of the stable convective column, and thus of the possible causes of slanting.

CHAPTER X

CONCLUSIONS

1. It is possible to confine magnetically, within the free-stream of a supersonic wind tunnel, a stable arc discharge sustained by an electric field essentially normal to the flow vector. A balance of forces on the column is provided by an external magnetic field with monotonic increase in transverse component from electrode-tip to electrode-base.

2. Root location for the stable confined arc is determined by processes in the column and is independent of material or flow conditions at the surface of the cathode. In this pure-magnetic mode of confinement, the arc occurs between the rails in a region where the electric field is essentially two-dimensional, at points determined by the streamwise location of the external field coils and by the conditions in the free-stream.

3. Pure-magnetic confinement is characterized by high spatial stability in the positive column.

4. The supersonic arc is characterized by a well-defined column, rather than a sheet discharge extending in the streamwise direction.

5. In a supersonic flow, the positive column of the stable arc assumes a slanted orientation with respect to the external electric field.

6. The direction of slant is the Hall direction for free-electron conduction:

$$\underline{j} \cdot (\underline{E} \times \underline{B}) < 0$$

7. The angle of slant is <u>not</u> affected by changes in arc current, free-stream pressure, or local magnetic induction (or corresponding changes in the Hall parameter, $\omega_e \tau_e$) by factors of about 2.

8. As determined from root location, the angle of slant with respect to the free-stream at M = 2.0 and 2.5 is equal to the Mach angle, which is very nearly equal to the angle for maximum value of the electric discharge parameter $E_{//}/P_s$ at the upstream boundary of the arc.

9. There are several possible phenomena which could contribute to arc slanting. Further investigation is needed to determine the dominant influence.

10. Only one angle of slant is observed for the stable column at M = 2.5. When requirements for continuity at the roots force the column to depart from this angle, column fluctuations appear. Such fluctuations characterize arcs which strike to an electrode tip or base.

11. The dimensionless ratio BI/Pd_e is a significant scaling parameter for the magnetically-stabilized convective arc.

APPENDIX A

LIMITS ON EXPERIMENTAL CONDITIONS

Many of the limits on experimental conditions for the wind-tunnel approach to convective arc research can be derived in advance. These include (1) limits related to the performance of the wind tunnel alone,[86] (2) limits related to the capability of the electrical power supply and control system,[82] and (3) limits imposed by the union of the tunnel and arc facilities.

Limits of types (1) and (2) for the present investigation are discussed in the cited references; they are outlined in the following table:

Mach number: 0.1 to 0.5; 1.4 to 4.0

Free-stream stagnation pressure: 0 to 30" Hg

Arc current: 0 to 2400 amp

Arc voltage: 0 to 600 v

Arc power: 0 to 1.5 megawatts

Limits of type (3) include those due to simple geometrical considerations:

1. A maximum electrode gap (about $1\frac{1}{4}$ in.) to avoid interaction with the tunnel boundary layer.

2. A maximum electrode length (around 6 in.) to keep within the test rhomboid.

3. A maximum magnetic induction (about 15,000 gauss) due to the tunnel width and structure.

4. A maximum permissible magnitude of column fluctuation (about 2 in.) to avoid arcing to the tunnel walls.

5. A maximum area for the cross-section of electrode and strut (about 0.7 $in.^2$ at M = 1.4 in 4" x 4" section) to allow tunnel starting.

Perhaps the most important limitation peculiar to wind-tunnel arc research is due to thermal blocking or choking of the tunnel flow. This phenomenon limits the ratio of arc power to free-stream stagnation pressure (W/P_{t_1}) for a given Mach number M. This can be shown as follows: assume that the energy from the arc is added uniformly to the free-stream. Then

$$q = W/\dot{m} \cong c_p(T_{o_2} - T_{o_1}) \tag{20}$$

where

W = arc power

$\dot{m}$ = mass flow rate

Q = heat added

C_p = specific heat

T_{o1} = initial stagnation temperature

T_{o2} = final stagnation temperature

The maximum heat addition permitted by the Rayleigh relation for the undisturbed free-stream is that given by

$$(W/\dot{m})_{MAX.} = C_p(T_o^{*H} - T_{o1}) \qquad (21)$$

where $T_o{}^{*H}$ is the stagnation temperature at the point where the Mach number is unity due to heat addition.[95] For a given test-section size the mass flow is a function of Mach number and stagnation pressure. For a 16 in.^{2} test section and T_{o1} = 530°R, the above equation becomes

$$(W/P_{t_1})_{MAX.} = (0.024\ MW/"Hg)\left[(T_o^{*H}/T_{o1})_{M'} - 1\right]/(A/A^*)_M \qquad (22)$$

where $(A/A^*)_M$ must be evaluated at the design test-section Mach number in order to give the proper relation between $\dot{m}$ and M, but where $(T_o{}^{*H}/T_{o1})_{M'}$ must be evaluated at the section where uniform heating is assumed to occur.

For rates of heat addition greater than that given by this equation, the nozzle flow can no longer remain undisturbed by the arc and must shock down and diffuse to a subsonic Mach number where $T_o{}^{*H}$ is great enough to accommodate the given rate of heat addition. The occurrence of thermal blocking would therefore be expected to cause dramatic changes in the flow configuration.

In the present case, thermal blocking is preceded somewhat by separation of the flow from the lower tunnel wall, as can be seen from Figure 75. This is probably due to feedback of the static pressure in the heated stream, which for near-maximum heat addition exceeds that required[96] to cause separation at the free-stream Mach number.

Figures 75 and 76 give examples of Schlieren pictures for two values of W/P_{t_1}. In Figure 75 it is clear that the flow is separated. Yet for Figure 76, with attached flow, the power level exceeds the maximum for heat blocking, and one would expect a normal shock to occur somewhere in the nozzle.

Figure 77 gives a plot of the experimental measurements of the separation limit. It is seen that the experimental maximum is considerably above that given by theory even when A' is taken to be the maximum value possible in the first 30 ft. of diffuser length, and even though the calculation does not account for diffuser friction. This discrepancy is probably due to heat losses to the electrodes and walls.

APPENDIX B

HALL EFFECT

The macroscopic behavior resulting from the Hall effect is profoundly influenced by the plasma configuration.[97-99] The calculation of Hall effects for the cylindrical plasma configuration represented by the arc column with transverse convection is beyond the scope of the present investigation. However, since the Hall effect represents a possible factor in arc slanting, it is relevant at least to consider its effect on a uniform plasma of infinite extent.

It is well known[100] that in the presence of perpendicular electric and magnetic fields a charged particle will, in the absence of collisions, drift in a direction normal to rather than parallel to the electric field. The drift velocity for a charge of either sign is given[100] by $(\underline{E}\times\underline{B})/B^2$ where $\underline{E}$ is a uniform electric field component normal to the uniform magnetic induction $\underline{B}$. Figure[78] illustrates this drift (with collisions) in a severely simplified way. The particle will follow a path such that there will be components of the drift velocity $\underline{V}_d$ parallel to and normal to the electric field, as shown in Figure 78. The angle that the drift velocity makes with the electric field is independent of the sense of the electric field, but changes sign with changes in the sense of $\underline{B}$. The current density $\underline{j}$ due to particles of charge q drifting at velocity $\underline{V}_d$ is given by

$$\underline{j} = nq\underline{v}_d \tag{23}$$

where n is the number density of the particles. Since in the presence of a magnetic field, $\underline{V}_d$ is not necessarily parallel to $\underline{E}$, the simple form of Ohm's Law

$$\underline{j} = \sigma\underline{E} \tag{24}$$

where σ is the scalar conductivity, must be modified. In the presence of a magnetic field additional terms must be added to Ohm's Law. For the latter case, assuming no ion slip, Ohm's Law can be approximately written[97]

$$\underline{j} = \sigma\underline{E} - \left(\frac{\omega_e \tau_e}{B}\right)\underline{j}\times\underline{B} \tag{25}$$

where

τ_e = electron mean free time between collisions

ω_e = electron cyclotron frequency

This equation is not exact even under the assumed conditions, but is useful for indicating trends. In the following, the uniform magnetic field is assumed to be in the positive y direction. The cyclotron frequency is given by:

$$\omega_e = qB/m \tag{26}$$

The mean free time τ_e for air varies with electron temperature and gas density in a rather complicated manner, especially when both neutral collisions and ion collisions

are important.[89] For $\omega_e \tau_e \ll 1$, equation (25) reduces to the simple form of Ohm's Law with scalar conductivity. The components of current density from equation (25) are as follows:

$$j_x = \sigma[E_x + \omega_e \tau_e E_z]/1 + (\omega_e \tau_e)^2 \tag{27}$$

$$j_z = \sigma[E_z - \omega_e \tau_e E_x]/1 + (\omega_e \tau_e)^2 \tag{28}$$

For the case where there is no component of the electric field in the x direction, the angle between the current density vector and the electric field E is given by:

$$\tan\theta = j_x/j_z = \omega_e \tau_e = q_e B \tau_e / m_e \tag{29}$$

Thus it is seen that, unless $\omega_e \tau_e \ll 1$, the electron current will flow at an angle with respect to the electric field. This angle varies with $\omega_e \tau_e$, and therefore with the magnitude and direction of $\underline{B}$. It is independent of the magnitude or direction of the electric field.

Note that although reversal in the direction of $\underline{E}$ results in no change in the Hall angle, a reversal in $\underline{E}$ while at the same time maintaining the same (upstream) direction of $\underline{E}$ x $\underline{B}$, requires reversal of B also, and this results in reversal of the direction of the Hall angle.

For the case where no current-flow in the x direction is possible, there must be an electric field E_x to prevent it:

$$j_x = 0; \quad \therefore \quad E_x = -\omega_e \tau_e E_z \tag{30}$$

Substituting this value of E_x in equation (28) gives

$$j_z = \sigma E_z \tag{31}$$

Thus, in this case the electrical conductivity in the z direction is unaffected by the presence of the magnetic field. In general, $\sigma_{\parallel}$, the analogue of conductivity parallel to the current is unaffected by the magnetic field (Tonk's theorem):

$$\sigma_{\parallel} = \underline{j} \cdot \underline{j} / \underline{j} \cdot \underline{E} = \sigma \tag{32}$$

It should be repeated that the above discussion applies to the highly idealized case of a uniform plasma.

Hall effects become important when $\omega_e \tau_e$ becomes appreciable. The cyclotron frequency for the electrons is very easily calculated from equation (26). For the induction of 3000 gauss, ω_e is 5.3×10^{10}/sec. The electron collision frequency depends on the gas temperature and density. For P_{t_1} = 20 in. Hg, a lower bound on the collision frequency

can be calculated from the minimum pressure possible in the column P_{∞} , and an assumed temperature, 8000°K, which is probably low for an arc of several hundred amperes.

A lower limit on the gas density corresponding to these conditions can be estimated from a table of properties for equilibrium air[101] to be $10^{-3.3}\,\rho_o$. From reference 89, the electron collision frequency corresponding to this density and temperature is 6×10^9 /sec. Thus, a rough upper limit for $\omega_e \tau_e$ at M = 2.5 and P_{t_1} = 20 in. of mercury, is 8.8. It is seen that under this fairly extreme condition there should be a significant Hall effect for a uniform gas. The actual value of $\omega_e \tau_e$ existing in the arc column must be determined experimentally of course, but it should be less than the above estimate, since the density and temperature in the column should be greater than assumed above - for a temperature of 12,000°K, $\omega_e \tau_e = 1.3$.

If it were assumed that the observed angle of arc slant is the same as the Hall angle for a uniform plasma, then it would follow that $\omega_e \tau_e = 2.4$ for all values of current, pressure, and local magnetic induction investigated.

REFERENCES

1. Stuhlinger, E. "Electric Propulsion." Astronautics, vol. 7, p. 60; November, 1962.

2. Rose, P., Powers, W. and Hritzay, D. "The Large High Pressure Arc Plasma Generator: A Facility for Simulating Missile and Satellite Re-entry." AVCO-Everett Research Lab. Everett, Mass., Research Report 56; June, 1959.

   Bond, C. E., Cordero, J., Curtiss, H. A., and Henshall, B. D. "The Development of a Ten Megawatt Multi-arc and Its Operational Use in Hypersonic Re-entry Vehicle Studies." IAS Paper No. 62-69; Jan. 22, 1962.

3. John, R. R., and Bade, W. L. "Recent Advances in Electric Arc Plasma Generation Technology," ARS Journal, vol. 31, no. 1., p. 4; January, 1961.

4. Covert, E. E., and Kerney, K. "A Review of the Literature of Plasma Physics." Massachusetts Institute of Technology, Naval Supersonic Laboratory Tech. Rpt. No. 373, WADC TR-59-486; July, 1959.

5. Secker, P. E., and Guile, A. E. "Magnetic Deflection of Arcs." Nature (London), vol. 181, p. 1615; June 7, 1958.

6. Guile, A. E., Lewis, T. J., and Mehta, S. F. "Arc Motion with Magnetized Electrodes." Brit. J. Appl. Phys., vol. 8, no. 11, p. 444; November, 1957.

7. Guile, A. E., Lewis, T. J., and Mehta, S. F. "Arc Movement and Electrode Magnetism." Nature (London), vol. 179, p. 1023; May 8, 1957.

8. Gönenc, Izzet. "Lichtbogenwanderung an runden Stäben." ETZ-A, vol. 81, no. 4, p. 132; 1960.

9. Guile, A. E., and Mehta, S. F. "Arc Movement Due to the Magnetic Field of Current Flowing in the Electrodes." Instn. of Elec. Eng. Proc., vol. 104, pt. A, no. 18, p. 533; December, 1957.

10. Secker, P. E., Guile, A. E., and Caton, P. S. "Skin Effect as a Factor in the Movement of Cold-Cathode Arcs." Brit. J. Appl. Phys., vol. 13, no. 6, p. 282; June, 1962.

11. Secker, P. E. "The Influence of Cathode Surface Conditions on Arc Movement." Proc. IV Conference on Ionization Phenomena, Uppsala, vol. 1, p. II B 350; August, 1959.

12. Eidinger, A., and Rieder, W. "Das Verhalten des Lichtbogens im transversalen Magnetfeld (Magnetische Blasung)." Arch. Elektrotech, vol. 43, no. 2, p. 94; 1957.

13. Secker, P. E., and Guile, A. E. "Arc Movement in a Transverse Magnetic Field at Atmospheric Pressure." Instn. of Elec. Eng. Proc., vol. 106, pt. A, no. 28, p. 311; August, 1959.

14. Winsor, L. P., and Lee, T. H. "Properties of a D-C Arc in a Magnetic Field." Trans. AIEE, p. 143; May, 1956.

15. Guile, A. E., and Secker, P. E. "Arc Cathode Movement in a Magnetic Field." J. Appl. Phys., vol. 29, no. 12, p. 1662; December, 1958.

16. Lee, T. H. "Properties of a D.C. Arc in a Magnetic Field" (unpublished Ph.D. dissertation, Dept. of Electrical Eng., Rensselaer Polytechnic Institute); 1954.

17. Lewis, T. J., and Secker, P. E. "Influence of the Cathode Surface on Arc Velocity." J. Appl. Phys., vol. 32, no. 1, p. 54; January, 1961.

18. Stolt, H. "Die Rotation des elektrischen Lichtbogens bei Atmosphärendruck." Ann. Phys., Vol. IV, bd. 61, no. 10, p. 80; 1924.

19. Guile, A. E., Lewis, T. J., and Secker, P. E. "The Motion of Cold-Cathode Arcs in Magnetic Fields," Instn. Elec. Eng. Proc., vol. 108, pt. C, no. 14, p. 463; May 1961.

20. Lewis, T. J., and Secker, P. E. "Effect of Cathode Surface Roughness and Oxidation on Arc Movement." Nature (London), vol. 186, p. 30; April 2, 1960.

21. Féchant, M. L. "Vitesses de déplacement d'arcs électriques dans L'air." Rev. Gen. Élec., vol. 68, no. 9, p. 519; September, 1959.

22. Kuhnert, Ekkehard. "Über die Lichtbogenwanderung im engen Isolierstoffspalt bei Strömen bis 200 kA." ETZ-A, bd. 81, H. 11, p. 401; 1960.

23. Angelopoulos, M. "Über magnetisch schnell fortebewegte Gleichstrom - Lichtbögen." ETZ-A, Bd. 79, h. 16, p. 572; 1958.

24. Smith, H. L., and Early, H. C. "Investigation of Heating of Air Stream in a Wind Tunnel by Means of an Electrical Discharge: Final Report." University of Michigan, ERI Report 2154-3-F; October, 1954.

25. Finkelnburg, W. and Maecker, H. "Elektrische Bögen und thermisches Plasma." Handbach der Physik, vol. XXII, p. 254. Springer-Verlag, Berlin-Götingen-Heidelberg; 1956. Also available in translation by Eckstein, B. H., Parma Research Laboratory, Union Carbide Corp., Parma, Ohio. ARL Report No. 62-302; April, 1962.

26. Compton, K. T. "The Electric Arc." Trans. AIEE, p. 868; June, 1927.

27. Gurevich, D. B., and Podmoshenskii, I. V. "The Relationship between the Excitation Temperature and the Gas Temperature in the Positive Column of an Arc Discharge." Optics and Spectroscopy (Trans.), vol. 15, no. 5, p. 319; November, 1963.

28. Loeb, L. B. "Basic Processes of Gaseous Electronics." University of California Press, Berkeley, Calif.; 1960 [1955].

29. Edels, H. "Properties and Theory of the Electric Arc." Instn. of Elec. Eng., paper no. 3498, p. 55, February, 1961.

30. Rompe, R., Thouret, W., and Weizel, W. "Zur Frage der Stabilisierung frei brennender Lichtbogen." Z. Phys., bd. 122, h. 1-4, p. 1; 1943.

31. Schmitz, G., and Uhlenbusch, J. "Zur mathematischen Beschreibung zylindersymmetrischer Lichtbögen." Z. Phys., vol. 159, no. 5, p. 554; 1960.

32. Krizhanskii, S. M. "Theory of the Positive Column of an Arc Discharge." Sov. Phys. - Tech. Phys. (trans.), vol. 7, no. 2, p. 129; August, 1962.

33. Maecker, H. "Messung und Auswertung von Bogencharakteristiken (Ar, N_2)." Z. Phys., vol. 158, no. 4, p. 392; 1960.

34. Maecker, H. "Über die Charakteristiken zylindrischer Bögen." Z. Phys., vol. 157, no. 1, p. 1; 1959.

35. Belousova, I. M., and Gurevich, D. B. "Calculation of the Temperature of a Mercury Arc and Its Experimental Verification." Sov. Phys. - Tech. Phys. (trans.), vol. 6, no. 11, p. 974; May, 1962.

36. Kolesnikov, V. N., and Sobolev, N. N. "Structure of the Column in an Argon Arc." Sov. Phys. - Tech. Phys. (trans.), vol. 7, no. 9, p. 801; March 1963.

37. Schmitz, G. and Uhlenbusch, J. "Angenäherte Berechnung Zylindrischer Lichtbögen unter Berücksichtigung der Abstrahlung." Ionization in Gases Conference Proceedings, p. 871, Munich; 1961.

38. Bauer, A. "Eine Näherungslösung der Elenbaas - Hellerschen Differentialgleichung." Z. angew. Phys., vol. 15, no. 6, p. 550; 1963.

39. Schmitz, G. "Zur Theorie der wandstabilisierten Bogensäule." Z. Naturforsche, vol. 5A, p. 571; 1950.

40. Rother, H. "Über den Einfluss der Konvektion auf einen Lichtbögen." Ann. Phys. (Leipzig), vol. 20, no. 1, p. 230; 1957.

41. Thiene, P. "Convective Flexure of a Plasma Conductor." Phys. Fl., vol. 6, no. 9, p. 1319; September, 1963.

42. Suits, C. G., and Poritsky, H. "Application of Heat Transfer Data to Arc Characteristics." Phys. Rev., vol. 55, p. 1184; June 15, 1939.

43. Champion, K. S. W. "The Energy Balance Equation for the Positive Columns of High Pressure Arcs." Proc. Phys. Soc. (London), B66, p. 169; 1953.

44. Patrick, R. M., and Brogan, T. R. "One-dimensional Flow of an Ionized Gas through a Magnetic Field." J. Fl. Mech., 5, p. 289; 1959.

45. Fowler, R. H. "Statistical Mechanics." The Macmillan Co., New York, N. Y.; 1936.

46. Kerrebrock, J. L. "Non-Equilibrium Effects on Conductivity and Electrode Heat Transfer in Ionized Cases." Daniel and Florence Guggenheim Jet Propulsion Center, California Institute of Technology, Tech. Note No. 4, AFOSR 165; November, 1960.

47. Kerrebrock, J. L. "Conduction in Gases with Elevated Electron Temperature." Proc. of the Second Symposium on the Engineering Aspects of Magnetohydrodynamics, Philadelphia, p. 327; March, 1961.

48. Elenbaas, W. "The High Pressure Mercury Vapour Discharge." Interscience Publishers Inc., New York, N. Y.; 1951.

49. Shvangiradze, R. R., Oganexov, K. A., and Chikhladze, B. Ya. "Study of the Direct Current Arc at Different Pressures of Argon and Air." Optics and Spectroscopy (trans)., vol. 13, no. 1, p. 14; 1962.

50. Demetriades, A. "Electric-Field Heating Threshold for Charged Particles." Reprint from Phys. of Fl., vol. 5, no. 9, Graduate Aeronautical Laboratories, California Institute of Technology, Pasadena, pub. no. 532; 1962.

51. Kitaeva, V. F., Kolesnikov, V. N., Obukhov-Denisov, V. V., and Sobolev, N. N. "Structure of the Column in an Argon Arc: I. Local Electrical Characteristics of the Column." Sov. Phys. - Tech. Phys. (trans.), vol. 7, no. 9, p. 796; March, 1963.

52. Suits, C. G. "The Temperature of High Pressure Arcs." J. Appl. Phys. vol. 10, p. 728, Oct. 1939.

53. Suits, C. G. "High Pressure Arcs in Common Gases in Free Convection." Phys. Rev., vol. 55, p. 561; March 15, 1939.

54. Secker, P. E. "Explanation of the Enhanced Arc Velocity on Magnetic Electrodes." Brit. J. Appl. Phys., vol. 11, no. 8, p. 385; August, 1960.

55. Hochrainer, A. "Die Bewegung des Kurzschluss-Lichtbogens in Hochspannungs-Schaltanlagen." ETZ-A, Bd. 77, H. 10, p. 302; 1956.

56. Secker, P. E., and Guile, A. E. "A Theory of Cold-Cathode Arc Movement in a Magnetic Field." Nature (London), vol. 190, p. 428; April 29, 1961.

57. Bron, O. B. "Motion of an Electric Arc in a Magnetic Field." Trans. by Technical Documents Liaison Office, Wright Patterson - Air Force Base, Ohio, ASTIA, AD No. 258489; 1961.

58. Dunkerley, H. S., and Schaefer, D. L. "Observations of Cathode Arc Tracks." J. Appl. Phys., vol. 26, p. 1384; 1955.

59. Winsor, L. P., and Lee, T. H. "Properties of a d-c Arc in a Magnetic Field." Phys. Rev., vol. 98, p. 562; 1955.

60. Burghoff, H. H. "Über die magnetische Ablenkung von Lichtbögen." Elektrotechn. und Masch., Bd. 52, H. 5, p. 49; February, 1934.

61. Freiberger, H. Lichtbogenwanderung in Schaltanlagen." ETZ, Bd. 61, H. 38, p. 865; September, 1940.

62. Nicol, J. "The Rotation of the Electric Arc in a Radial Magnetic Field." Proc. Roy. Soc. A82, p. 29 October, 1909.

63. Miyagawa, N. "On the Movements of Arc Cathode Spot and of Ball-of-Fire in a Transverse Magnetic Field." Sci. Papers I.P.C.R., vol. 56, no. 1; 1962.

64. Smith, C. G. "Retrograde Arc Motion of Supersonic Speed." Phys. Rev., Ser. 2, v. 84, p. 1075; 1951.

65. Minorsky, M. N. "La Rotation de l' Arc Électrique dans un Champ Manétique Radial." J. Phys. et. Rad., vol. 9, p. 127; 1928.

66. St. John, R. M., and Winans, J. G. "Motion and Spectrum of Arc Cathode Spot in a Magnetic Field." Phys. Rev., vol. 98, no. 6; June 15, 1955.

67. Ecker, G., and Müller, K. G. "Theorie der Retrograde Motion." Z. Phys., Bd. 151, H. 5, p. 577; 1958.

68. Ecker, G., and Müller, K. G. "Theory of the Retrograde Motion." J. Appl. Phys., vol. 29, no. 11, p. 1606; November, 1958.

69. Ecker, G. "Electrode Components of the Arc Discharge." Ergebn. d. exakt. Naturw. XXXIII, p. 1; 1959.

70. Smith, C. G. "Cathode Dark Space and Negative Glow of a Mercury Arc." Phys. Rev. vol. 69, nos. 3 and 4, p. 96; February 1 and 15, 1946.

71. Hernqvist, K. G., and Johnson, E. O. "Retrograde Motion in Gas Discharge Plasmas." Phys. Rev., vol. 98, no. 6, p. 1576; June 15, 1955.

72. Smith, C. G. "Motion of an Arc in a Magnetic Field." J. App. Phys., vol. 28, no. 11, p. 1328; November, 1957.

73. Zei, D., and Winans, J. G. "Motion of High Speed Arc Spots in Magnetic Field." J. Appl. Phys., vol. 31, no. 11, p. 1813; November, 1959.

74. Robson, A. E., and von Engel, A. "Motion of a Short Arc in a Magnetic Field." Phys. Rev., vol. 104, no. 1, p. 15; October 1, 1956.

75. Robson, A. E., and von Engel, A. "Origin of Retrograde Motion of Arc Cathode Spots." Phys. Rev., vol. 93, p. 1121; 1954.

76. Robson, A. E. "The Motion of an Arc in a Magnetic Field." Proc. IV Conference on Ionization Phenomena, Uppsala, vol. 1, p. II B 346; August, 1959.

77. Kesaev, I. G. "On the Causes of Retrograde Arc Cathode Spot Motion in a Magnetic Field." Dokl. Akad. Nauk. (USSR), vol. 112, no. 4, p. 619 (trans.) Sov. Phys. Dokl., vol. 2, no. 1, p. 60; 1957.

78. Thiene, P. G. "Basic Study of Energy Exchange Process between an Electric Arc and a Gas Flow: Final Report." Plasmadyne Corp., Santa Ana, Calif., AFOSR 1264; ASTIA AD 263203; February, 1961.

79. Early, H. C., and Miller, D. B. "Heating a Supersonic Stream with a Corona Discharge." University of Michigan, ERI Report No. 2147-16-T; April, 1957.

80. Kaufmann, W. "Elektrodynamische Eigenümlichkeiten leitender Gase." Ann. der Physik, vol. 2, no. 5, p. 158; 1900.

81. Chetayev, N. G. "The Stability of Motion." Transl. by M. Nadler. Pergamon Press, New York, N. Y.; 1961.

82. Bond, C. E. "An Investigation of the Magnetohydrodynamics of the Positive Column of a Direct Current Electric Arc Moving at High Velocity Under the Impetus of a Strong External Magnetic Field - Phase I." University of Michigan, ORA. Report No. 05220-1-P; February, 1963.

83. Boatwright, W. B., Stewart, R. B., and Grimand, J. E. "Description and Preliminary Calibration Tests of a Small Arc-Heated Hypersonic Wind Tunnel." NASA TN D-1377; December, 1962.

84. Mayo, R. F., and Davis, D. D. "Magnetically Diffused Radial Electric-Arc Air Heater Employing Water-Cooled Copper Electrodes." ARS preprint no. 2453-62; March, 1962.

85. Powers, W. E., and Patrick, R. M. "A Magnetic Annular Arc." AVCO-Everett Research Lab., Everett, Mass., Research Report 129; May, 1962.

86. Amick, J. L., Liepman, H. P., and Reynolds, T. "Development of a Variable Mach Number Sliding Block Nozzle and Evaluation in the Mach Number Range 1.3 to 4.0." University of Michigan, WADC Tech. Report No. 55-88; March 1955.

87. Bailey, H. E., and Kuethe, A. M. "Supersonic Mixing of Jet and Turbulent Boundary Layers." University of Michigan, ERI Report No. 2270-11-F; June, 1957.

88. Janes, G. S. "Magnetohydrodynamic Propulsion." AVCO-Everett Research Lab., Everett, Mass., Research Report 90; August, 1960.

89. Shkarofsky, I. P., Bachynski, M. P., and Johnston, T. W. "Collision Frequency Associated with High Temperature Air and Scattering Cross-Sections of the Constituents." RCA Victor Co., Ltd., Research Lab., Montreal, Canada, Research Report No. 7-801.

90. King, L. A. "Theoretical Calculation of Arc Temperatures in Different Gases." Colloquium Spectroscopicum International VI, Amsterdam. Pergamon Press Ltd., London, p. 152; 1956.

91. Yamamura, S. "Immobility Phenomena and Reverse Driving Phenomena of the Electric Arc." J. Appl. Phys., vol. 21, no. 3, p. 193; March, 1950.

92. Loeb, L. B. "Electrical Breakdown of Gases with Steady or Direct Current Impulse Potentials." Hanbuch der Physik, vol. XXII, p. 445. Springer - Verlag, Berlin, Göttingen, Heidelberg; 1956.

93. Robben, F. "Electronic Rate Processes in Non-Equilibrium Plasmas." Presented at the AIAA Aerospace Sciences Meeting, New York, N. Y., Jan. 20-22, 1964 AIAA Preprint No. 64-56.

94. Weymann, H. D. "Electron Diffusion Ahead of Shock Waves in Argon." Phys. Fl., vol. 3, no. 4, p. 545; July-August, 1960.

95. Shapiro, A. H. "The Dynamics and Thermodynamics of Compressible Fluid Flow." Vol. I. The Ronald Press Co., New York, N. Y.; 1953.

96. Love, E. S. "Pressure Rise Associated with Shock-Induced Boundary-Layer Separation." NACA TN 3601; December, 1955.

97. Rosa, R. J. "Hall and Ion-Slip Effects in a Non-uniform Gas." Phys. Fl., vol. 5, no. 9, p. 1081; 1962.

98. Rosa, R. J. "Physical Principles of Magnetohydrodynamic Power Generation." Phys. Fl., vol. 4, no. 2, p. 182; 1961.

99. Hurwitz, H., Kilb, R. W., and Sutton, G. W. "Influence of Tensor Conductivity on Current Distribution in a MHD Generator." J. Appl Phys., vol. 32, no. 2, p. 205; 1961.

100. Spitzer, L. "Physics of Fully Ionized Gases." Interscience Publishers, Inc., New York, N. Y.; 1956.

101. Hilsenrath, J., and Klein, M. "Table of Thermodynamic Properties of Air in Equilibrium Including Second Virial Corrections from 1,500° K to 15,000° K." Arnold Engineering Development Center, Tullahoma, Tenn. AEDC-TDR-63-161; August, 1963.

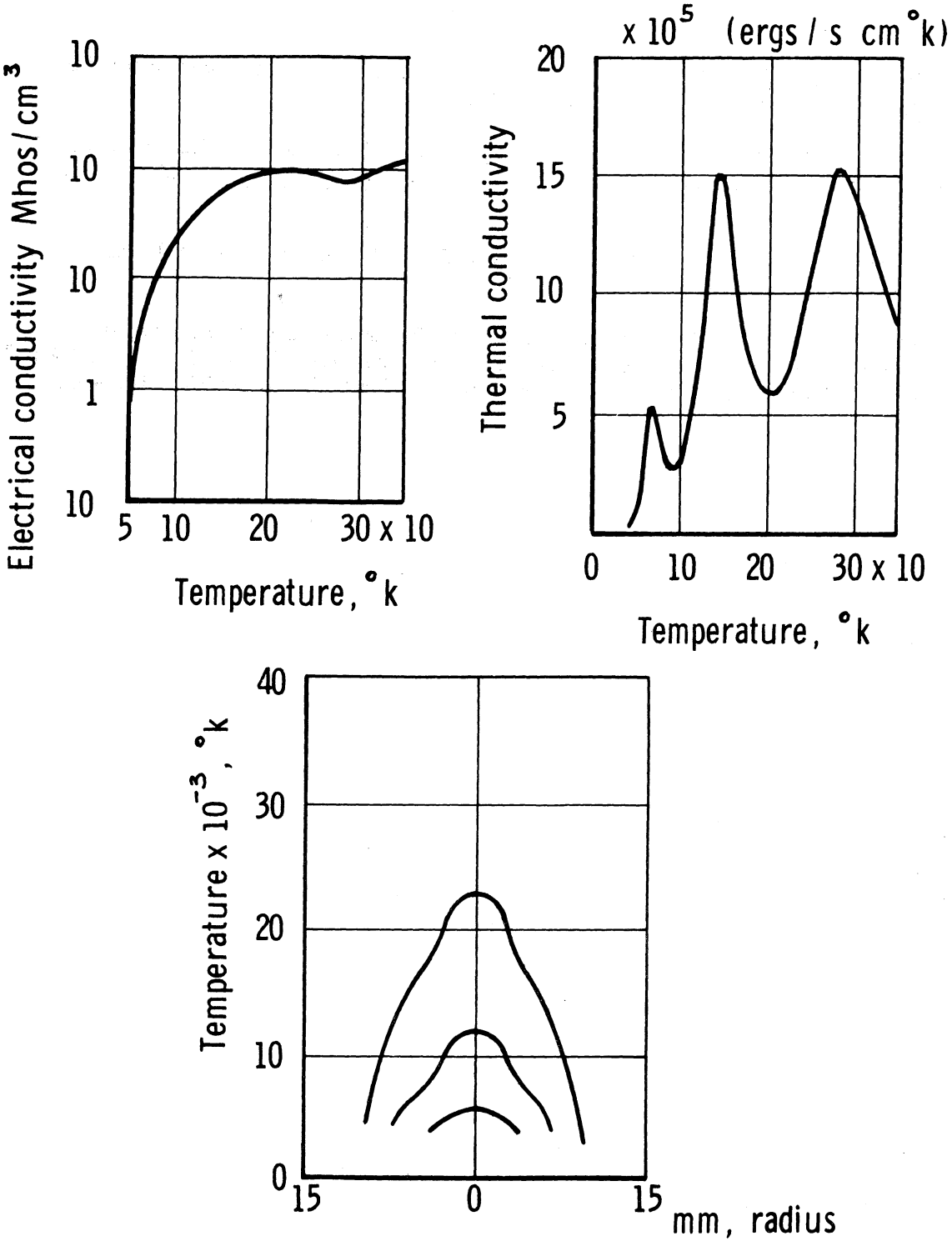

Fig. 1 Material Properties of Nitrogen and Resulting Temperature Distributions for the Non-Convective Arc (from King[90])

a. Model Assumed by Rother[40]

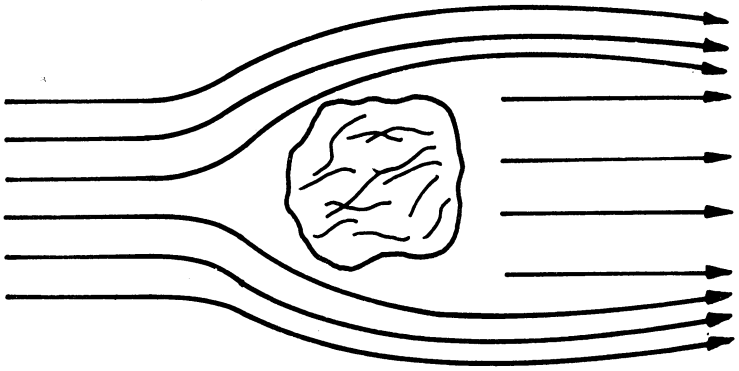

b. Model with Deflected Flow

Fig. 2 Flow Patterns for the Convective Arc

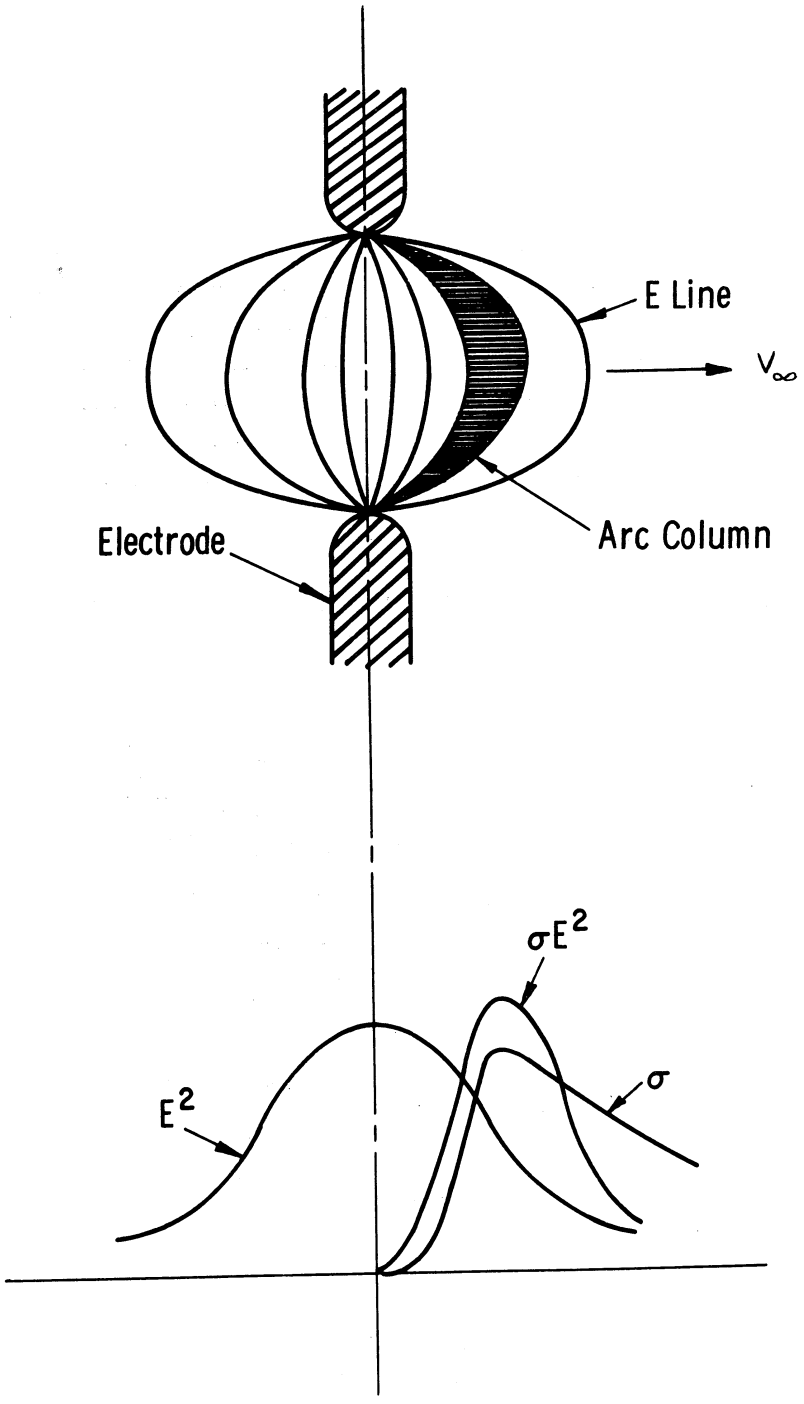

Fig. 3. Model for Blown Arc, Used by Rother[40]

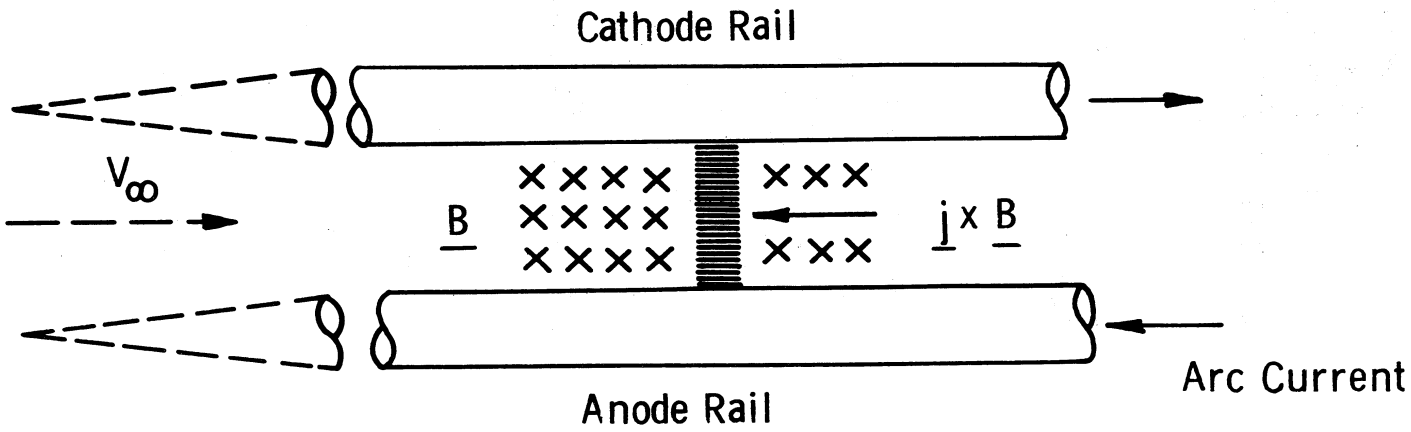

Fig. 4 Rail-Accelerator Setup

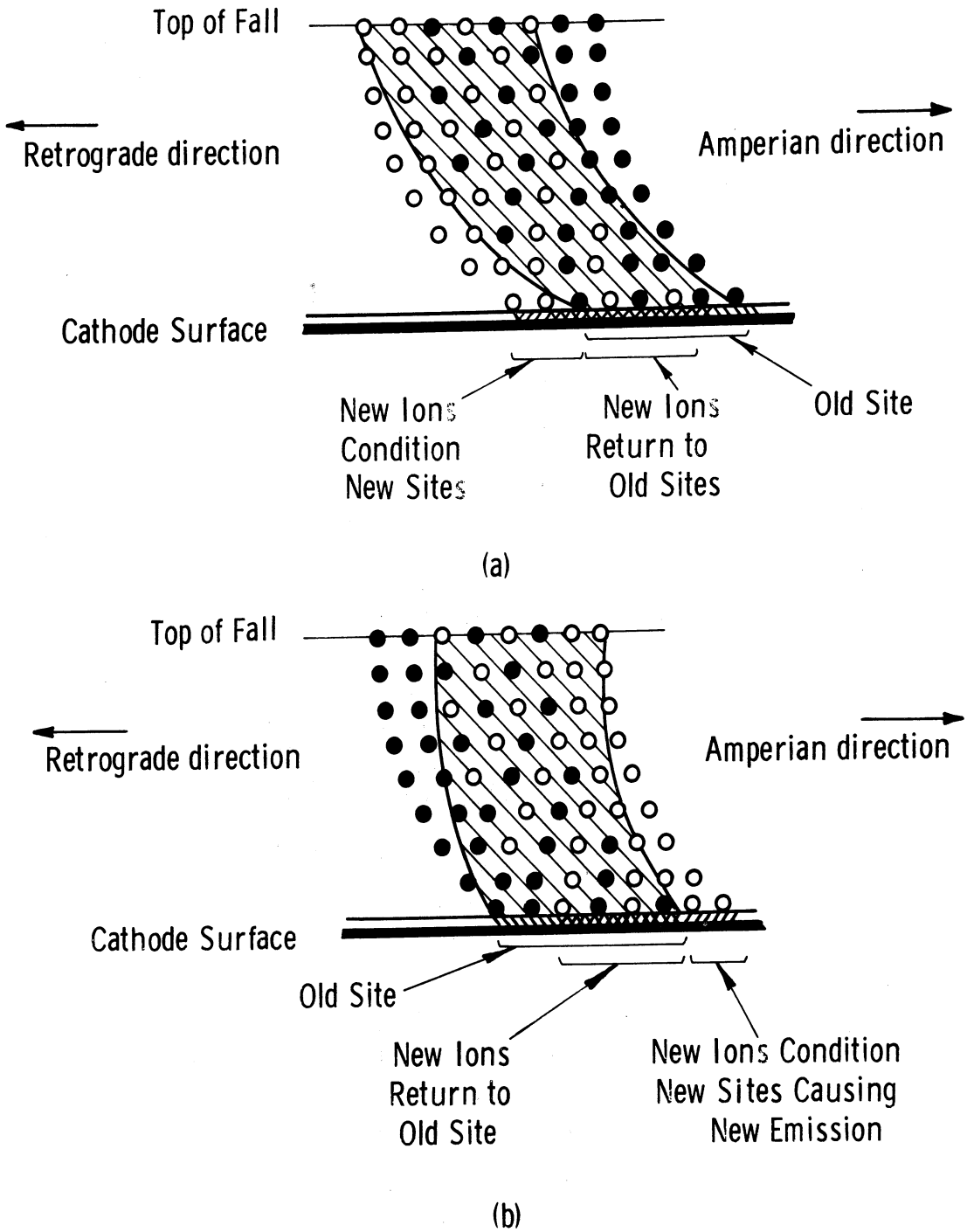

Fig. 5. Model for Cathode Spot Motion from Ref. 19.

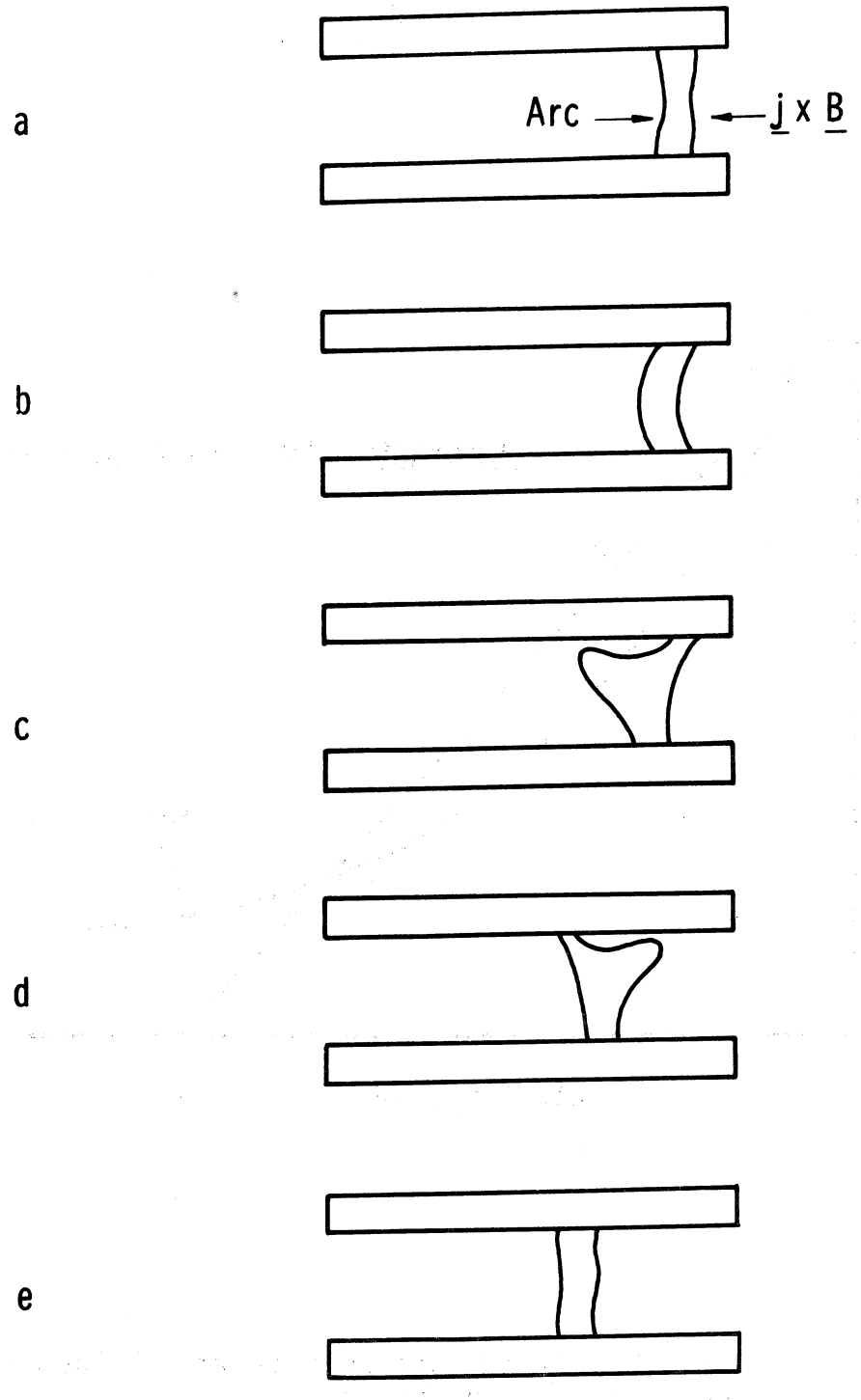

Fig. 6. Root Motion by the Stepping Mechanism (after Dunkerley and Schaefer[58])

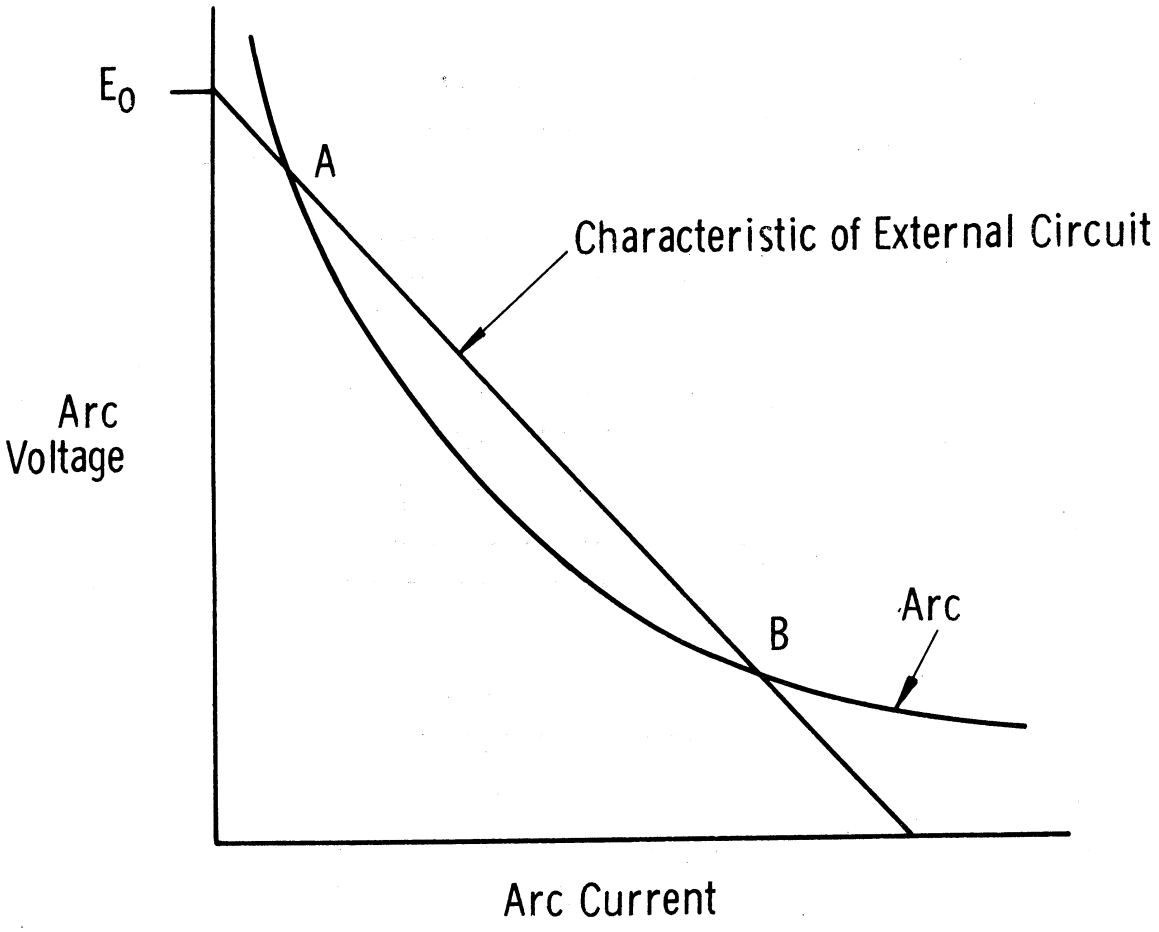

Fig. 7. Typical Static Characteristic and Points of Equilibrium for an Electric Arc.

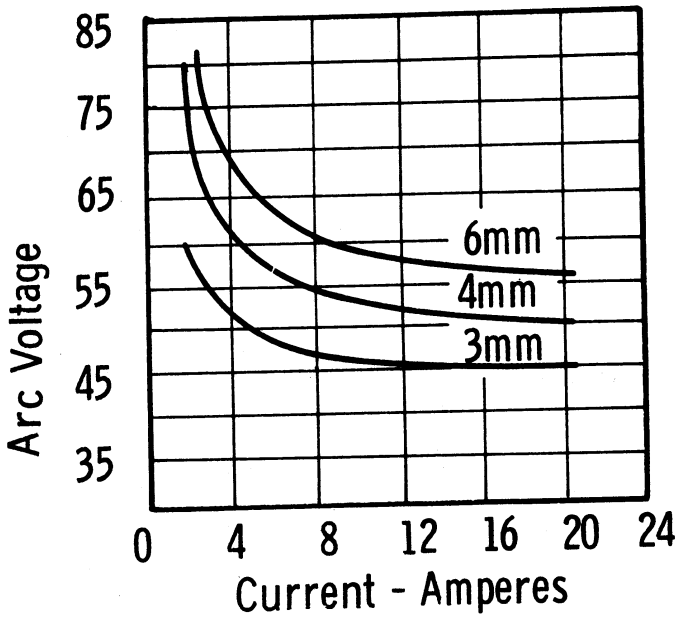

Fig. 8 Ayrton's Voltage-Current Traces for Non-Convective Arcs (from Ref.25)

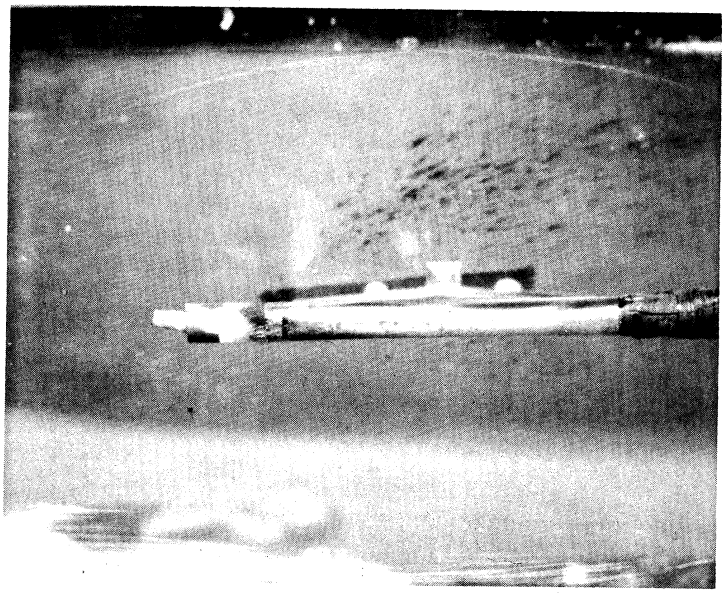

(a) Carbon Electrode Fracture

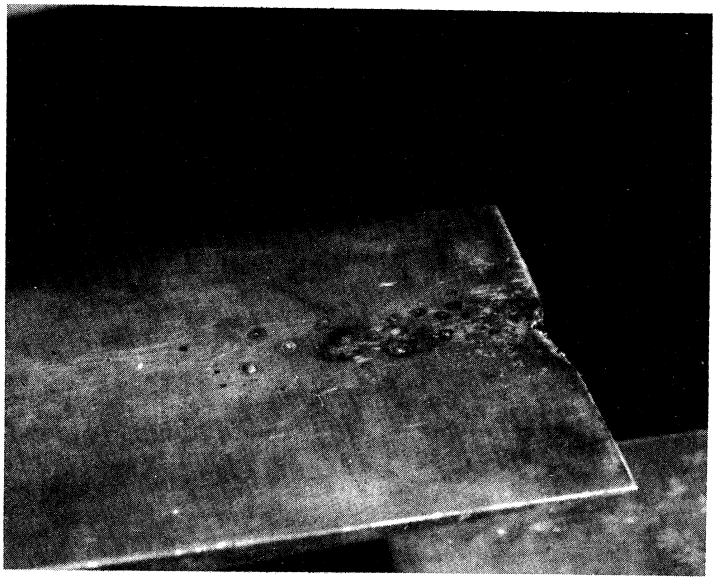

(b) Arc Strike to Lower Tunnel Wall
Due to Excess Power and Flow Reversal

Fig. 9 Confinement Hazards

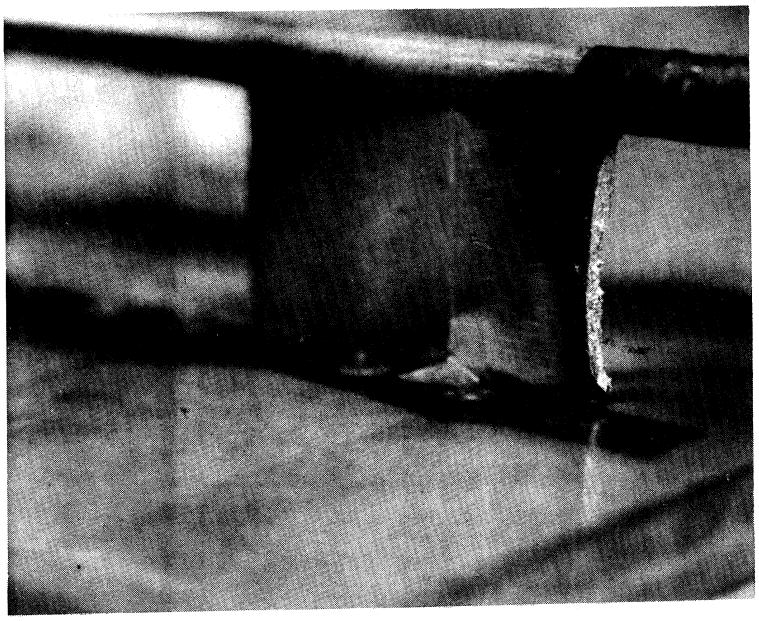

(a) Strike to Downstream Edge of Cathode Support Strut

(b) Strike to Anode Cable

Fig. 10 Arc Mislocation

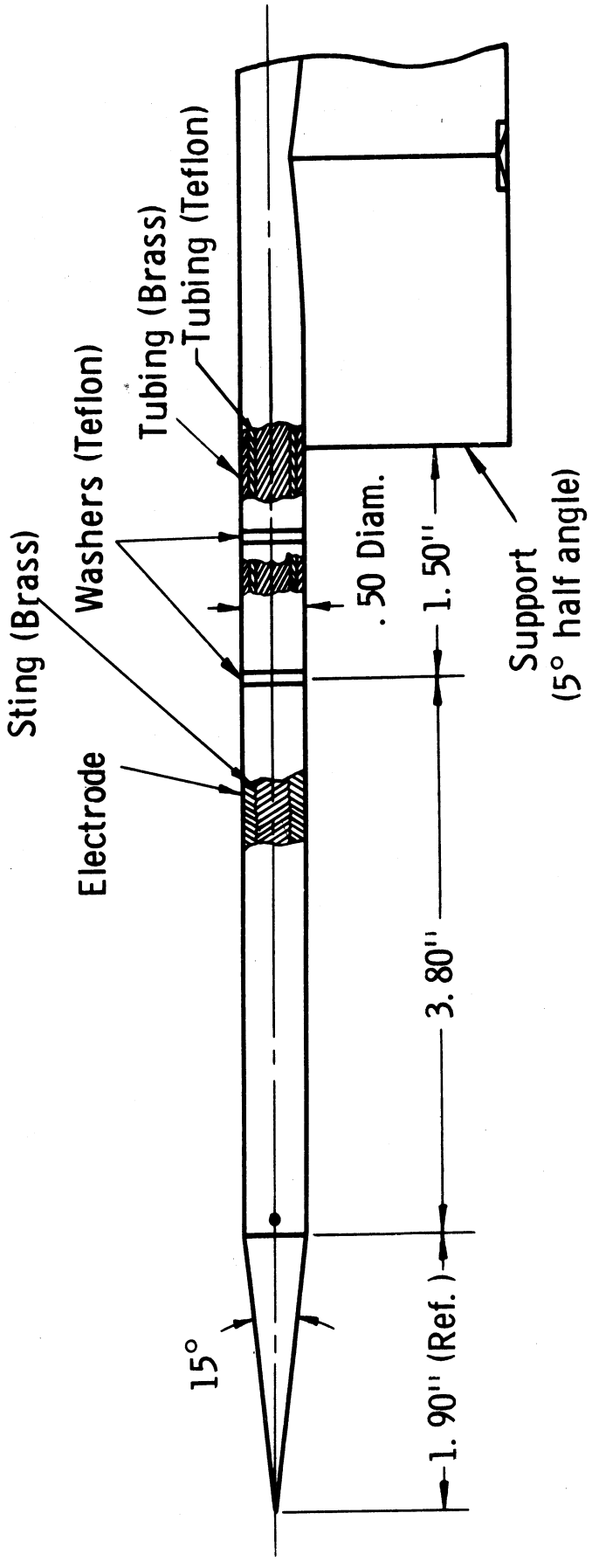

Fig. 11 Details of Electrode Design

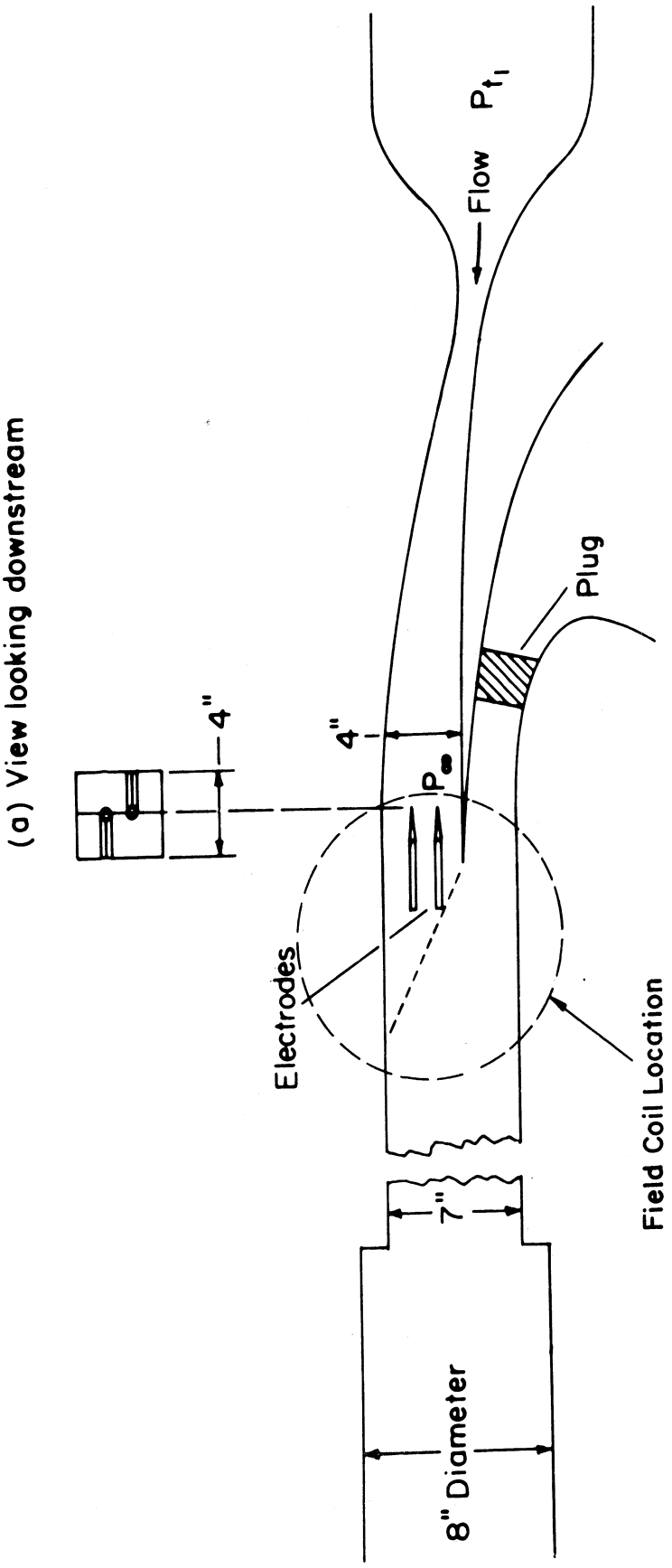

Fig. 12 Experimental Setup

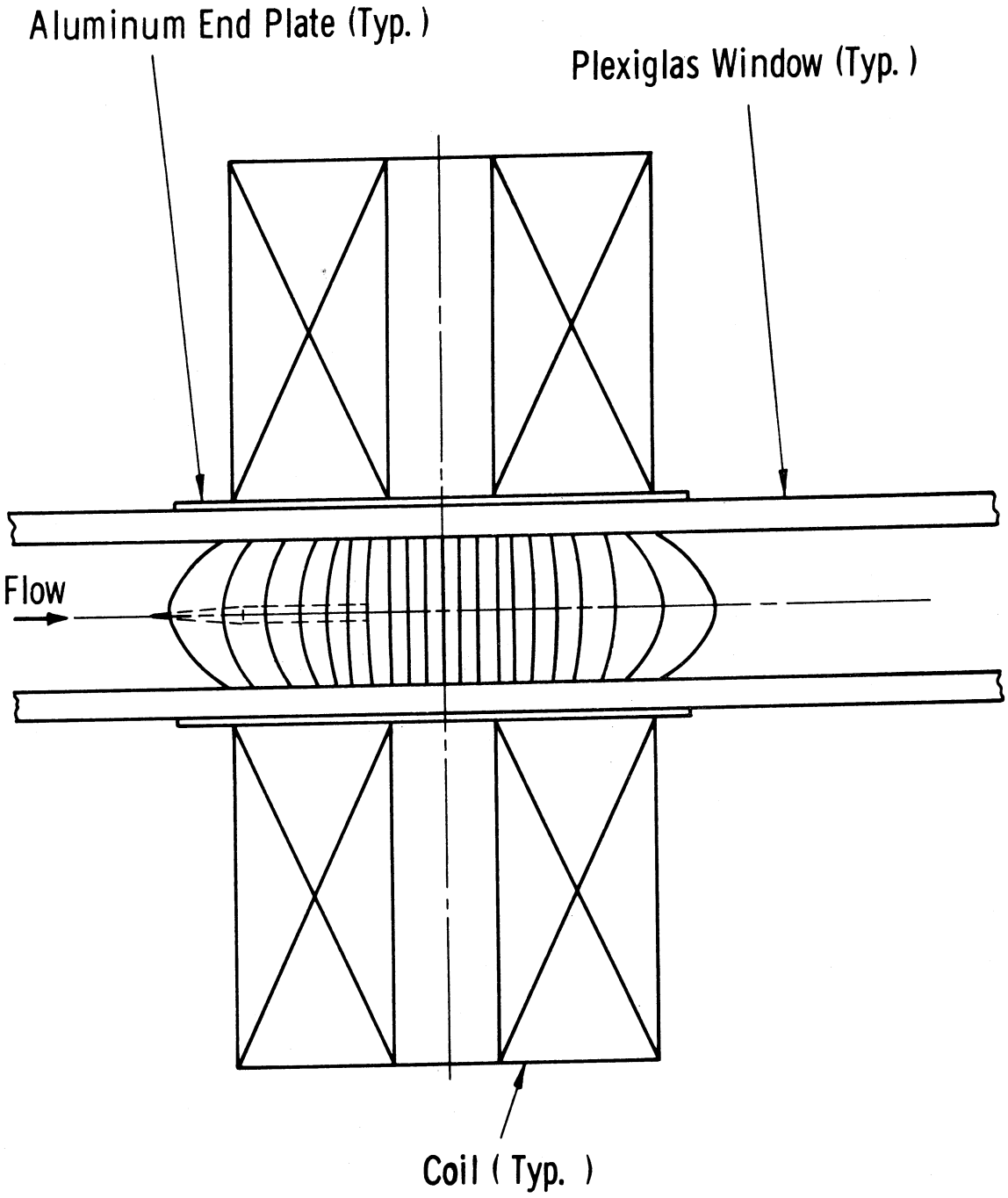

Fig. 13 Schematic Representation of Magnetic Field Lines

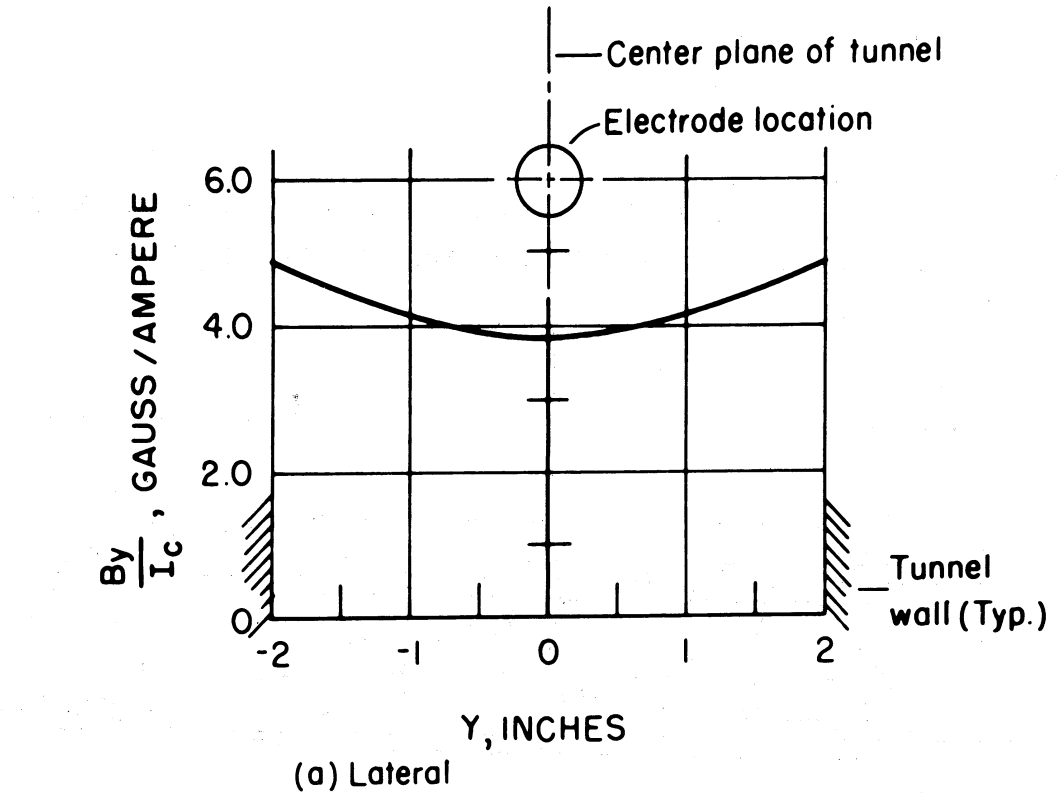

(a) Lateral

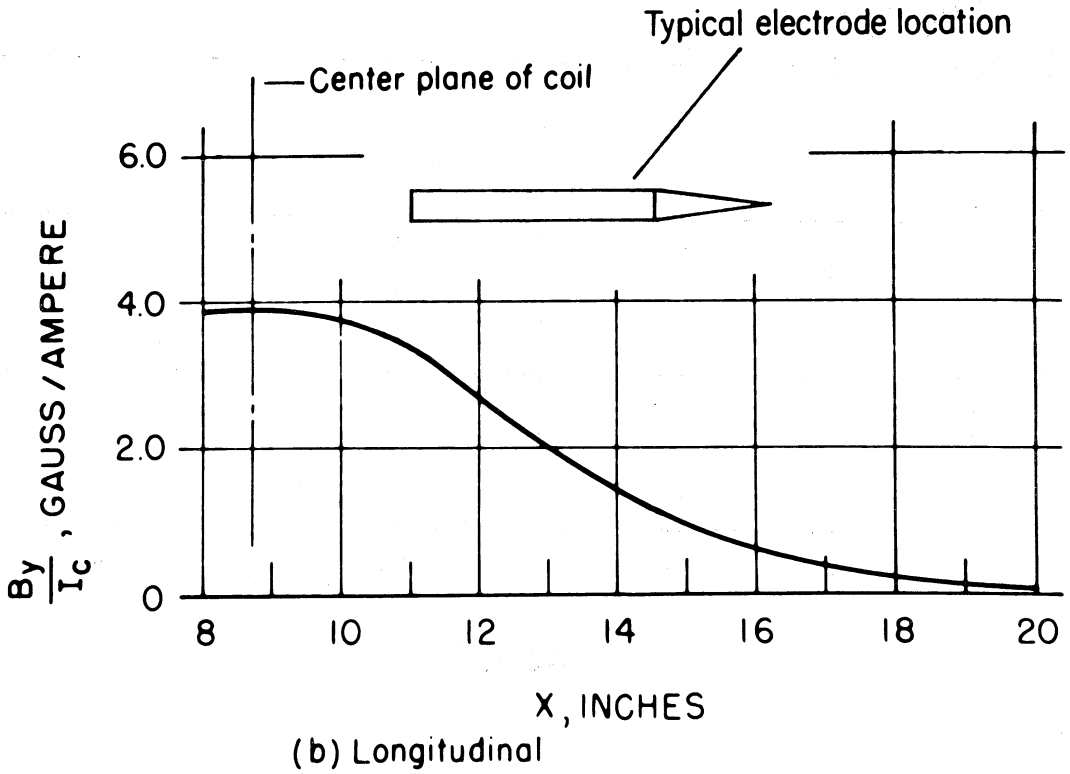

(b) Longitudinal

Fig. 14 Calculated Spatial Variation in B_y

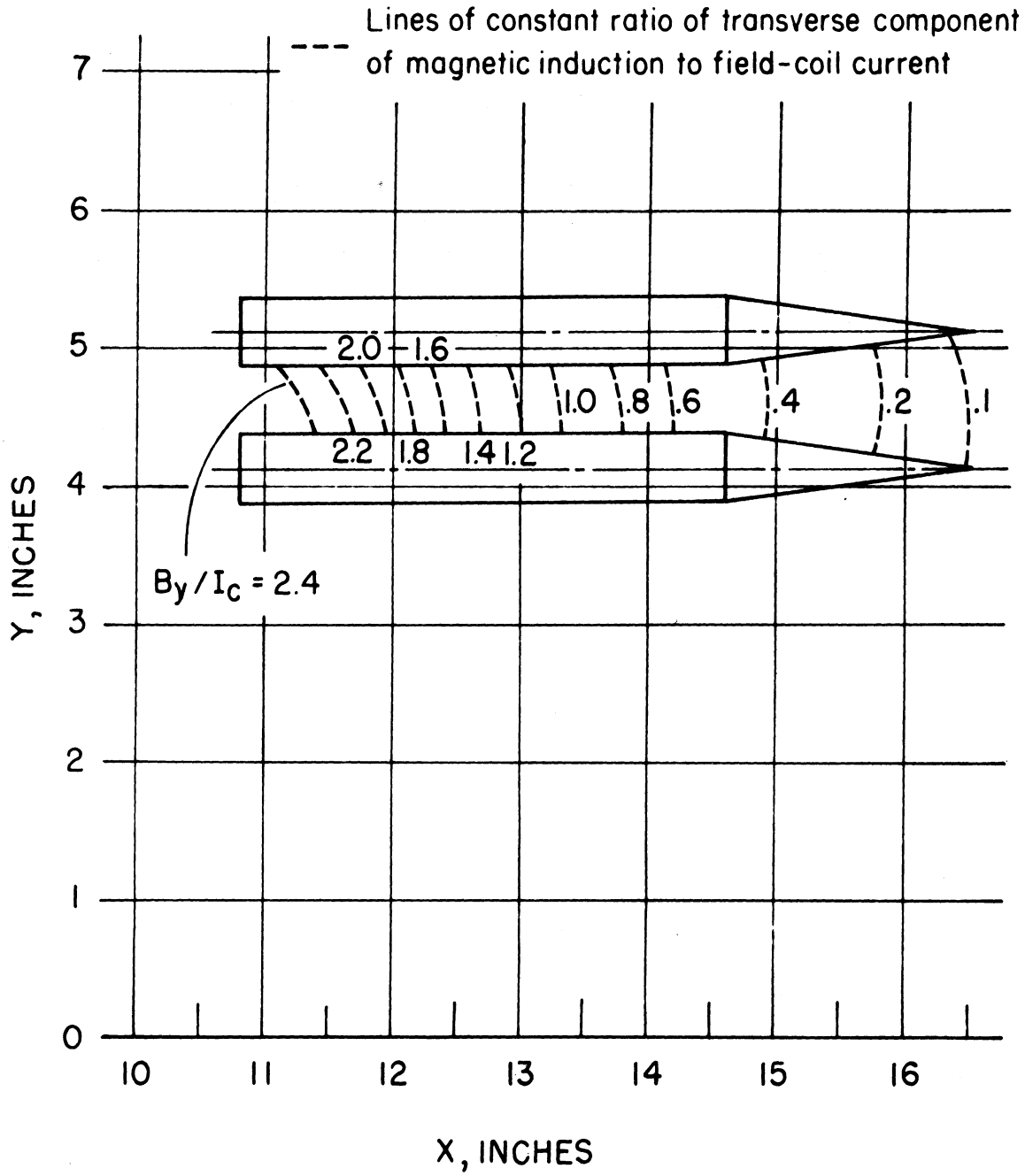

Fig. 15 Measured Spatial Variation in B_y
(Electrodes Shown with 0.6" Gap)

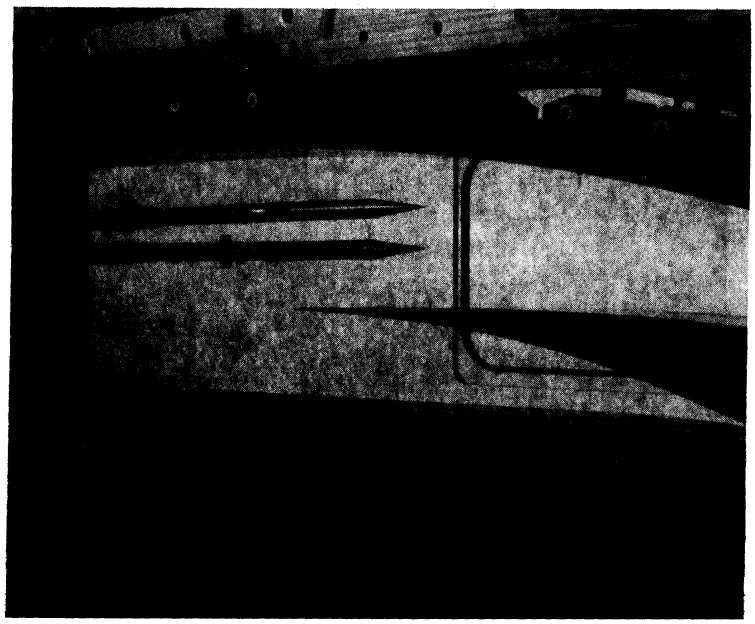

(a) Without Field Coils

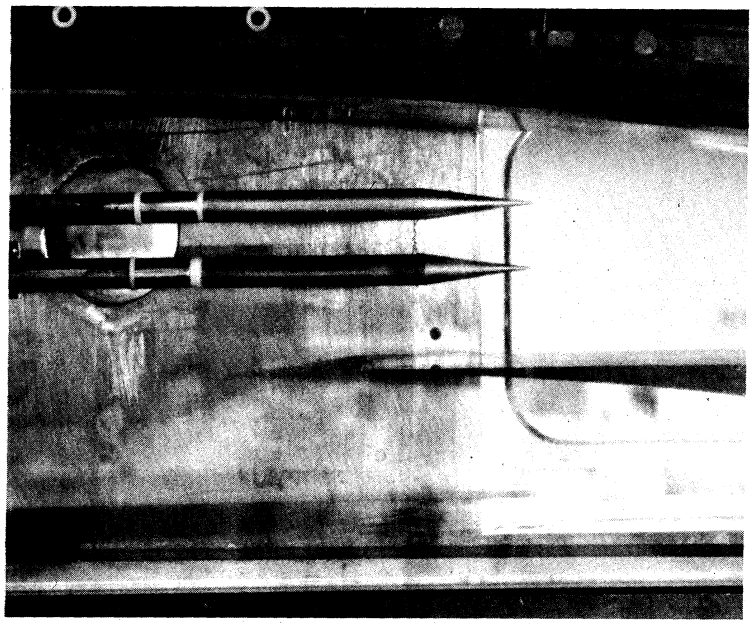

(b) With One Field Coil Installed

Fig. 16 Electrode Installation

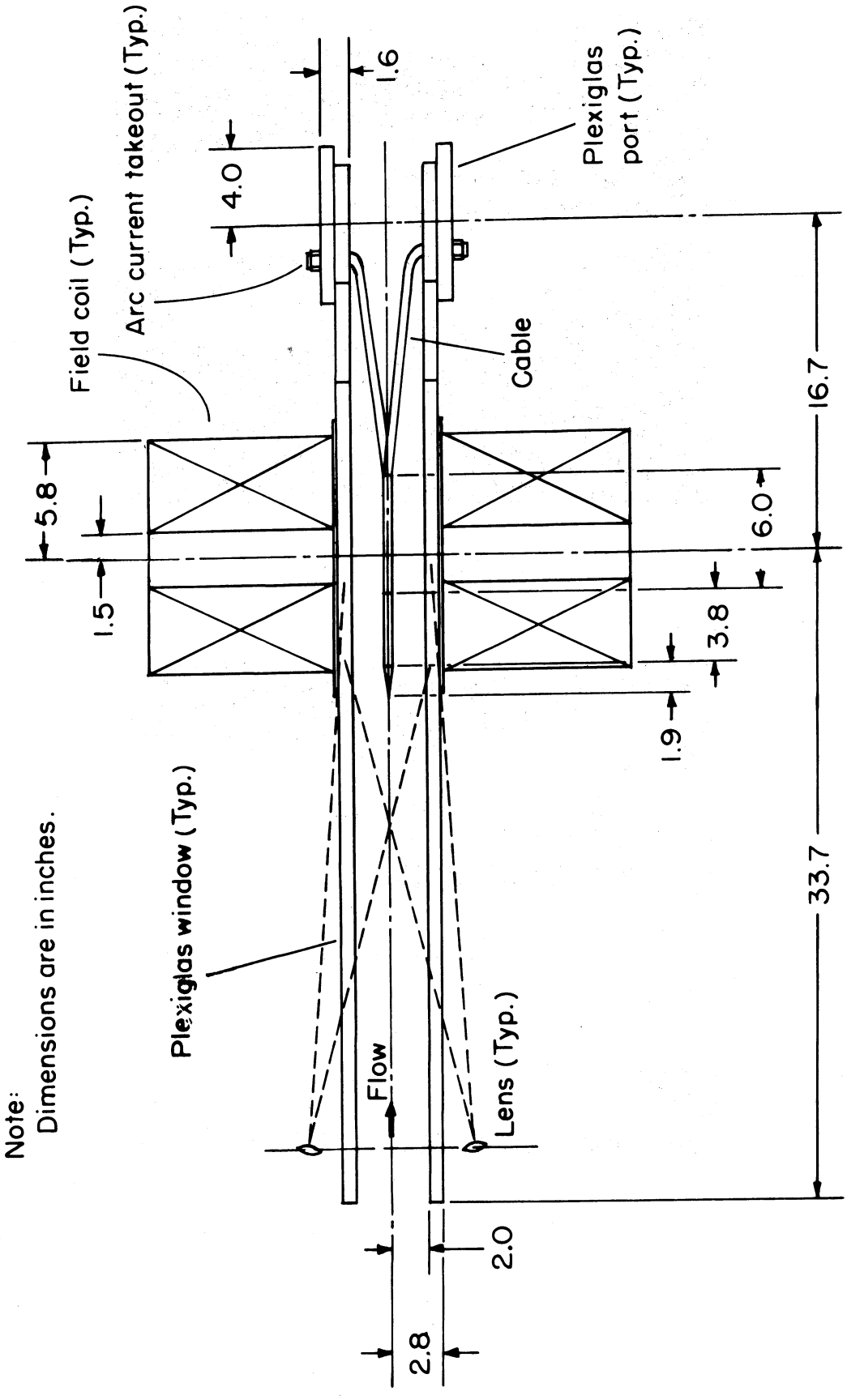

Fig. 17 Top View of Experimental Setup

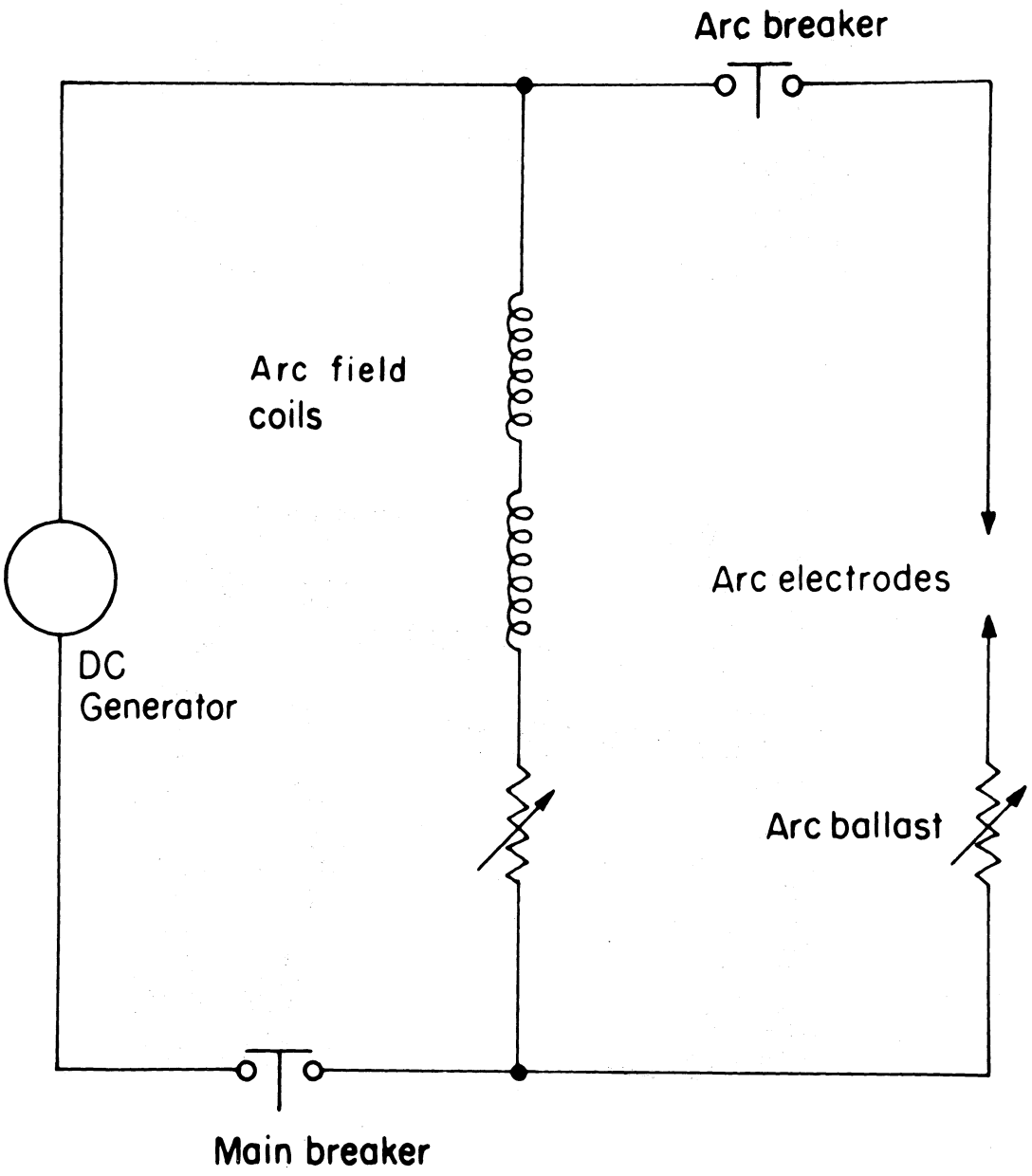

Fig. 18 Schematic Diagram of Power Circuit

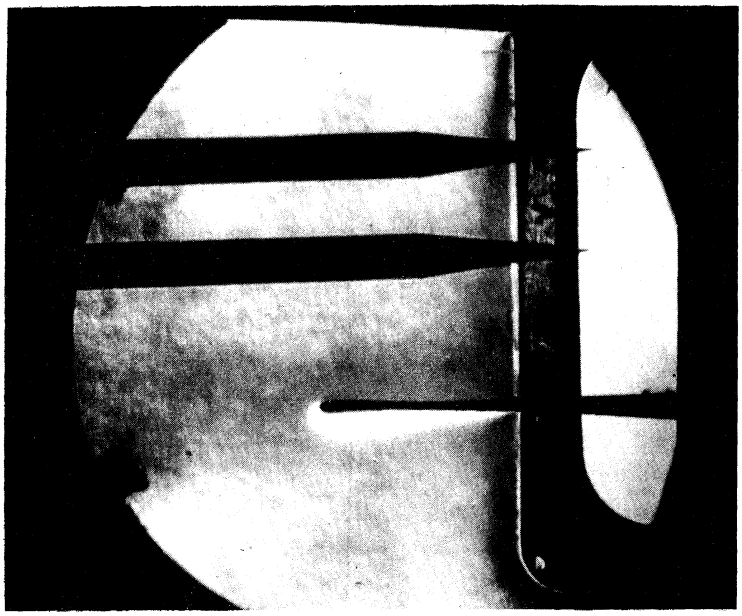

(a) Vacuum, No Flow

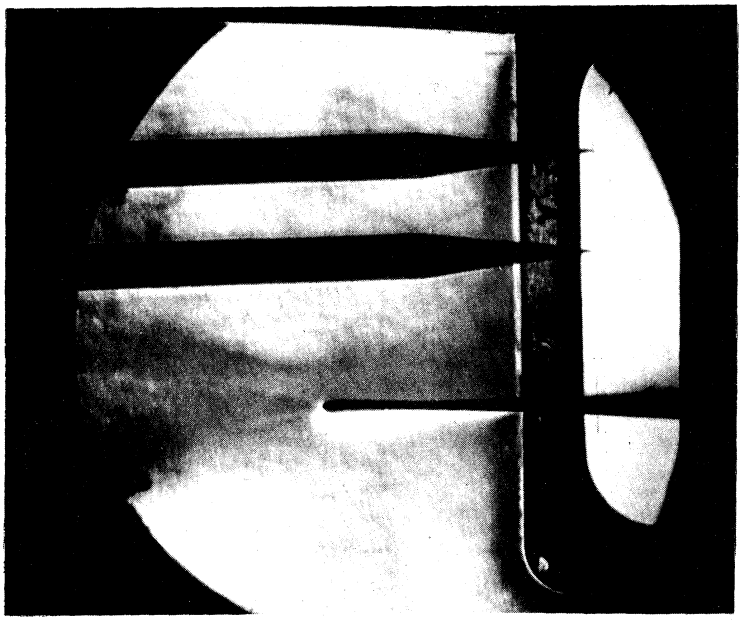

(b) Flow at M = 2.5

Fig. 19 Schlieren Photographs (through 3/4" Plexiglas Windows) of Installed Electrodes.

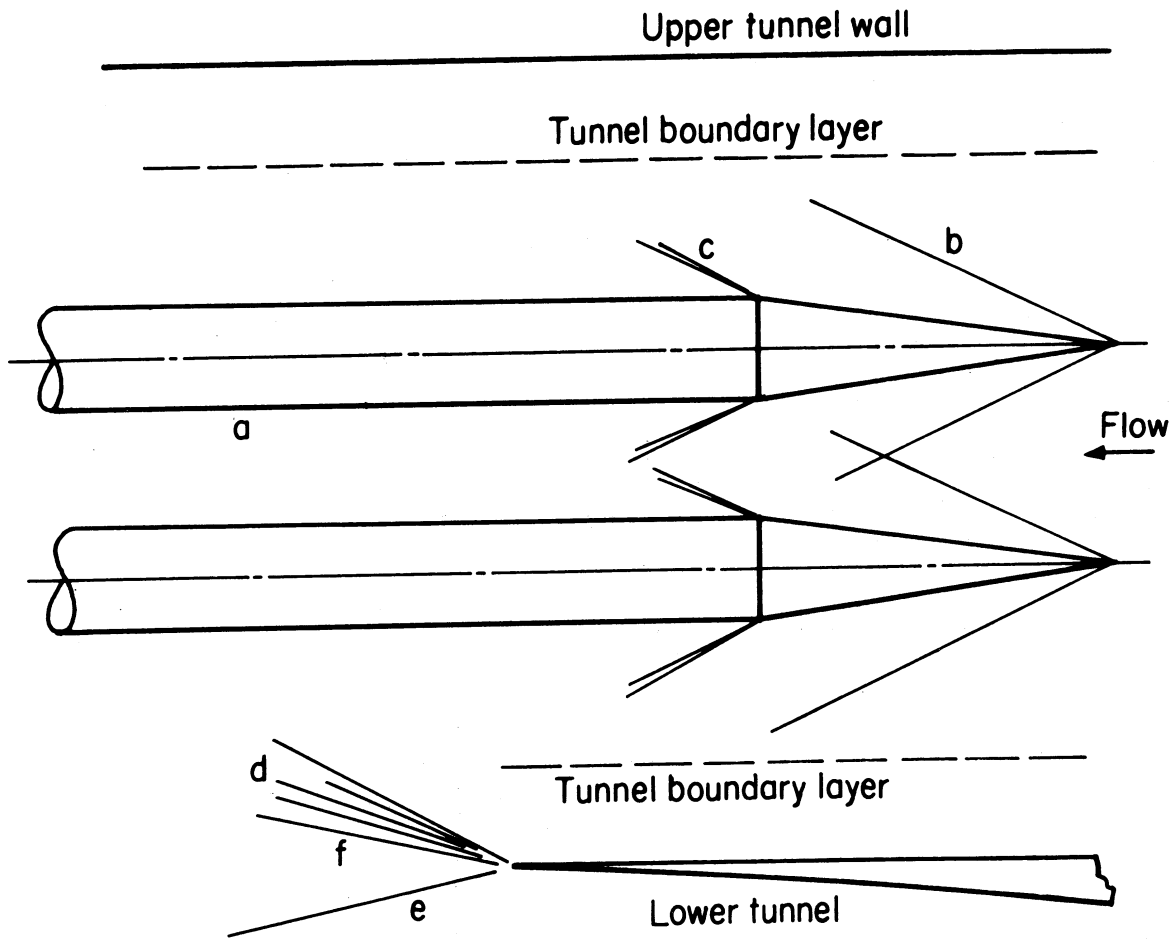

a. Electrode
b. Weak conical shock
c. Conical expansion fan
d. Expansion fan
e. Slip line
f. Lip shock

Scale: Actual size

c. Interpretation of Schlieren Photograph

Fig. 19 (Continued)

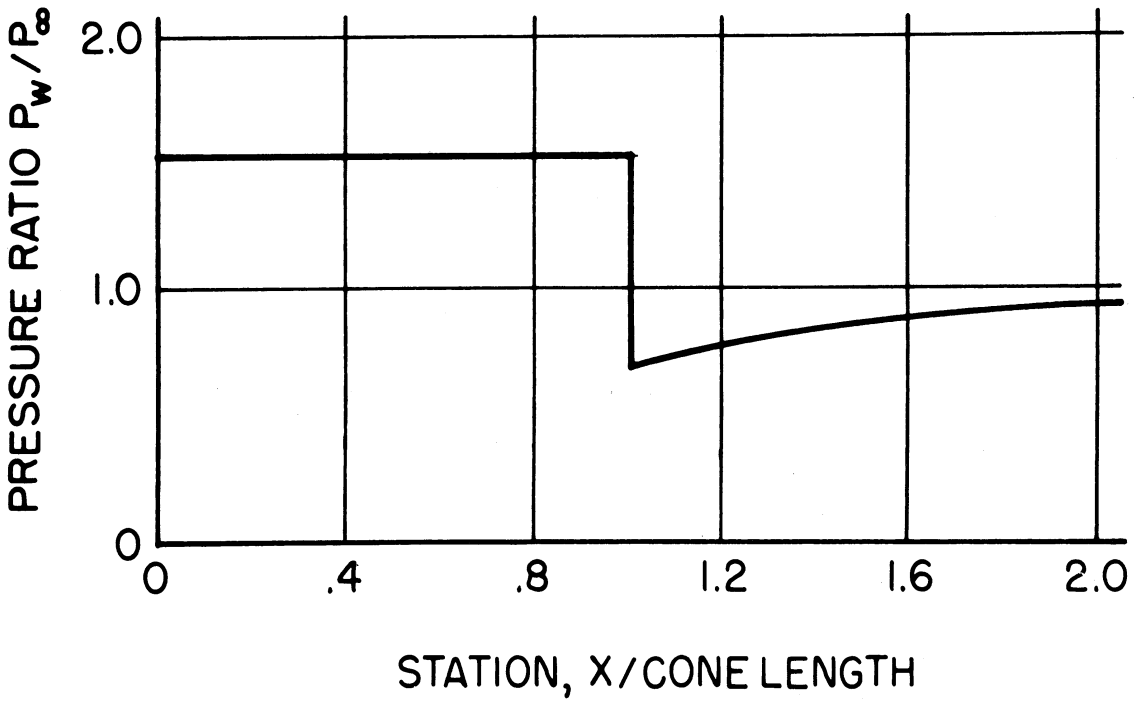

M = 3.0 fineness ratio = 3.0

Fig. 20 Pressure Distribution Typical of Cone Cylinders (from NACA TN 3527)

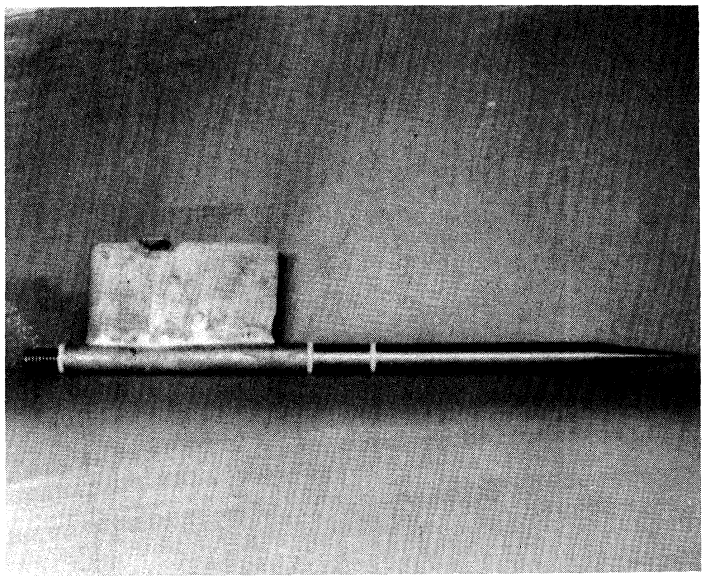

Fig. 21 **Electrode Assembly**

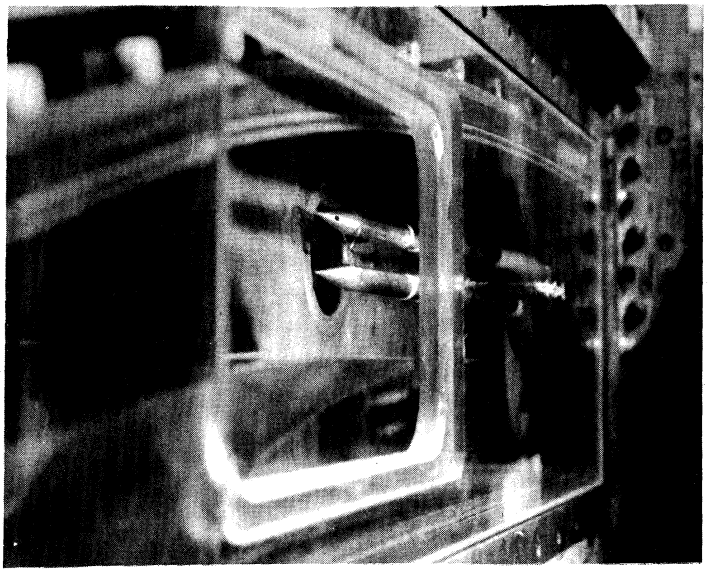

Fig. 22 Electrode Installation Approximately as Seen in Fastax Film Sequences

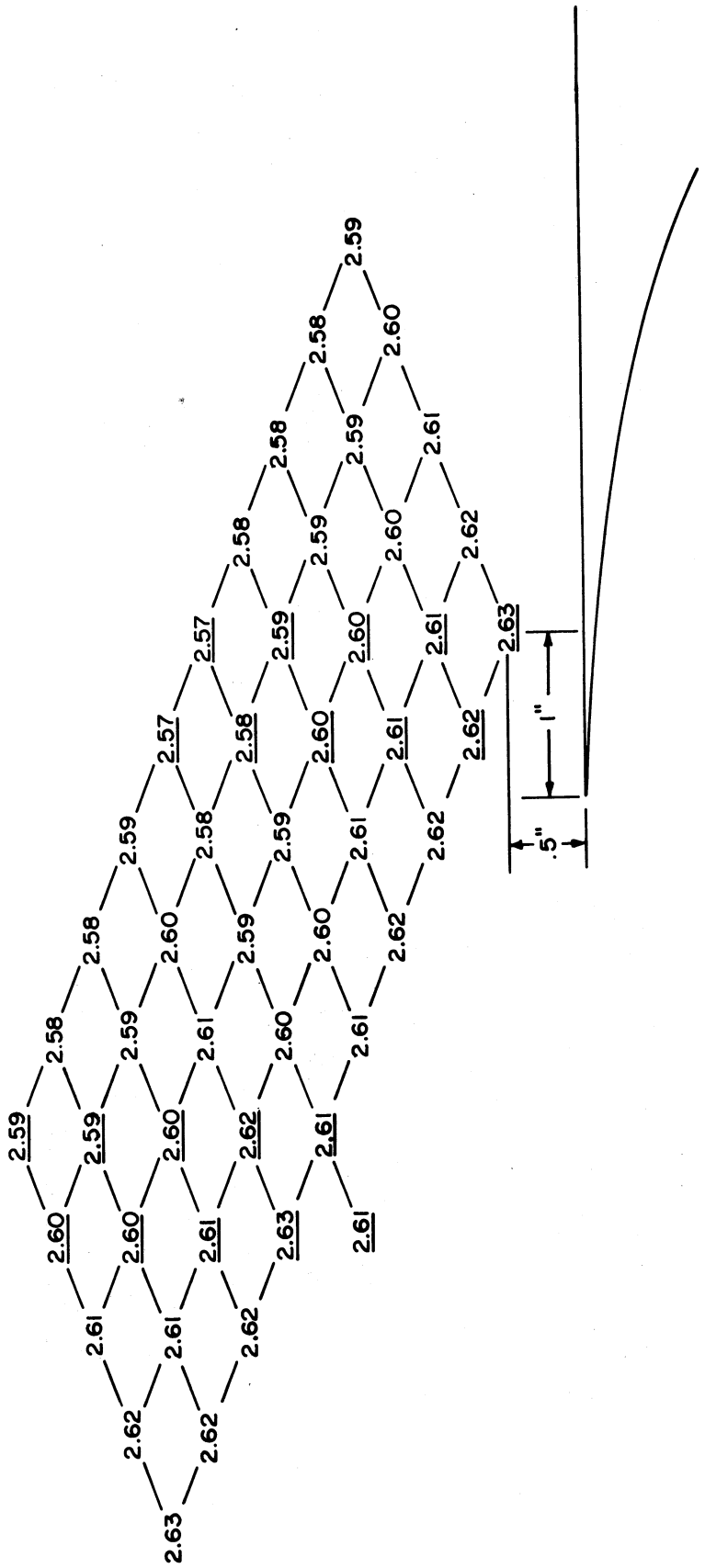

Fig. 23 Mach Number Distribution at M = 2.6

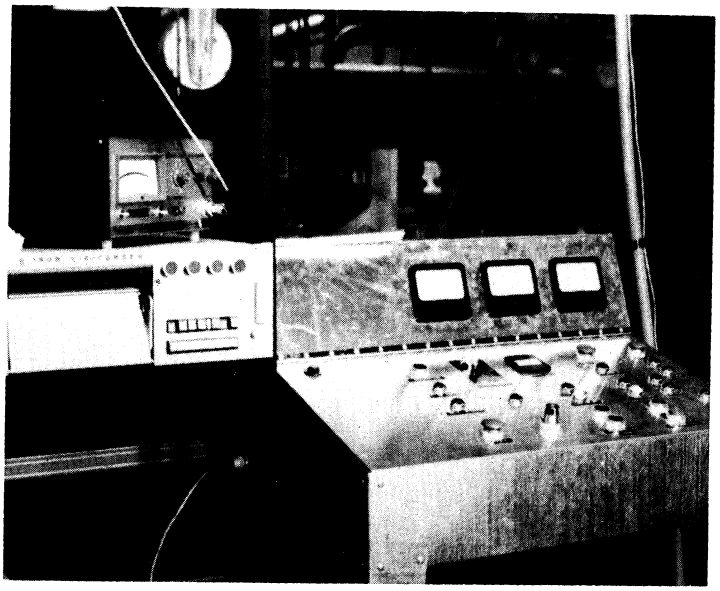

Fig. 24 Control Panel, Visicorder, and Gaussmeter

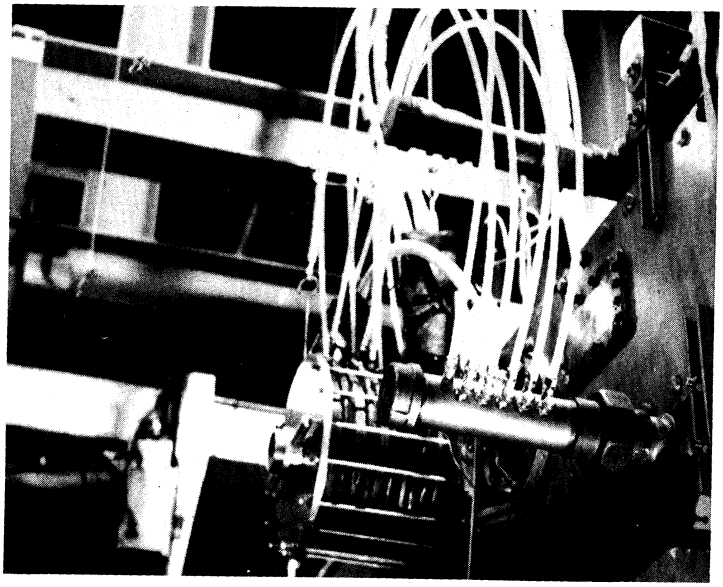

Fig. 25 External Field Coil and Water-Cooling Lines

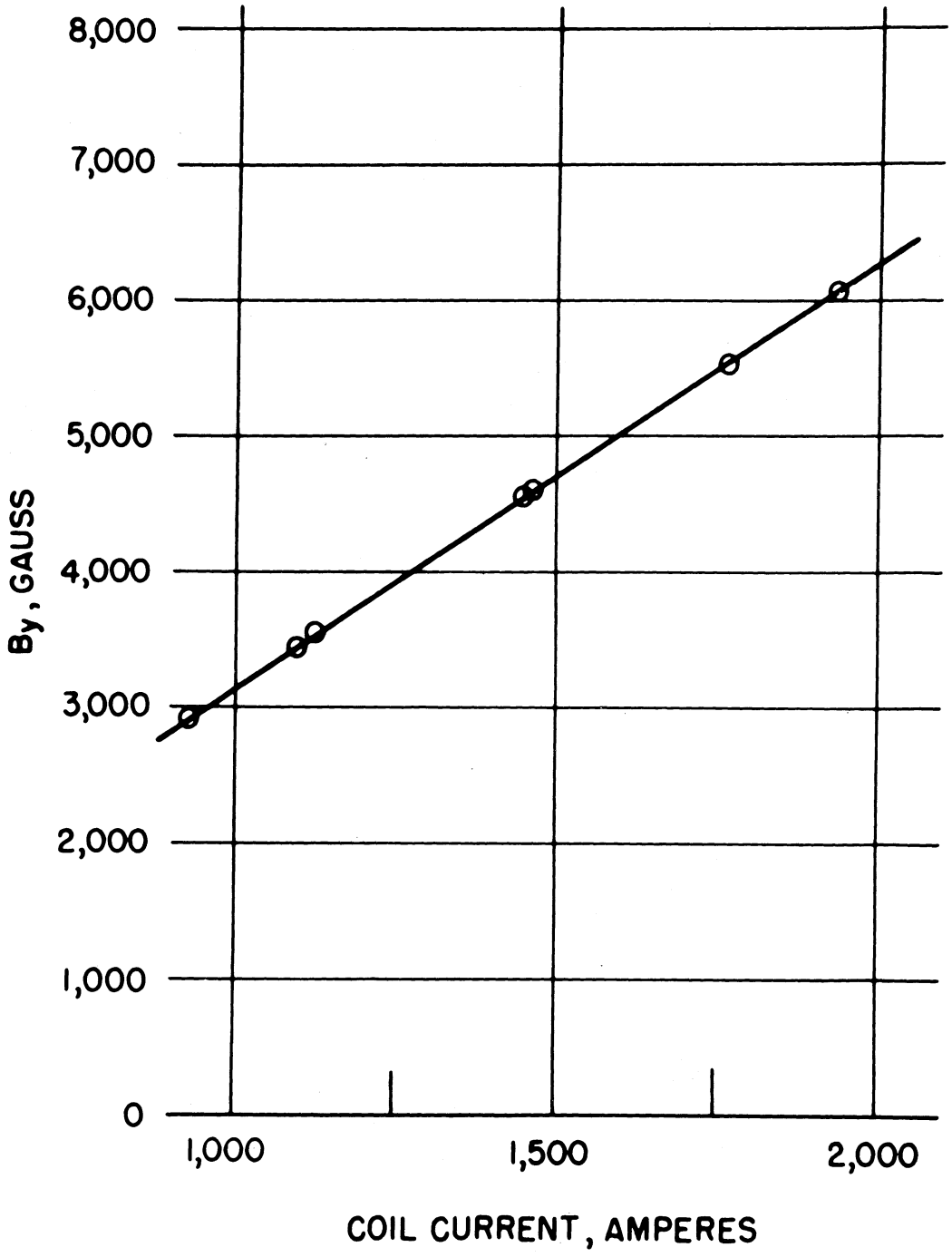

Fig. 26 Typical Measured Variation of B_y with Field-Coil Current

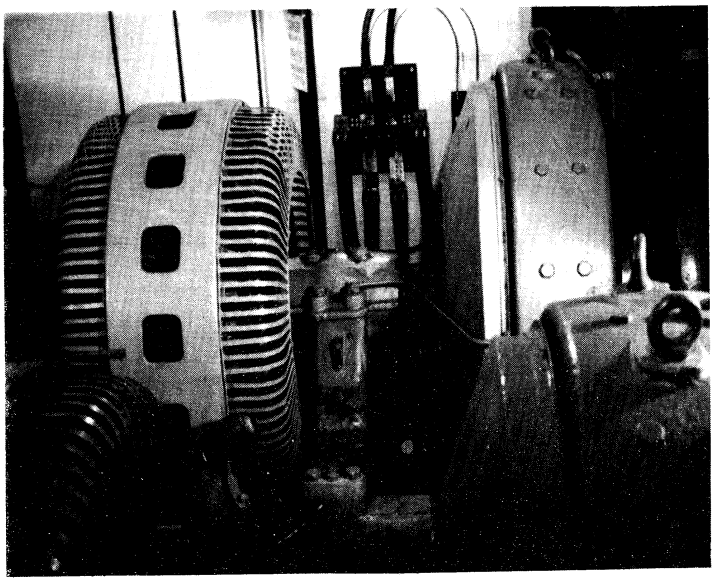

(a) Motor Generator and Armature Switch

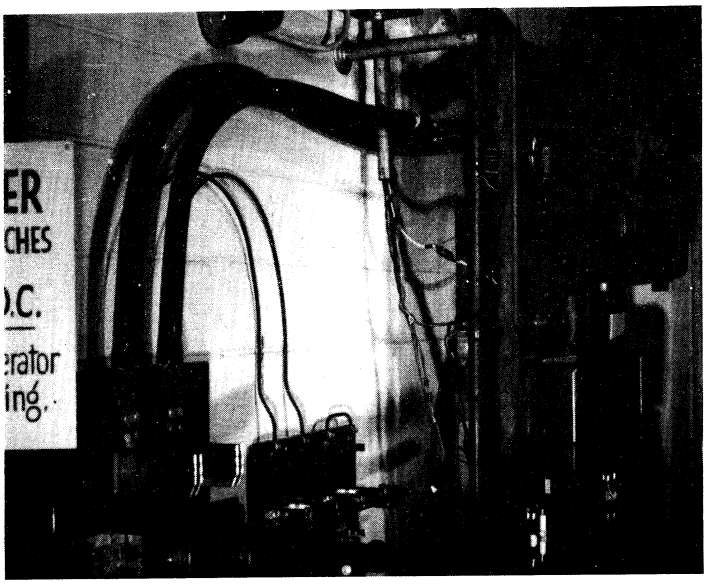

(b) Armature, Field Switches, and Circuit Breakers

Fig. 27 Power Plant Modifications

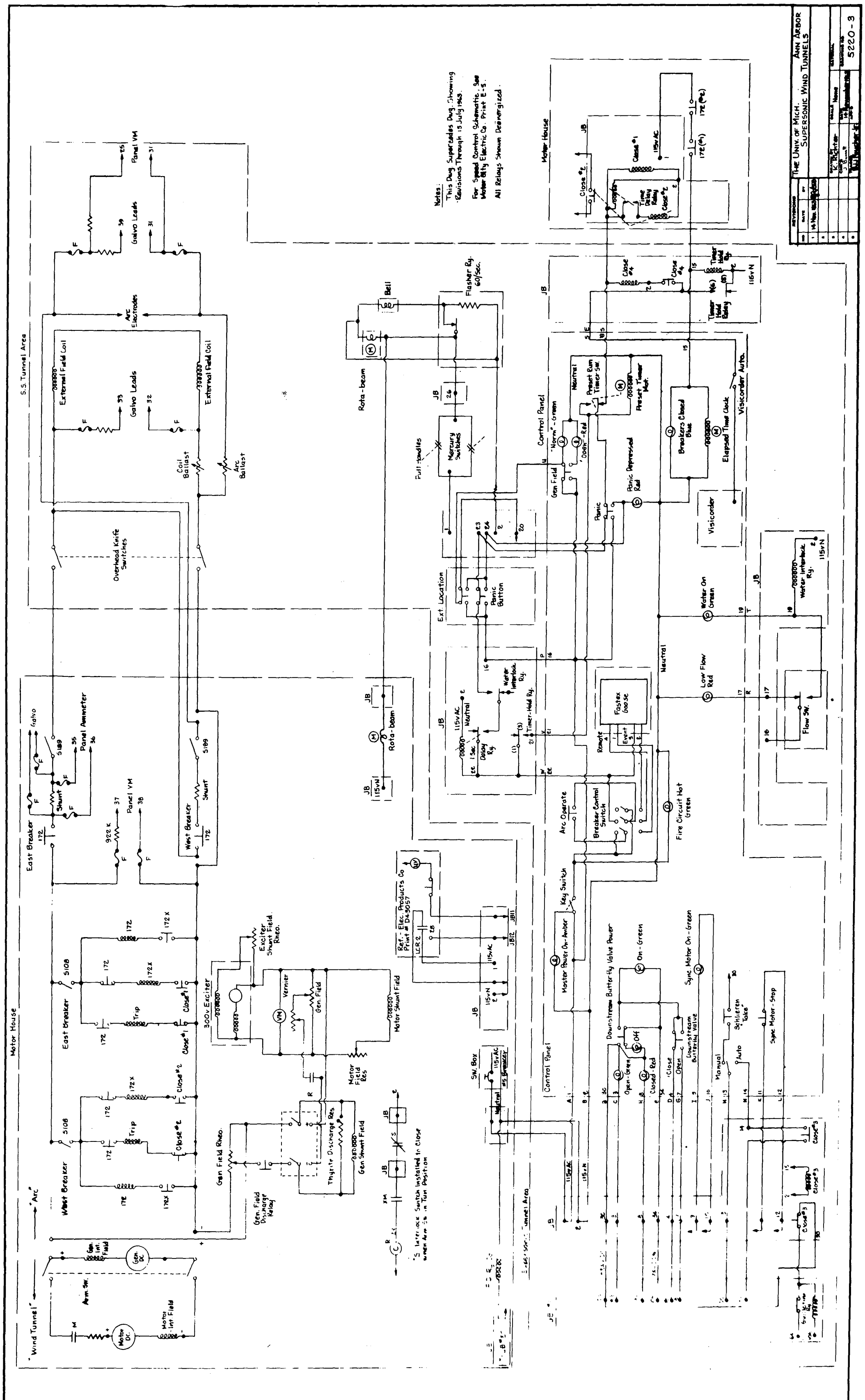
The Univ. of Mich. Ann Arbor
Supersonic Wind Tunnels
5220-3
Notes:
This Dwg. Supersedes Dwg. Showing Revisions Through 15 July 1963.
For Speed Control Schematic, See Westinghouse Elec. Co. Print E-5.
All Relays Shown De-energized.
Motor House
S.S. Tunnel Area
Control Panel
Ext. Location
East Breaker
West Breaker
Overhead Knife Switches
External Field Coil
Arc Electrodes
Galvo Leads
Panel VM
Panel Ammeter
Coil Ballast
Arc Ballast
300v. Exciter
Motor Shunt Field
Gen Field
Vernier
Exciter Shunt Field Rheo.
Motor Field Res
Gen Field Rheo.
Thyrite Discharge Res
Gen Shunt Field
Gen. Field Discharge Relay
Rota-beam
Flasher Ry. 60/sec.
Bell
Mercury Switches
Panic Button
Water Interlock Ry.
Timer-Hold Ry.
Delay Ry
Fastex Loose
Breaker Control Switch
Arc Operate
Key Switch
Master Power On-Amber
Fire Circuit Hot Green
Low Flow Red
Water On Green
Flow Sw.
Visicorder
Visicorder Auto.
Breakers Closed Blue
Elapsed Time Clock
Panic Depressed Red
Preset Timer Mot.
Preset Run Timer Sw.
Downstream Butterfly Valve Power
Downstream Butterfly Valve
Sync Motor On-Green
Sync Motor-Stop
Schlieren "take"
Manual
Auto
Time Delay Relay
Timer Hold Relay
Wind Tunnel
Arc

Fig. 28

(a) Overhead Knife Switches

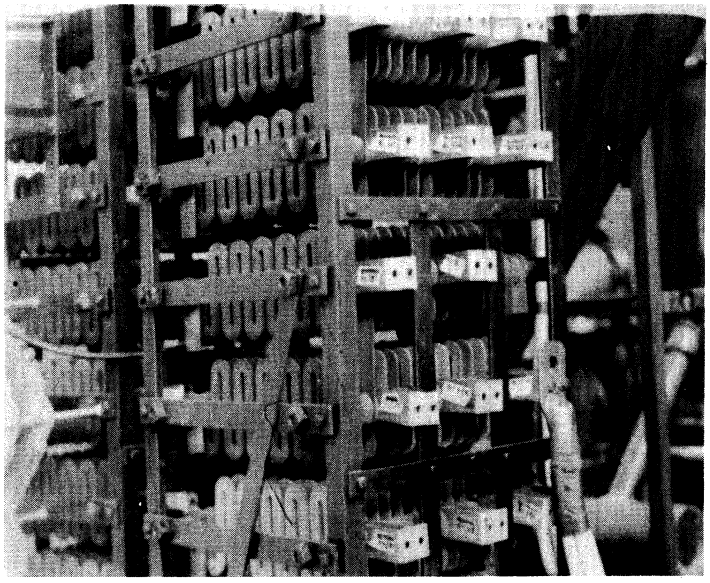

(b) Ballast Resistors, Coil Ballast in Foreground

Fig. 29 Circuit Components

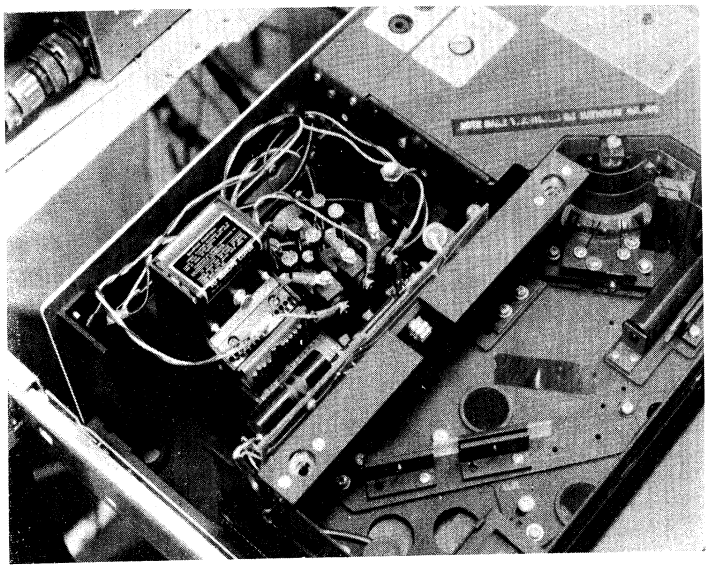

(a) Hathaway Galvanometer Installation (Note Bare Terminals)

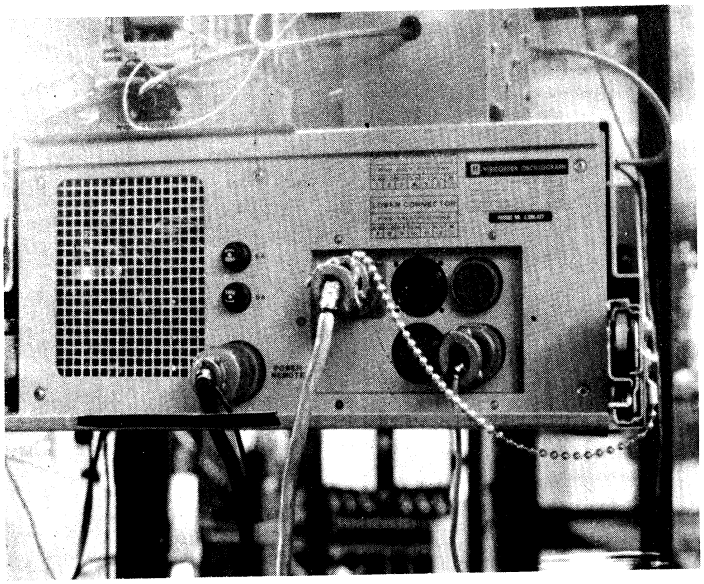

(b) Safety Chain

Fig. 30 Visicorder Modifications

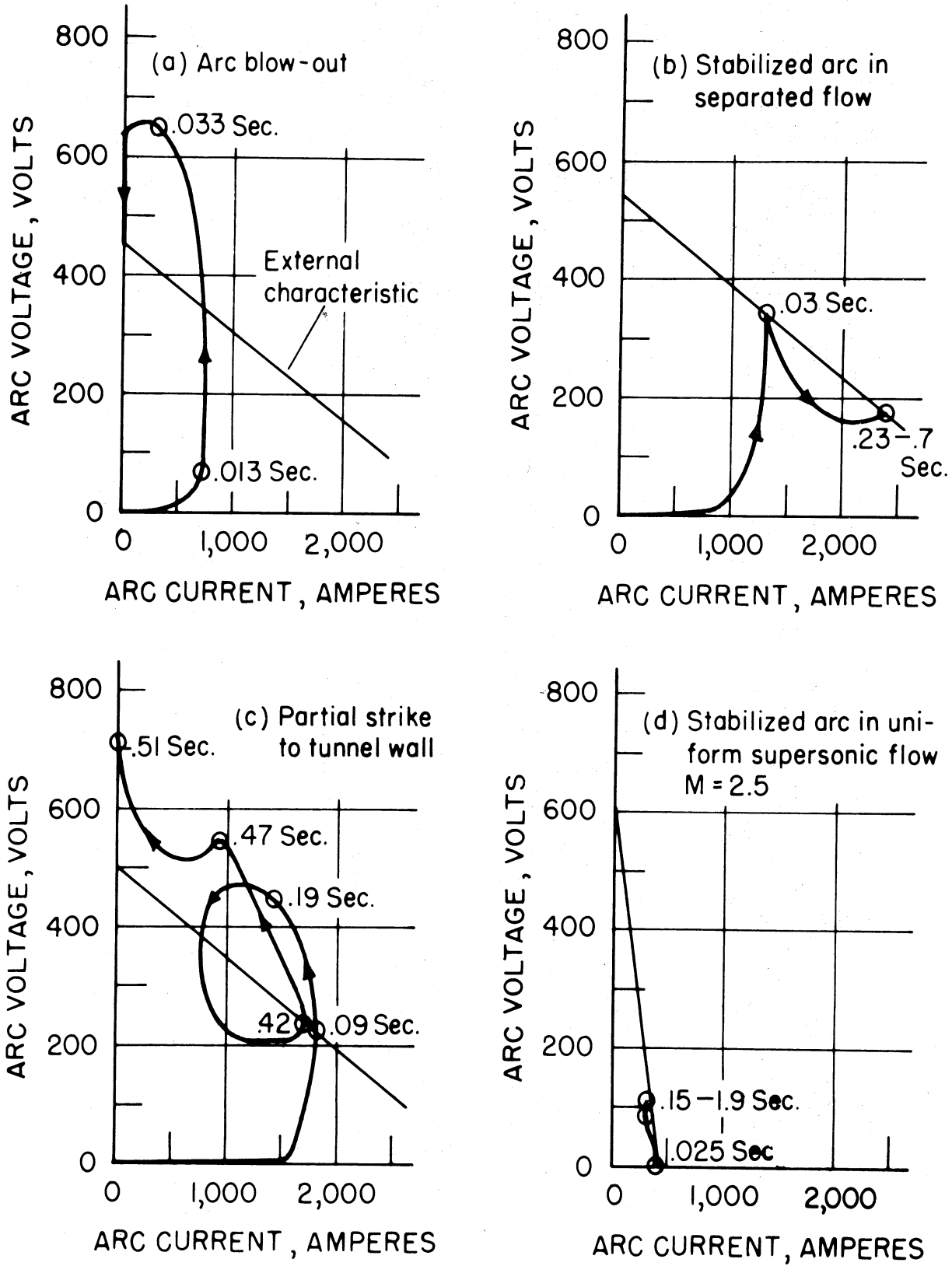

Fig. 31 Voltage-Current Time Histories

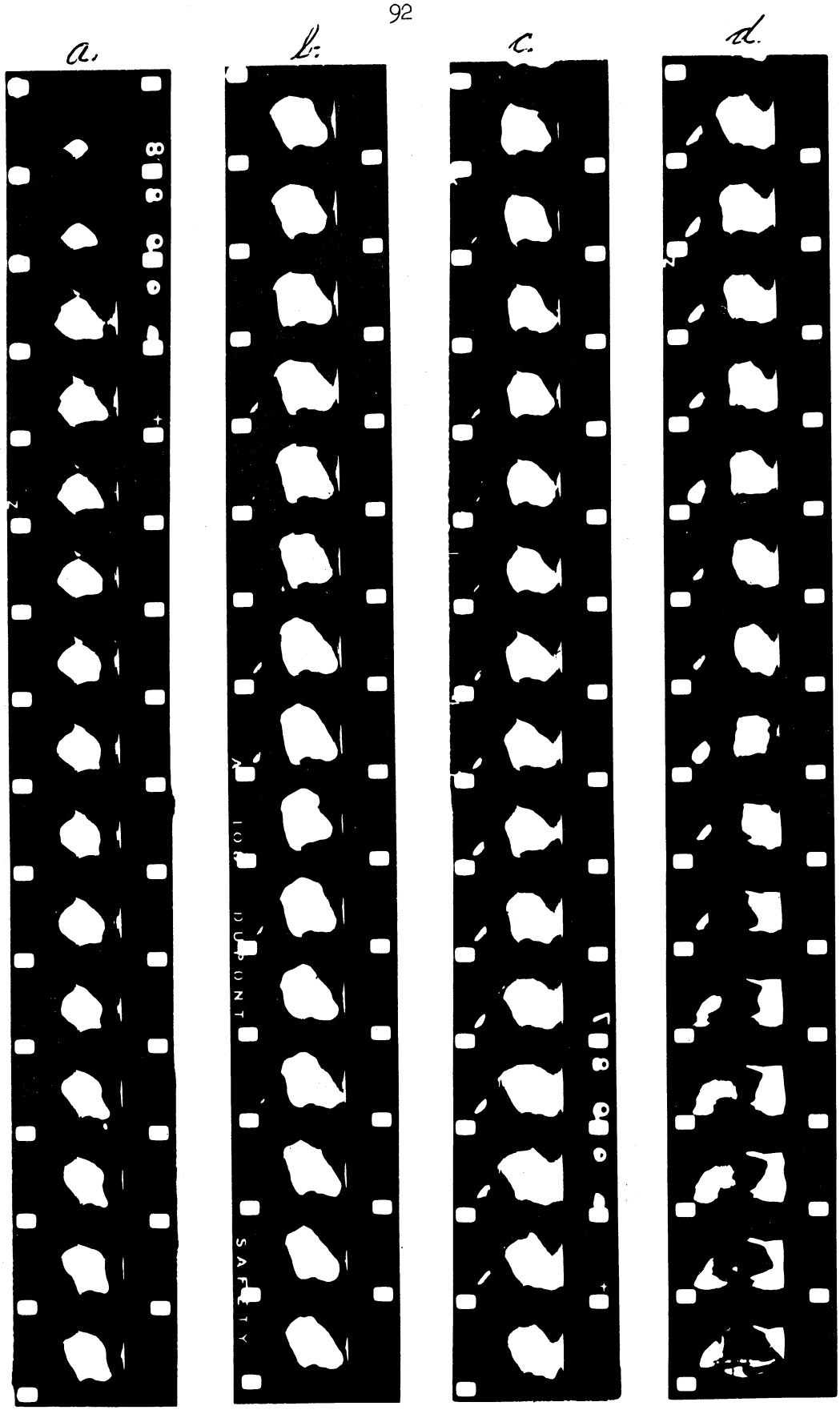

Fig. 32 Fastax Sequence Showing Arc Blown from Rails. M = 2.5, I = 1100 amp, P_{t_1} = 29.5 in. Hg, g = $1\frac{1}{4}$ in. Camera Speed about 3,000 frames/second.

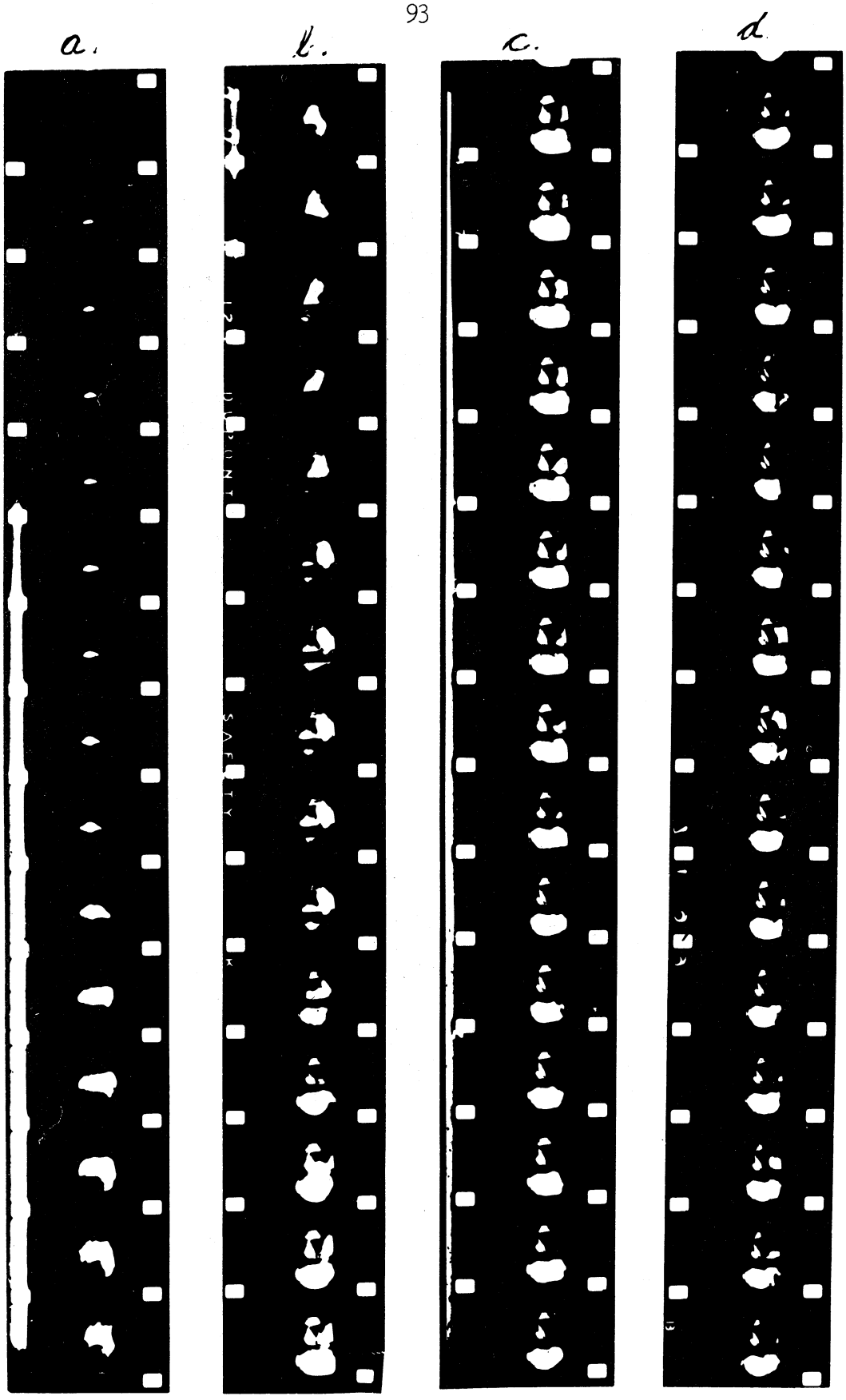

Fig. 33 Fastax Sequence Showing Arc Blown from Rectangular Electrodes and Re-Established between Power Cables, Passing through Lower Tunnel Boundary Layer. M = 2.5, I = 800 amp, P_{t_1} = 29.5 in. Hg, g = $1\frac{1}{4}$ in. Camera Speed about 3,000 frames/sec.

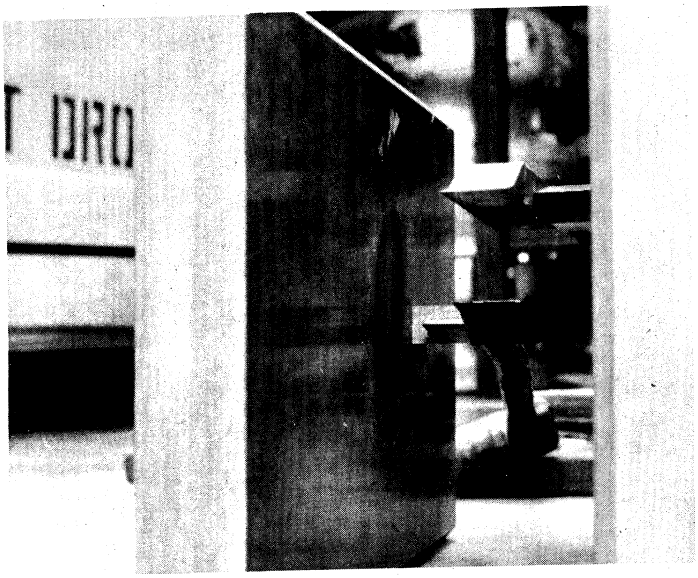

(a) Electrode Orientation

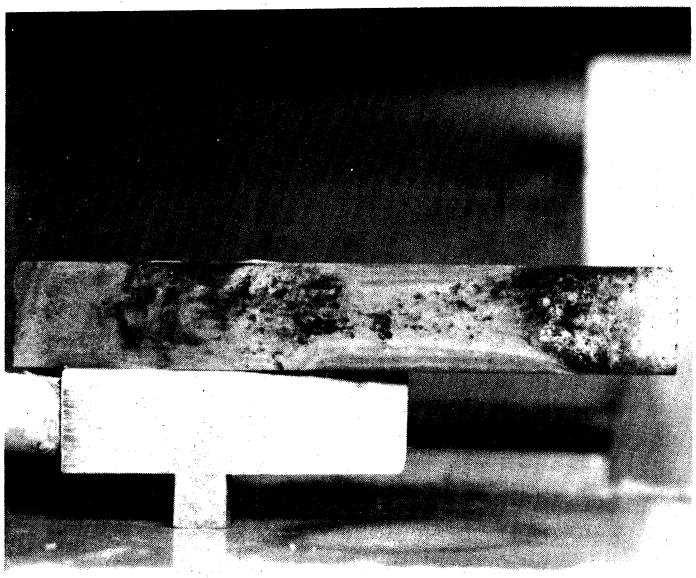

(b) Strike Marks Along Edge of Cathode

Fig. 34 Rectangular Electrodes

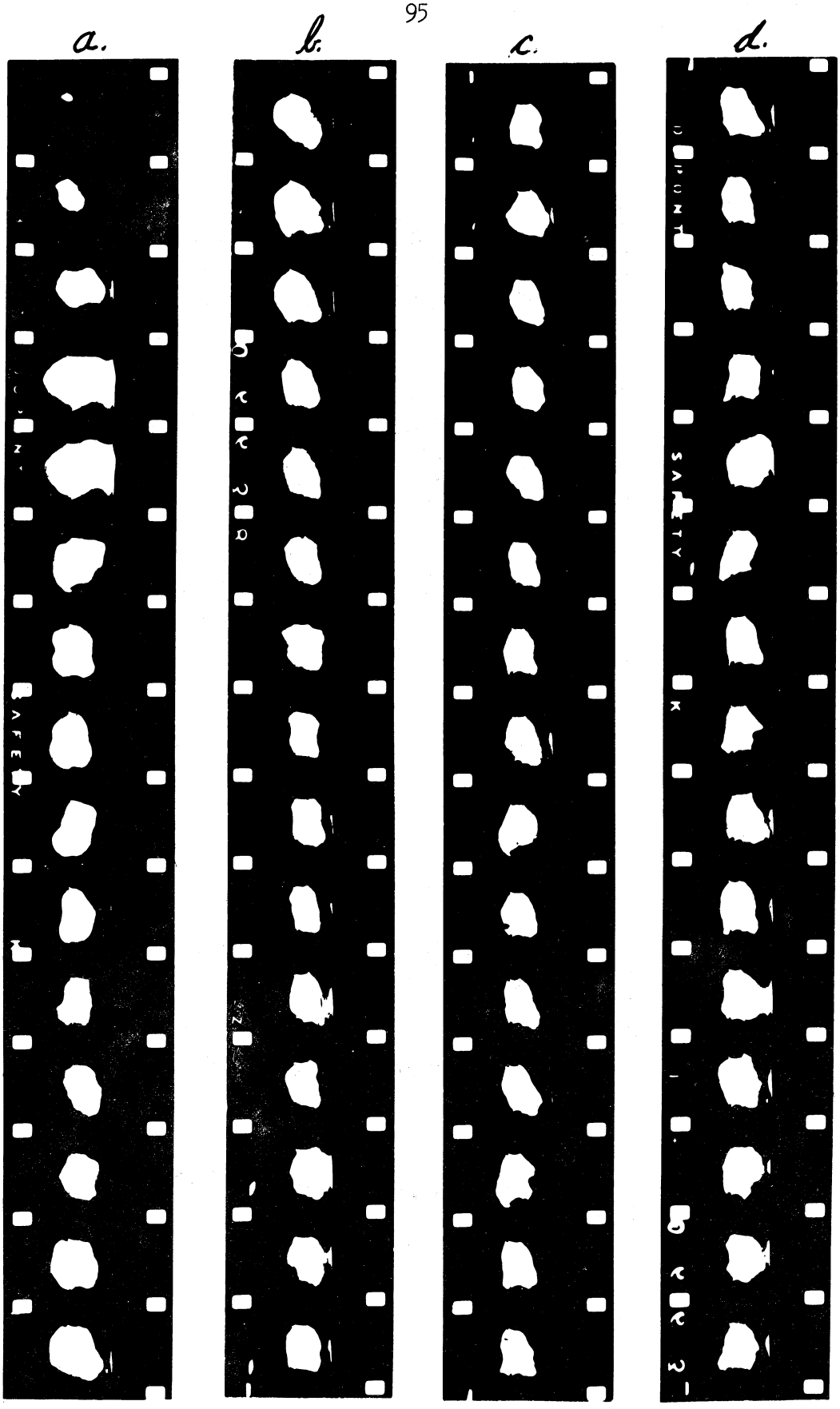

Fig. 35 Fastax Sequence Showing Arc Behavior in Flow Separated due to Excess Heat Addition. M = 2.5, W/Pt_1 = .015 mw/in. Hg, g = $1\frac{1}{2}$ in. Camera Speed about 3,000 frames/second.

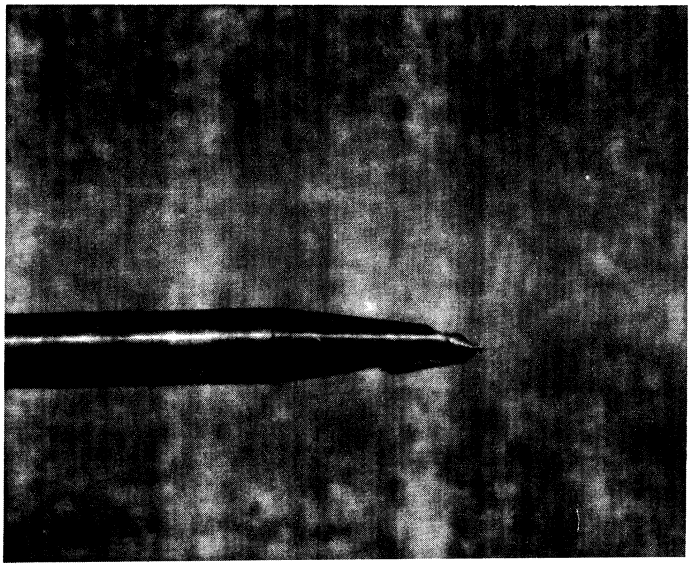

Fig. 36 Anode Tip Strike M = 2.5, I = 380 amp, P_{t_1} = 8.8 in. Hg, g = 0.75 in.

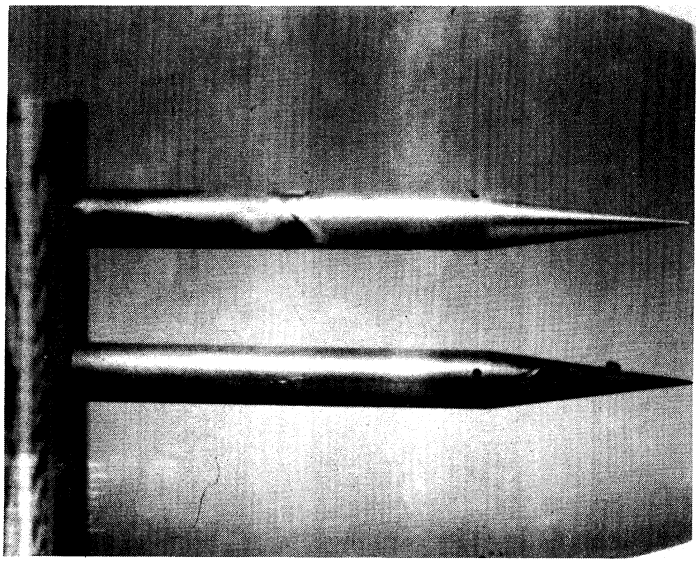

Fig. 37 Root Marks for Tip Strike M = 2.5, P_{t_1} = 10.2 in. Hg, I = 263 amp, g = 0.75 in.

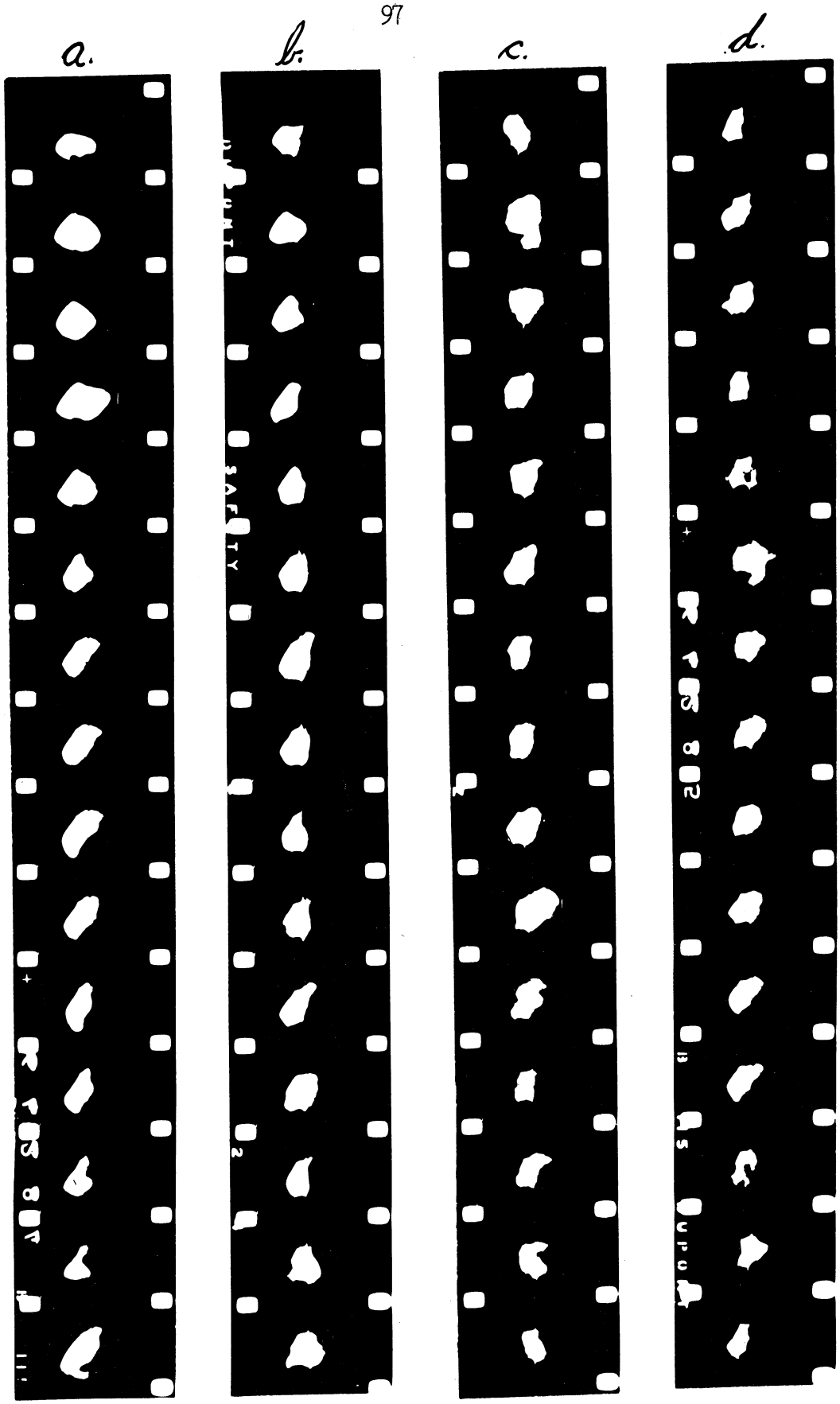

Fig. 38 Fastax Sequence Showing Arc Behavior with Anode Root at Tip of Anode. M = 2.5, I = 900 amp, P_{t_1} = 9.7 in. Hg, g = 0.75 in. Camera Speed about 3,000 frames/second.

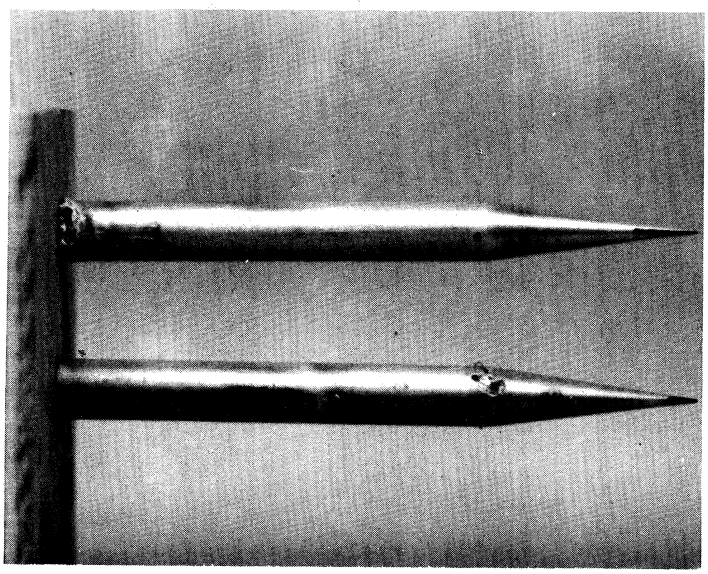

Fig. 39 Root Marks for Base-Strike; M = 2.5, P_{t_1} = 19.9 in. Hg, I = 244 amp, g = 0.75 in. (Top : Near Side of Cathode)

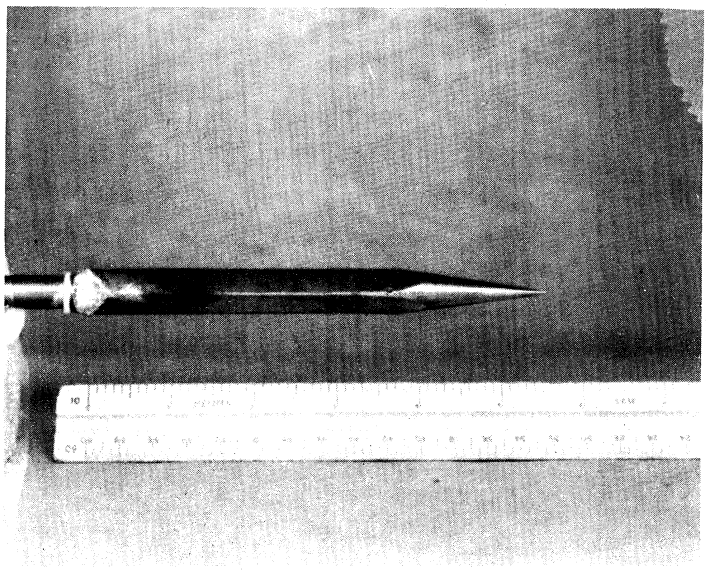

Fig. 40 Effect of Knife Edge on Cathode Root Location for Base-Strike Conditions

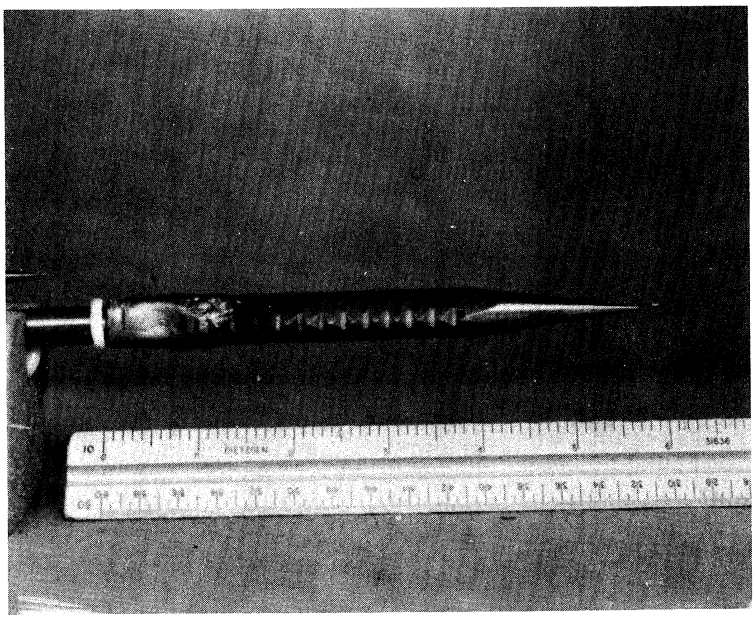

Fig. 41 Effect of Saw-Tooth on Cathode Root Location for Base-Strike Conditions

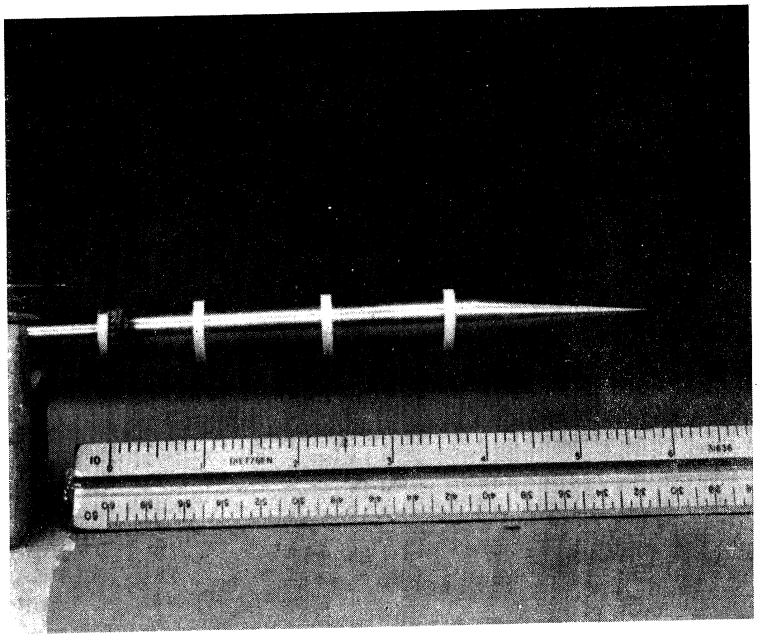

Fig. 42 Effect of Teflon Baffles on Cathode Root Location for Base-Strike Conditions

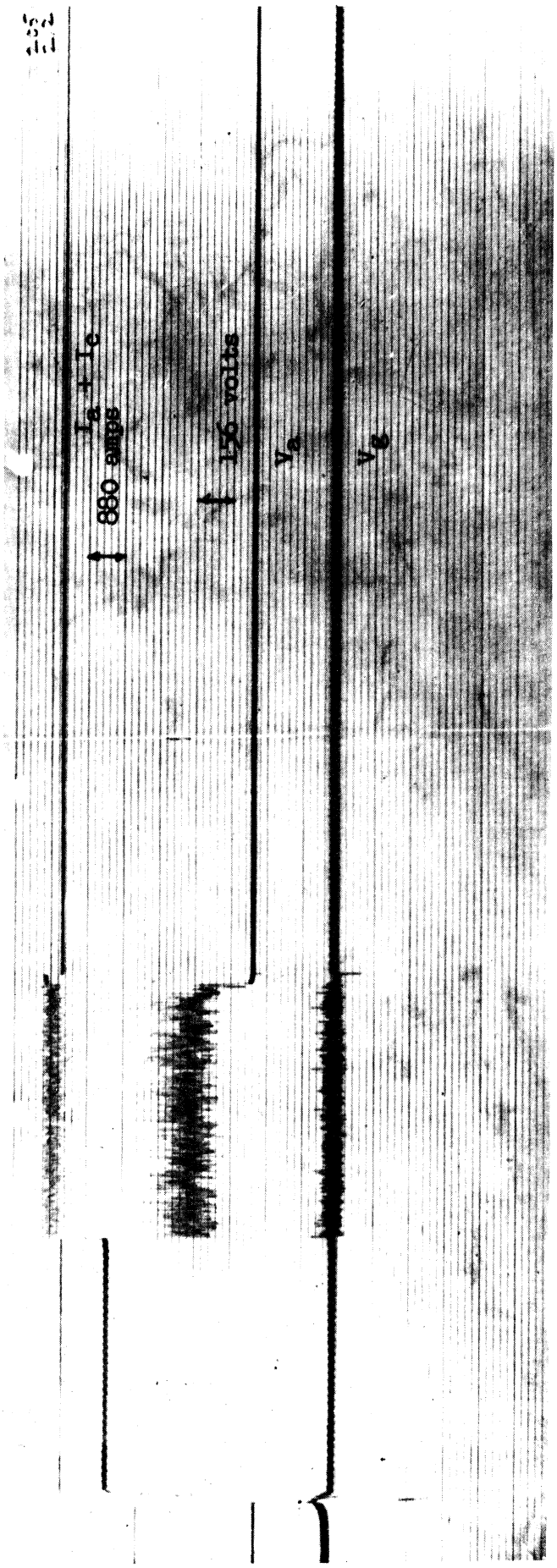

Fig. 43 Oscillograph Trace for Base-Strike Run.

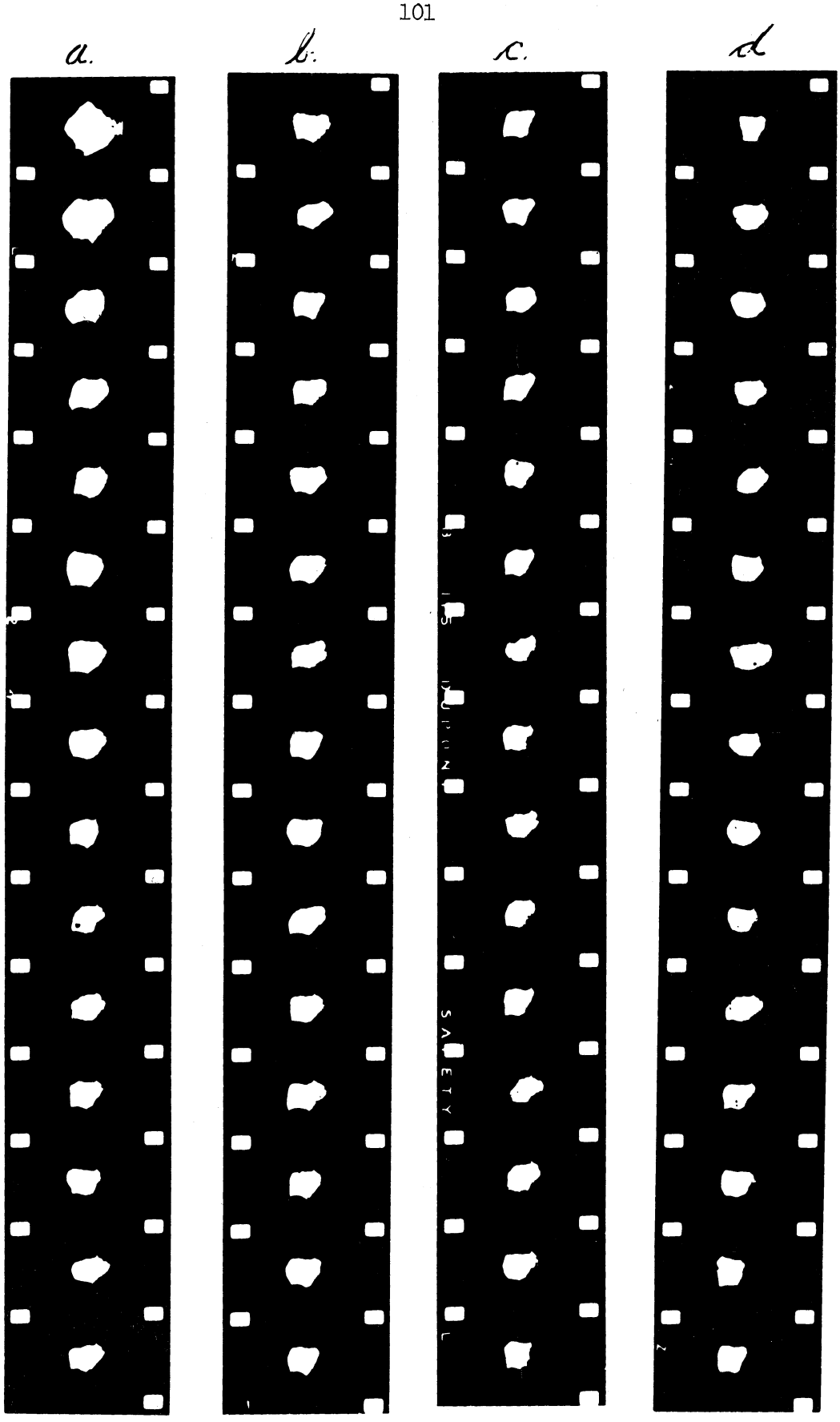

Fig. 44 Fastax Sequence Showing Arc Behavior with Cathode Root at Base of Cathode. M = 2.5, I = 900 amp, P_{t_1} = 29.5 in. Hg, g = 0.75 in. Camera Speed about 3,000 frames/second.

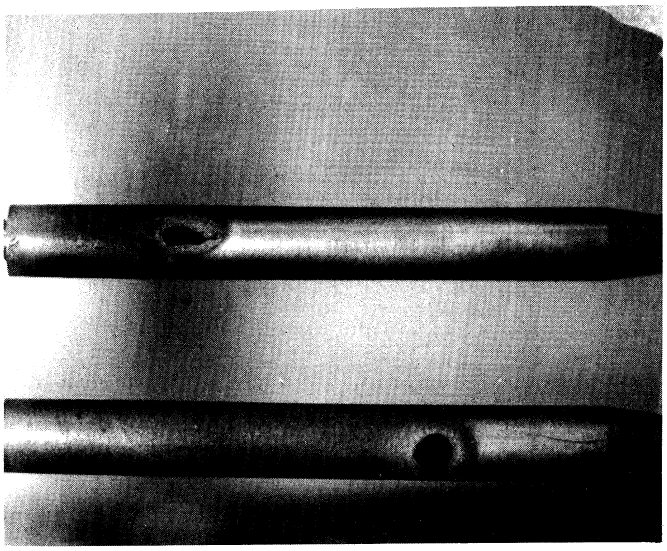

Fig. 45 Root Marks on Carbon Electrodes; M = 2.5, I = 233 amp, P_{t1} = 20.6 in. Hg, g = 0.6 in. (Top : Cathode)

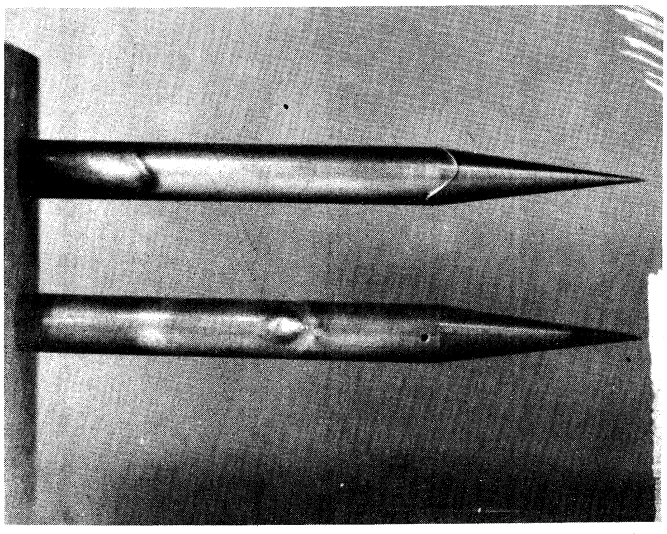

Fig. 46 Root Marks from Run Showing that Anode Root Need Not Strike Near Anode Cone for Stable Arc; M = 2.5, P_{t1} = 19.4 in. Hg, I = 340 amp, g = 0.6 (Top : Cathode)

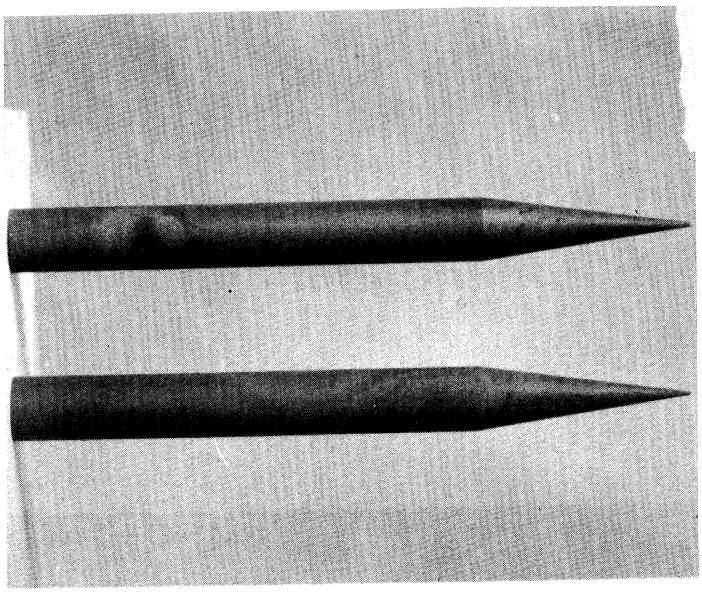

(a) Without Baffle: M = 2.5, P_{t_1} = 15.6 in. Hg, I = 300 amp, g = 0.75 in., W/P_{t_1} = .003

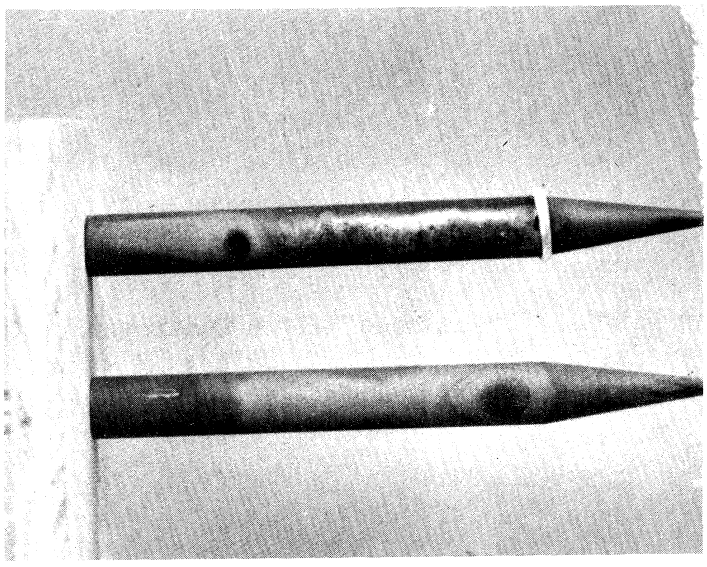

(b) With Baffle: M = 2.5, P_{t_1} = 15.5 in. Hg, I = 280 amp, g = 0.75 in., W/P_{t_1} = .002

Fig. 47 Effect of Flow Baffle on Root Location

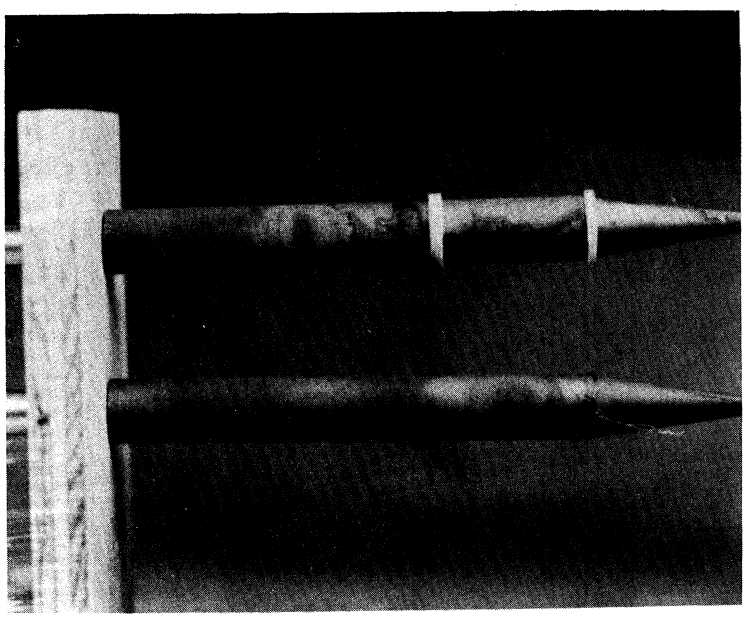

(c) Three Baffles (Downstream Baffle Destroyed by Arc Due to Extra Current in Field Coil); M = 2.5, P_{t_1} = 15.7 in. Hg, I = 420 amp, g = 0.75 in., W/P_{t_1} = .003

Fig. 47 Continued

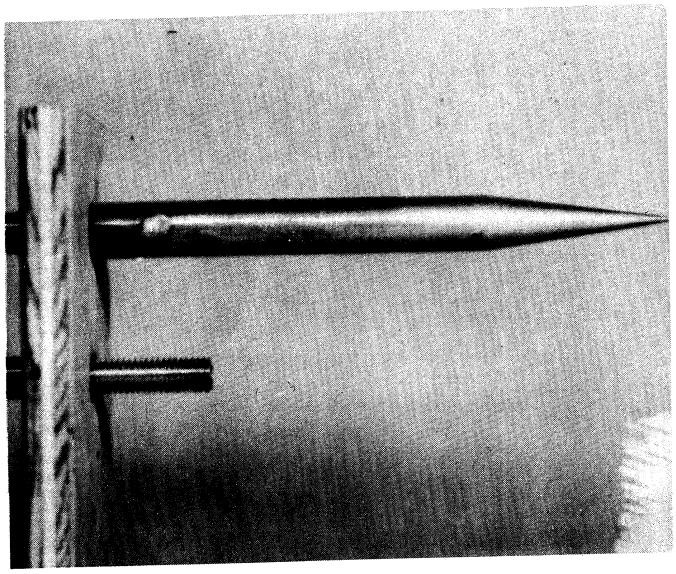

Fig. 48 **Cathode Root Mark for Stable Arc Shown in Fig. 60 (Anode Mark Accidentally Erased); M = 2.5, I = 132 amp, P_{t_1} = 20.2 in. Hg, g = 1.1 in.**

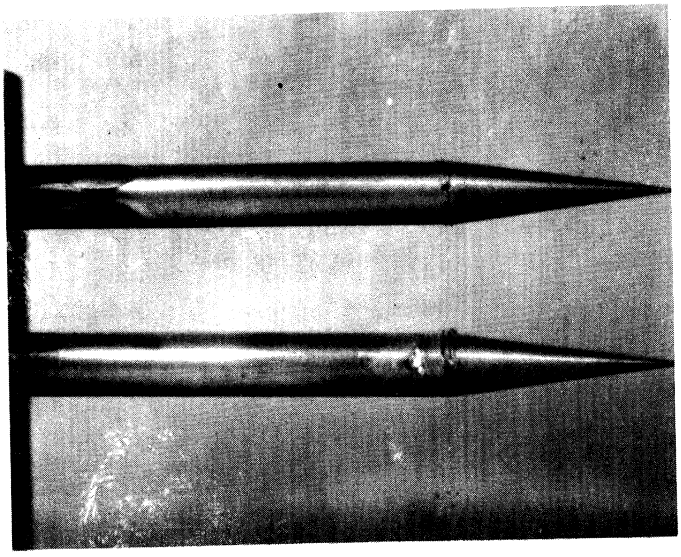

Fig. 49 Root Marks from Run where Cathode Root Switched Far-Side Locations During Run; M = 2.5, P_{t_1} = 17.7 in. Hg, I = 282 amp, g = 1.1 in. (Top : Far Side of Cathode)

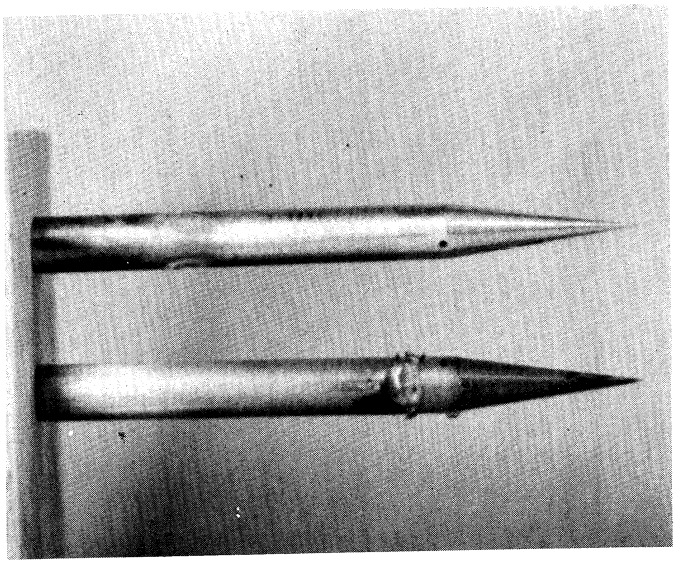

Fig. 50 **Root Marks for Stable Arc Shown in Fig. 57-8; M = 2.5, P_{t_1} = 15.6 in. Hg, I = 330 amp, g = 0.75 in.**

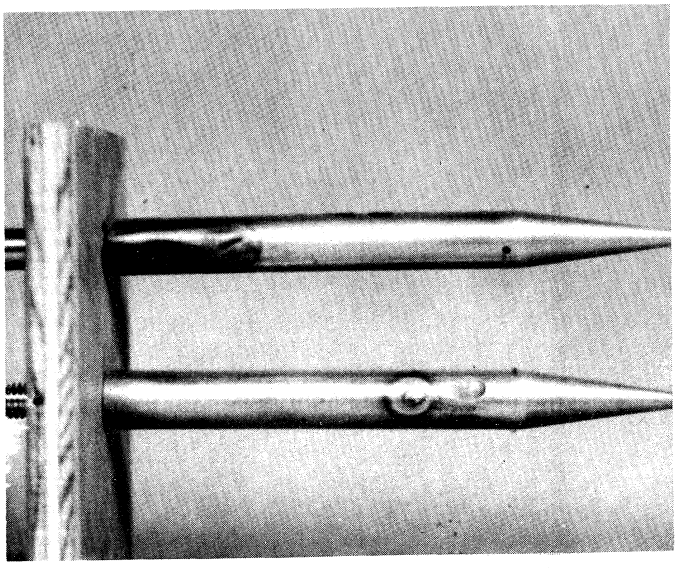

Fig. 51 Root Marks for Stable Arc Shown in Fig. 59 (Upstream Anode Mark from a Previous Run); M = 2.5, P_{t_1} = 20.2 in. Hg, I = 150 amp, g = 0.6 in.
(Top : Far Side of Cathode)

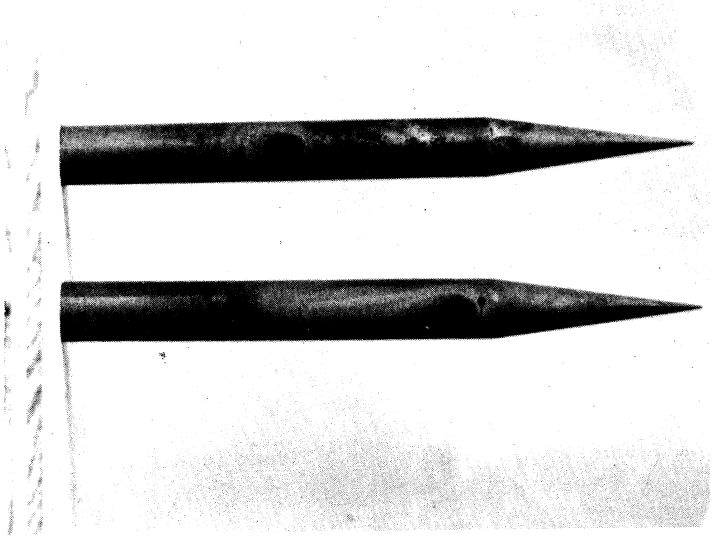

Fig. 52 Root Marks from Run with Normal Polarity; M = 2.5, P_{t_1} = 9.8 in. Hg, I = 340 amp, g = 0.6 in. (Top : Cathode)

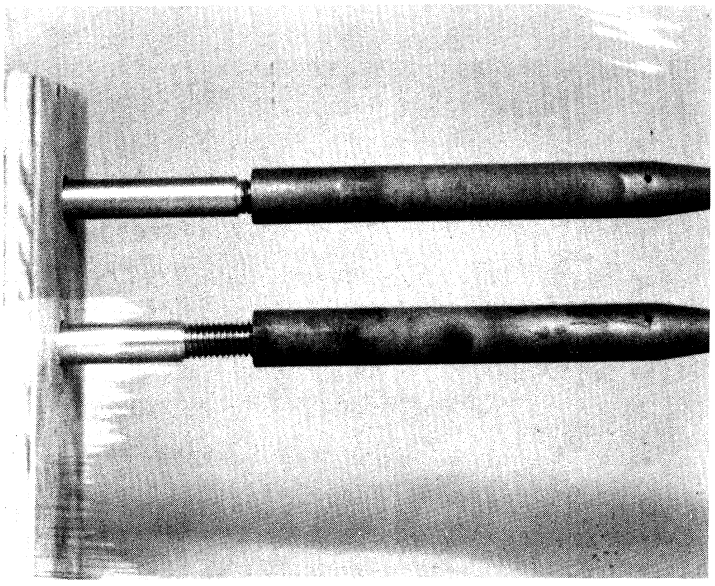

Fig. 53 Root Marks from Run with Reversed Polarity; M = 2.5, P_{t_1} = 9.3 in. Hg, I = 320 amp, g = 0.6 in. (Top : Anode)

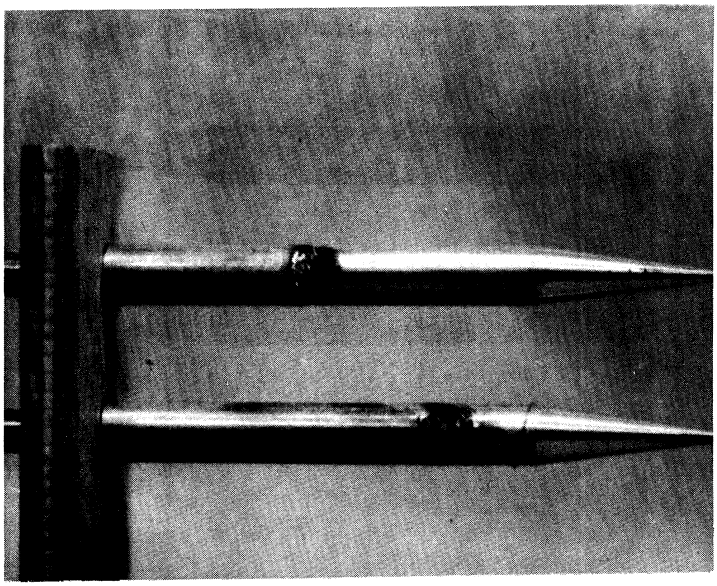

Fig. 54 Root Marks on Brass Electrodes; M = 2.0, I = 301 amp, P_{t_1} = 14.9 in. Hg, g = 0.6 in. (Top : Cathode)

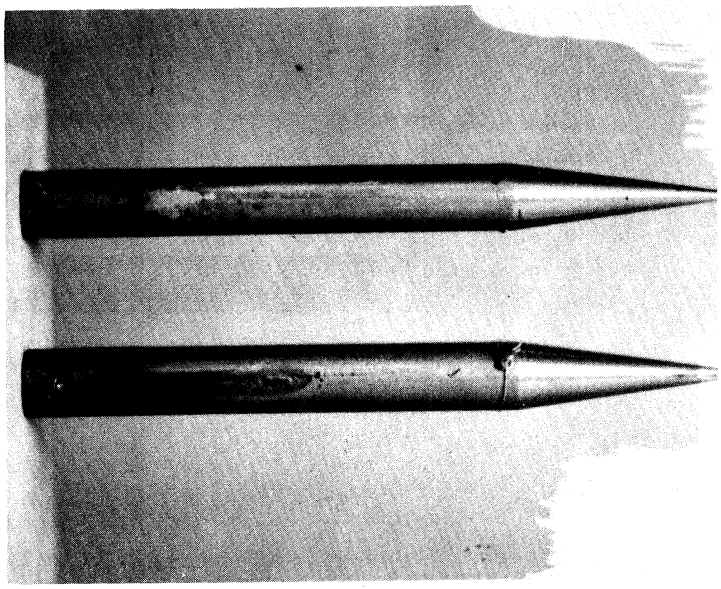

Fig. 55 Root Marks on Steel Electrodes; M = 2.5, P_{t_1} = 14.2 in. Hg, I = 320 amp, g = 0.6 in. (Top : Cathode)

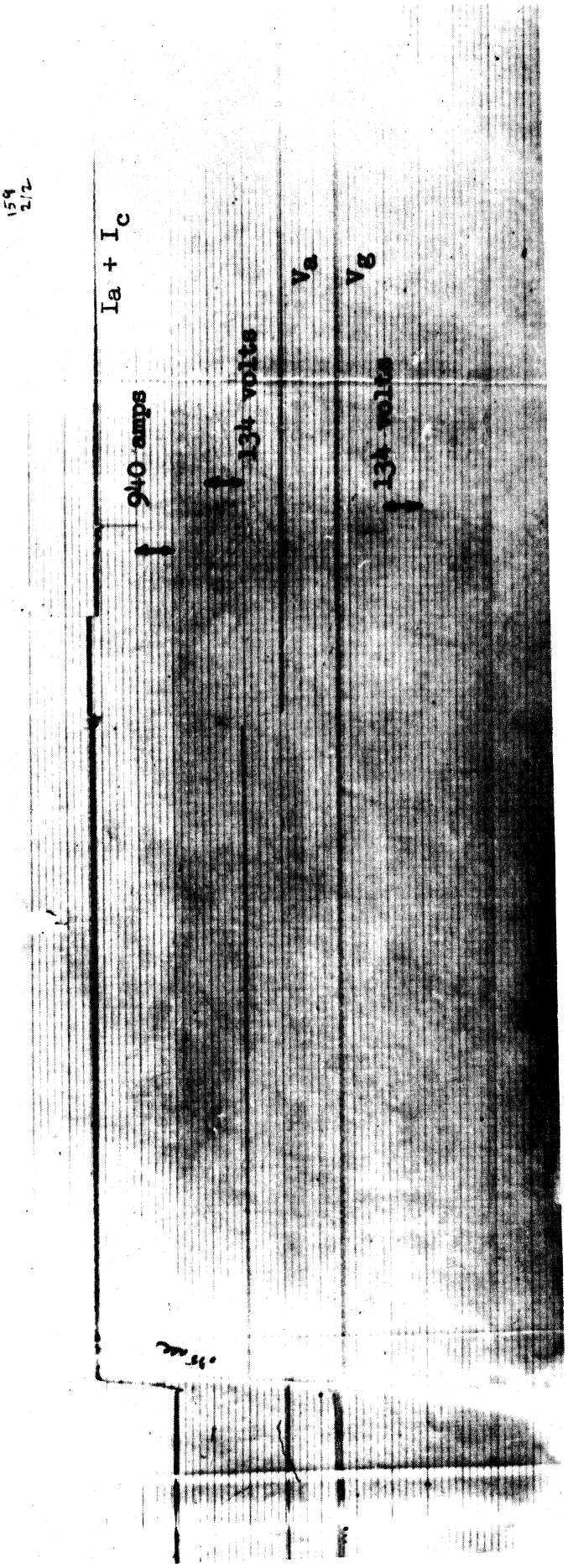

Fig. 56 Oscillograph Trace for the Stable Arc of Fig. 60

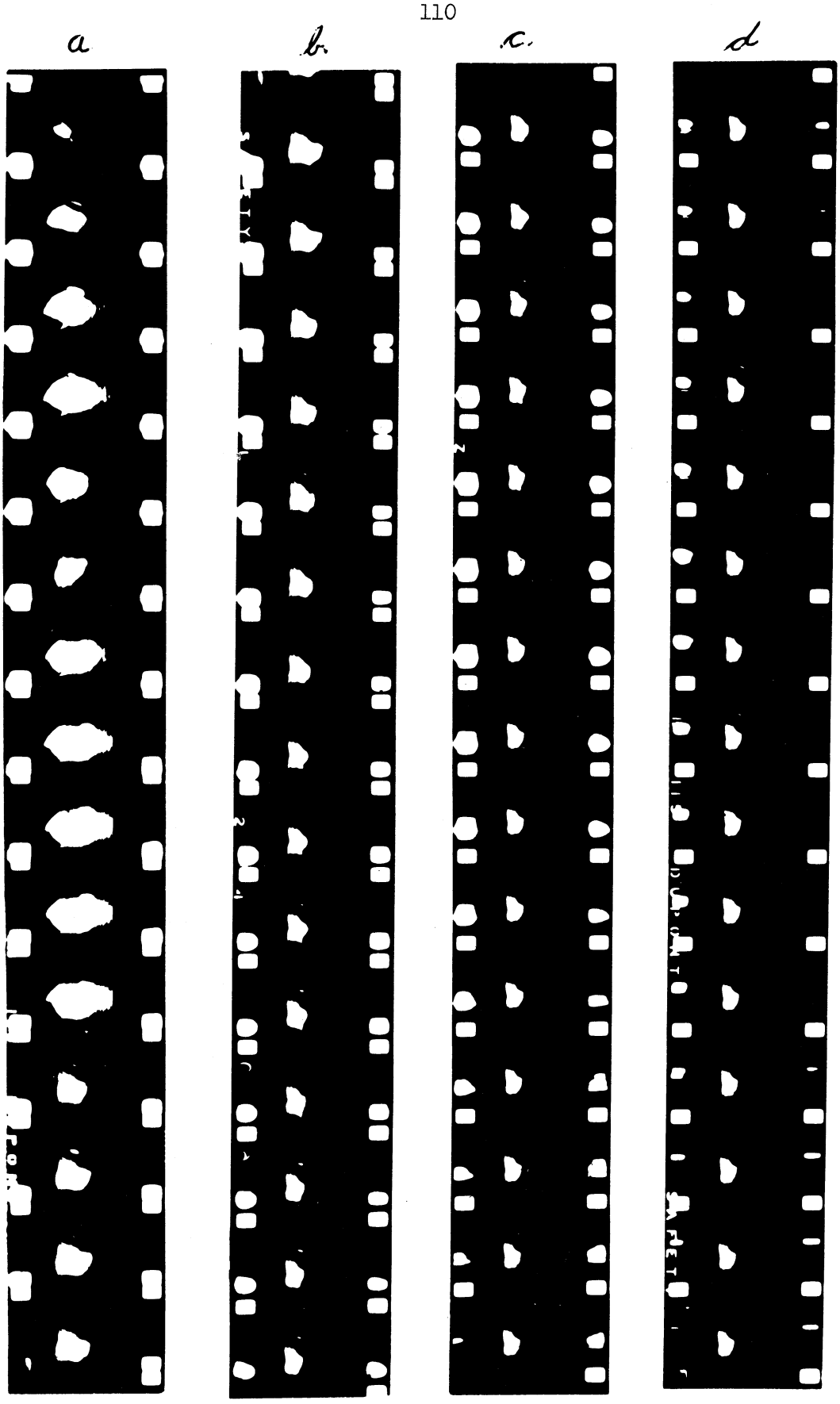

Fig. 57 Fastax Sequence Showing Stable Arc. M = 2.5, I = 320 amp, P_{t_1} = 15.6 in. Hg, g = 0.75 in. Camera Speed about 2,000 frames/ second.

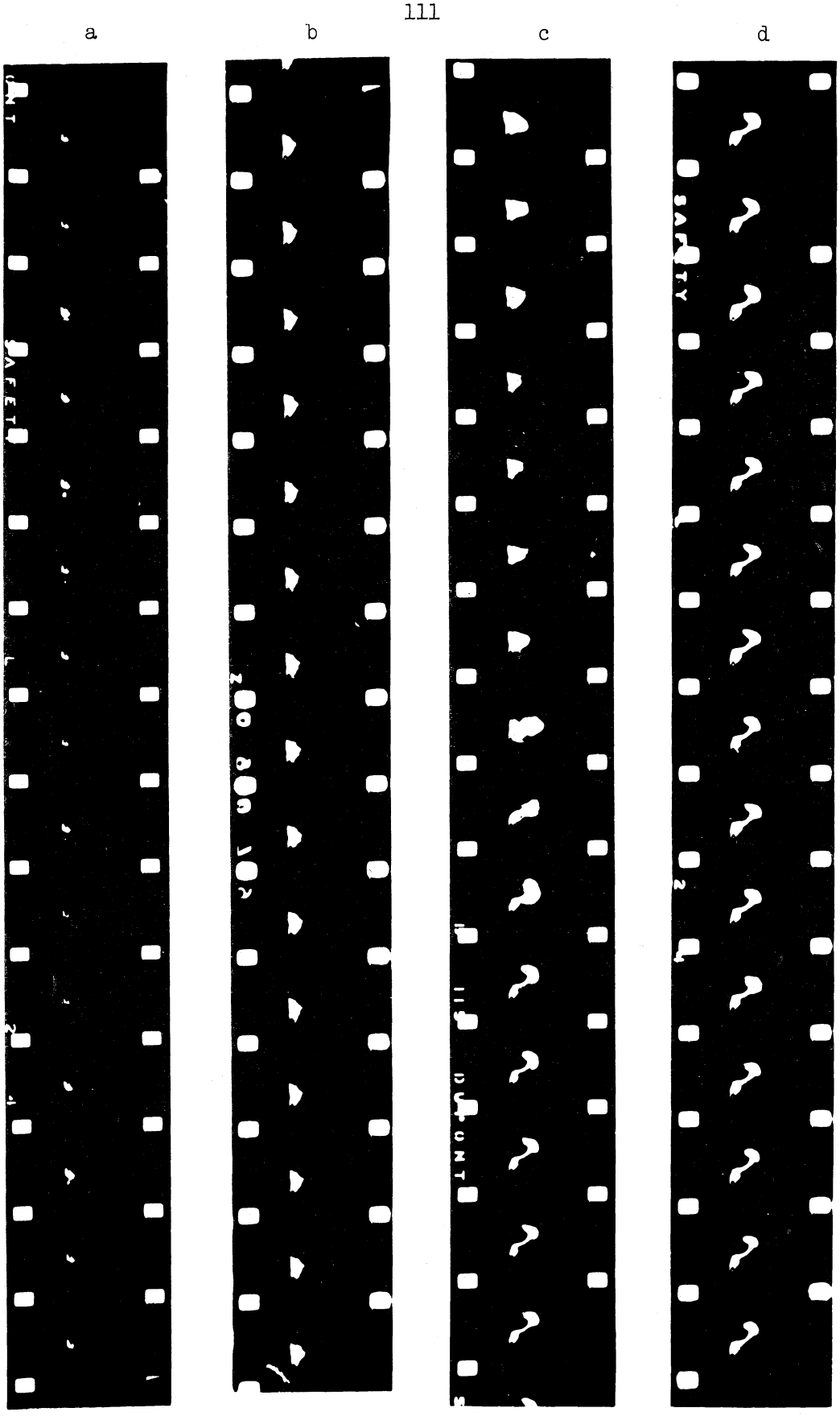

Fig. 58 Fastax Sequence Showing Switch from One Far-Side Strike Location to the Other. M = 2.5, I = 320 amp, P_{t_1} = 15.6 in.Hg, g = 0.75 in. Camera Speed about 2,500 frames/second.

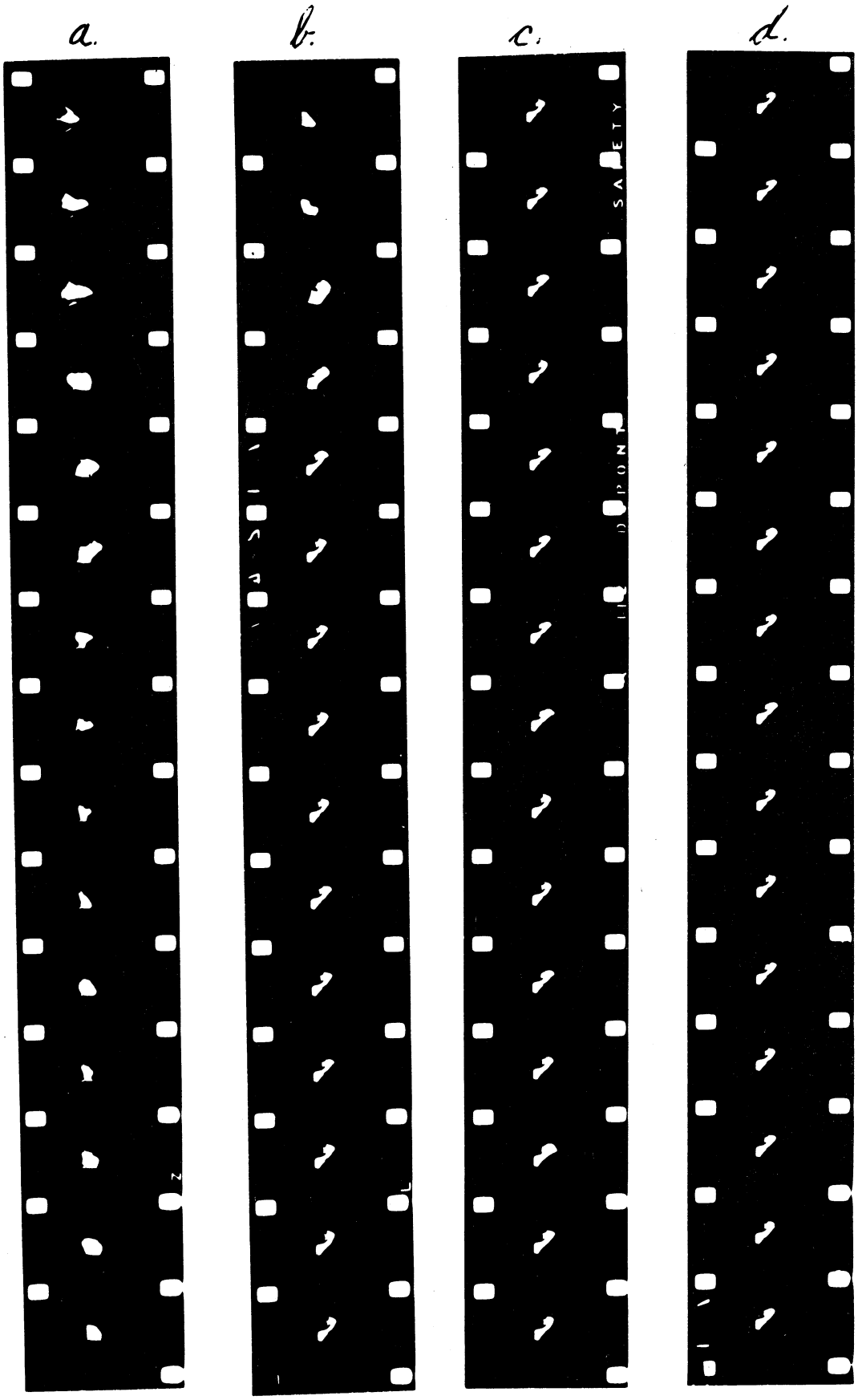

Fig. 59 Fastax Sequence Showing Establishment of Stable Arc. M = 2.5, I = 150 amp, P_{t_1} = 20.2 in. Hg, g = 0.6 in. Camera Speed about 2,500 frames/second.

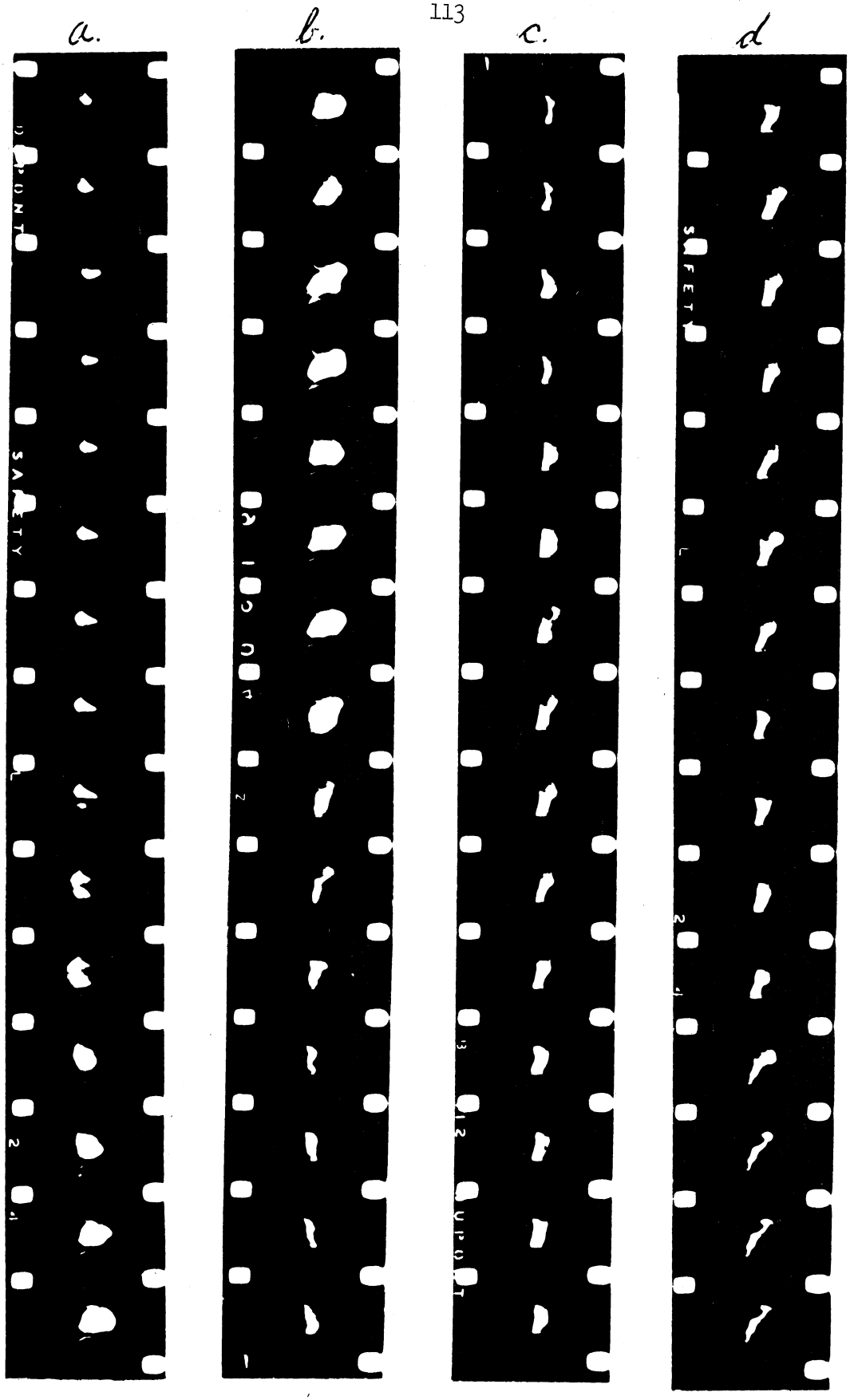

Fig. 60 Fastax Sequence Showing Establishment of Stable Arc. M = 2.5, I = 130 amp, P_{t_1} = 20.2 in. Hg, g = 1.1 in. Camera Speed about 2,500 frames/second. (contd.)

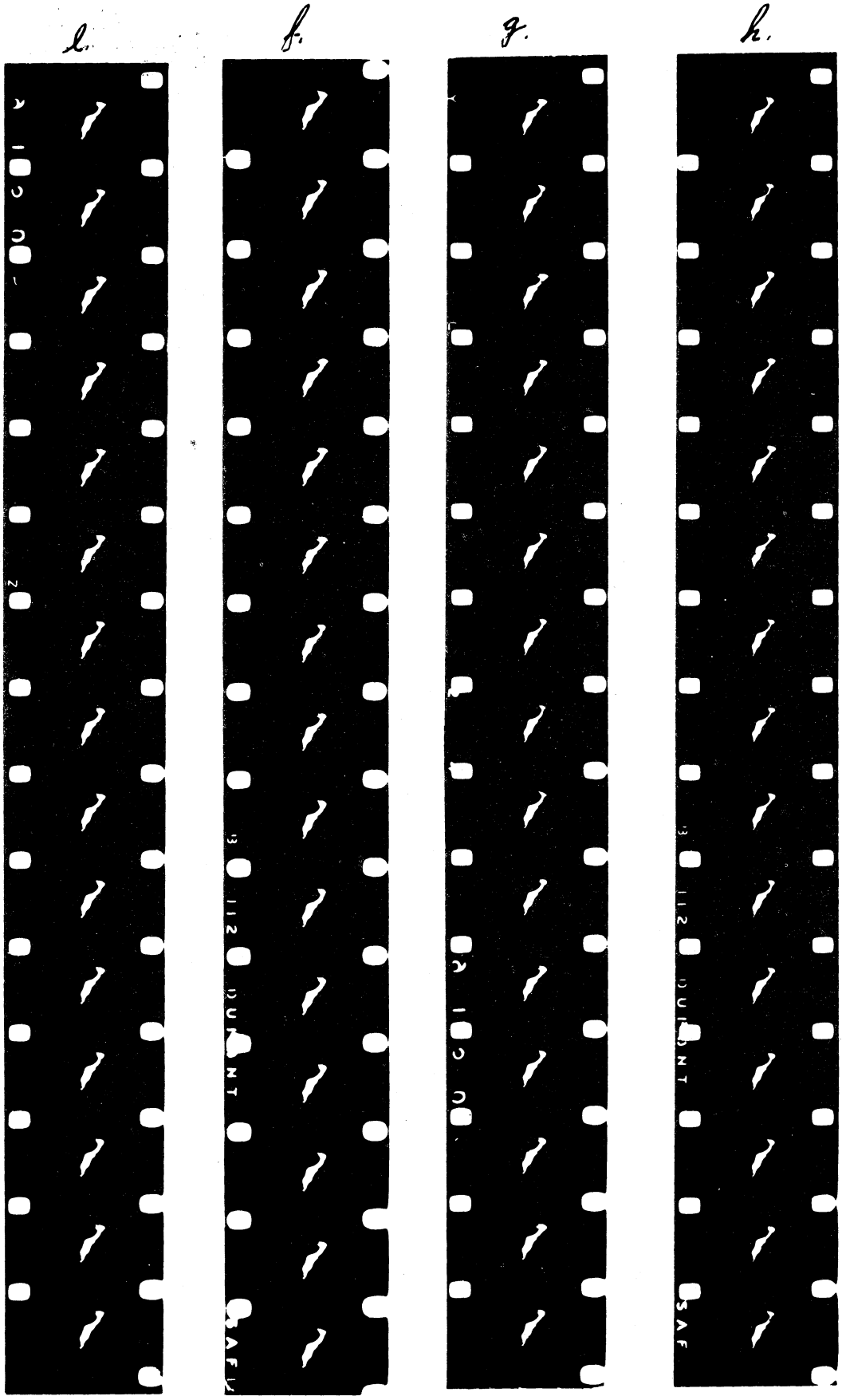

Fig. 60 Continued.

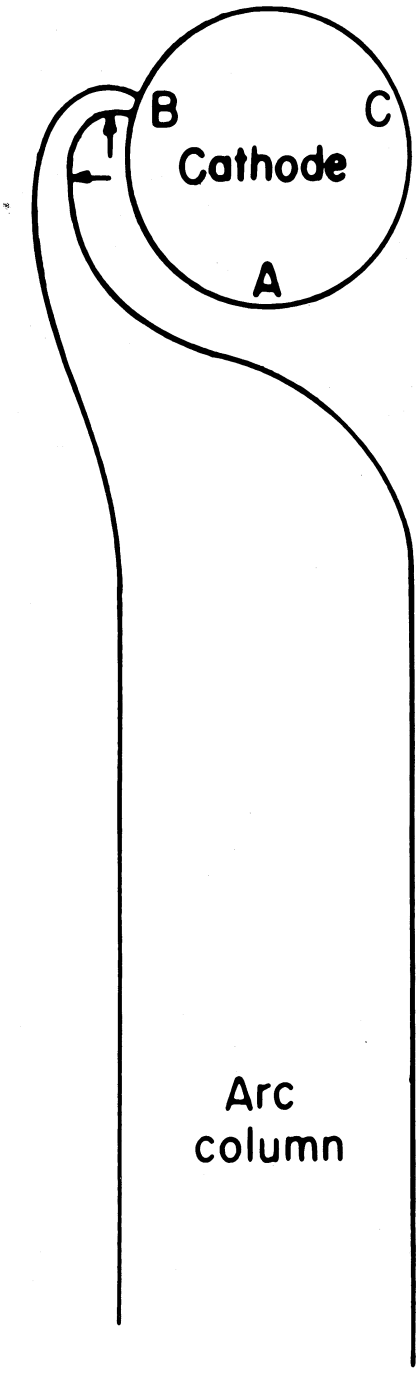

Fig. 61 Lorentz Forces Due to B_x

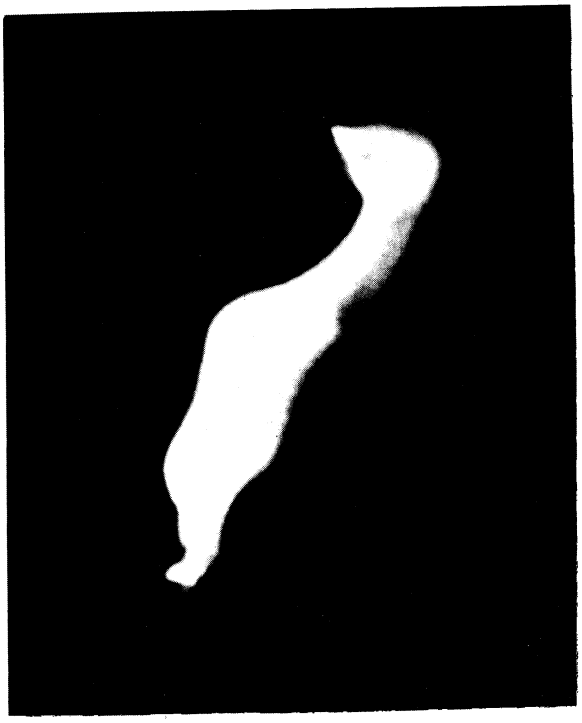

(a) Single Fastax Frame of Stable Arc; M = 2.5, P_{t_1} = 20.2 in. Hg, I = 132 amp, g = 1.1 in. Camera Speed about 2,500 frames/second

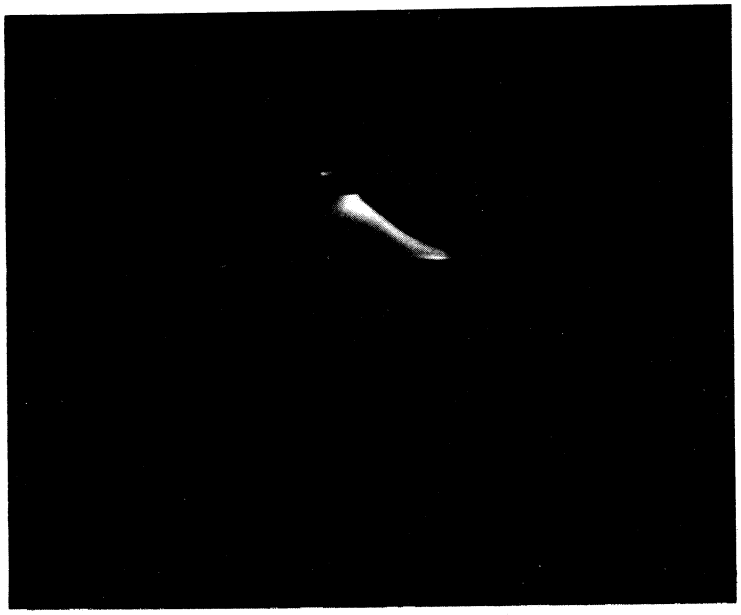

(t) Polaroid Photograph of Arc Reflection; M = 2.5, P_{t_1} = 15.9 in. Hg, I = 280 amp, g = 1.1 in.

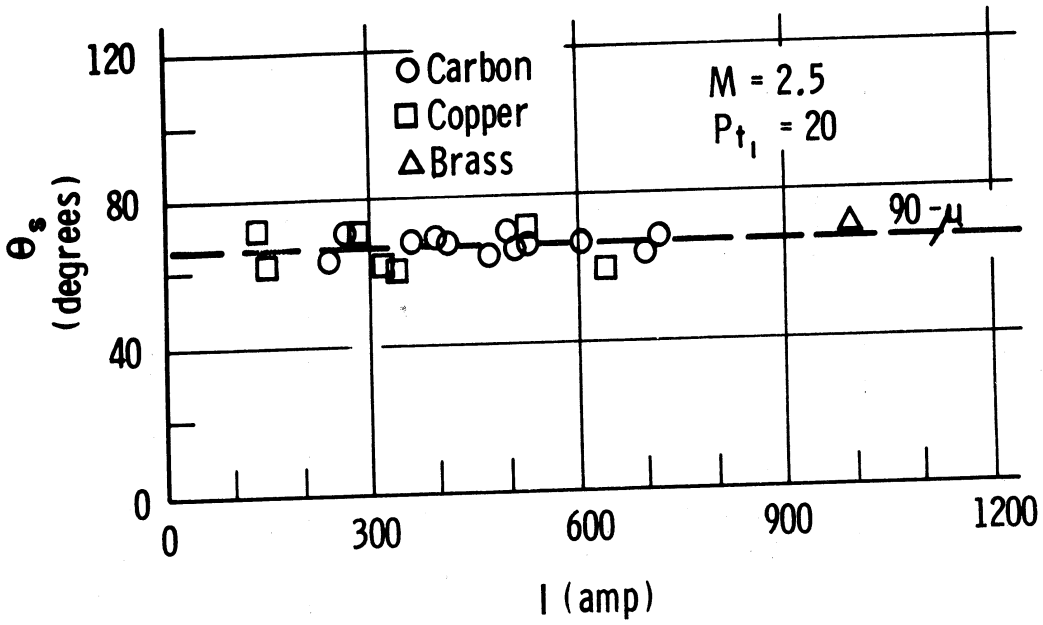

Fig. 63 Variation of Arc Slant Angle with Current

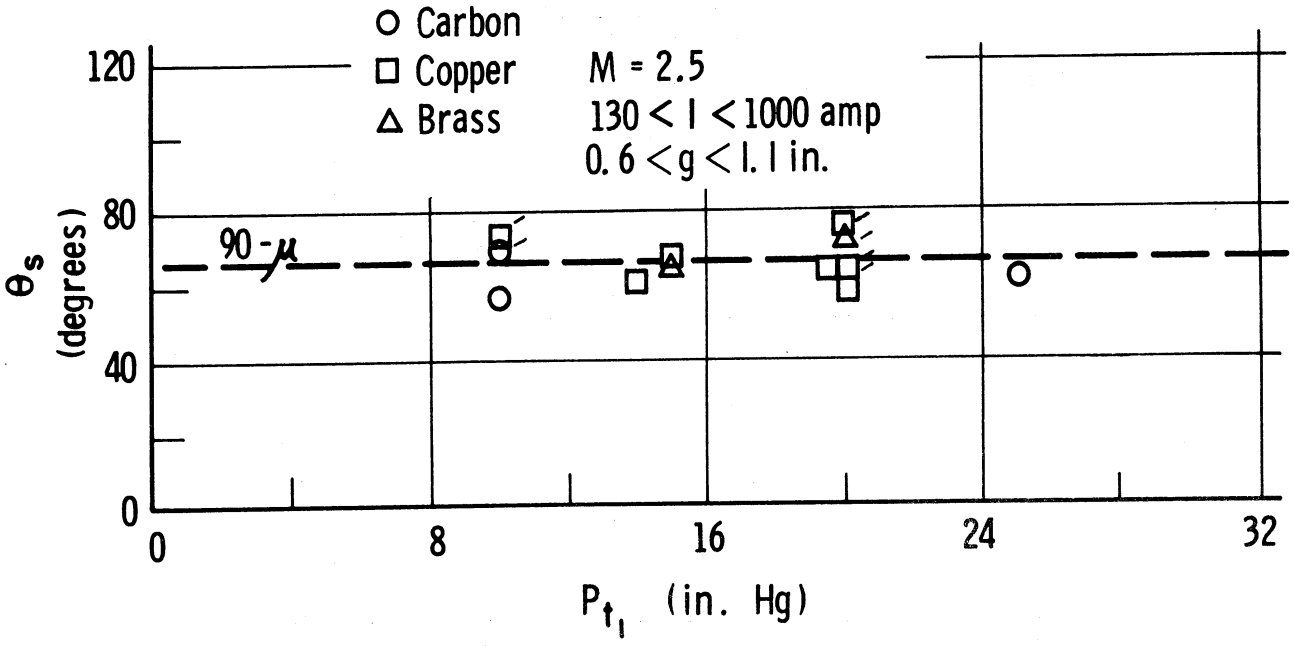

Fig. 64 Variation of Arc Slant Angle in Free-Stream Stagnation Pressure

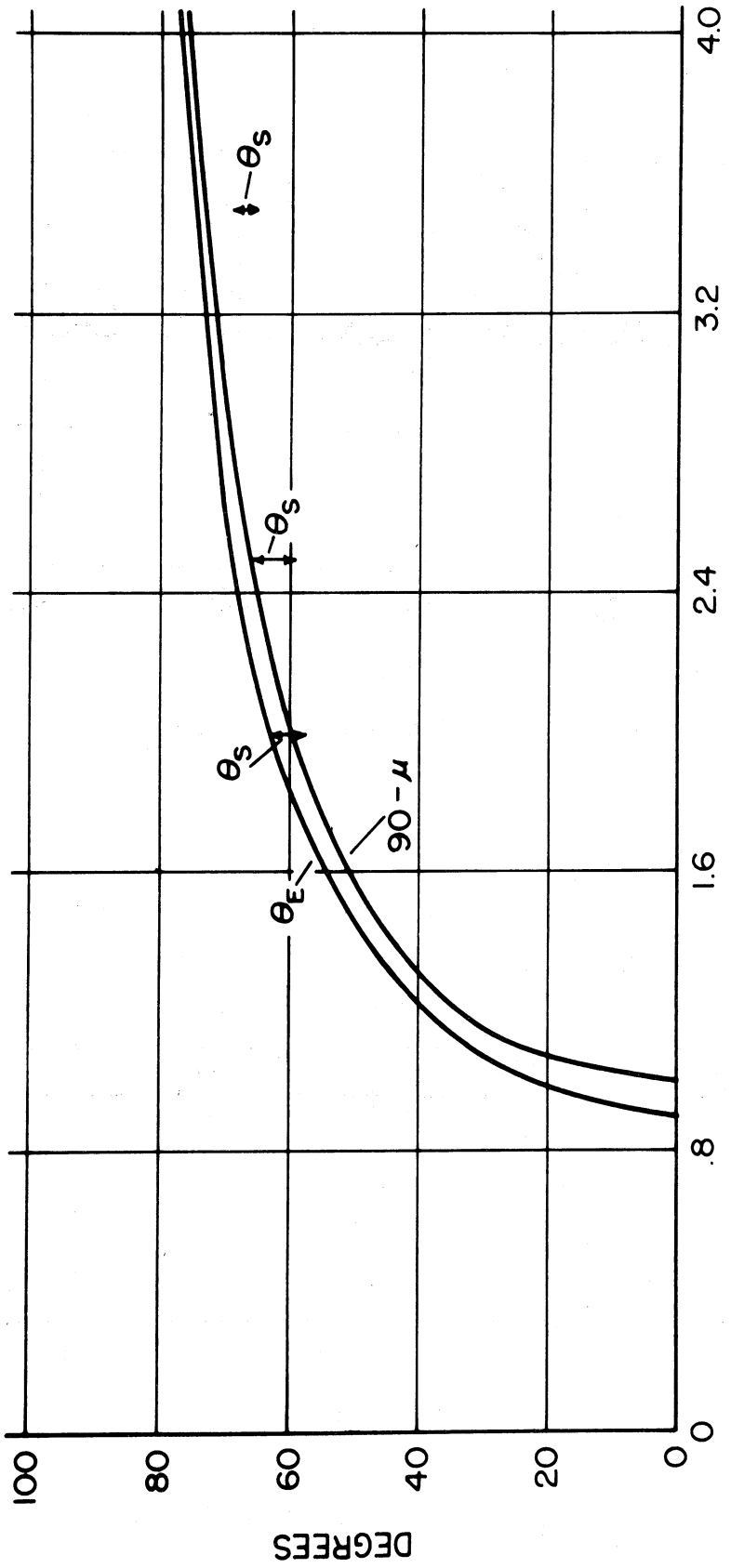

Fig. 65 Variation of Mach Angle, Angle of Maximum E_{11}/P_s, and Arc Slant Angle with Mach Number

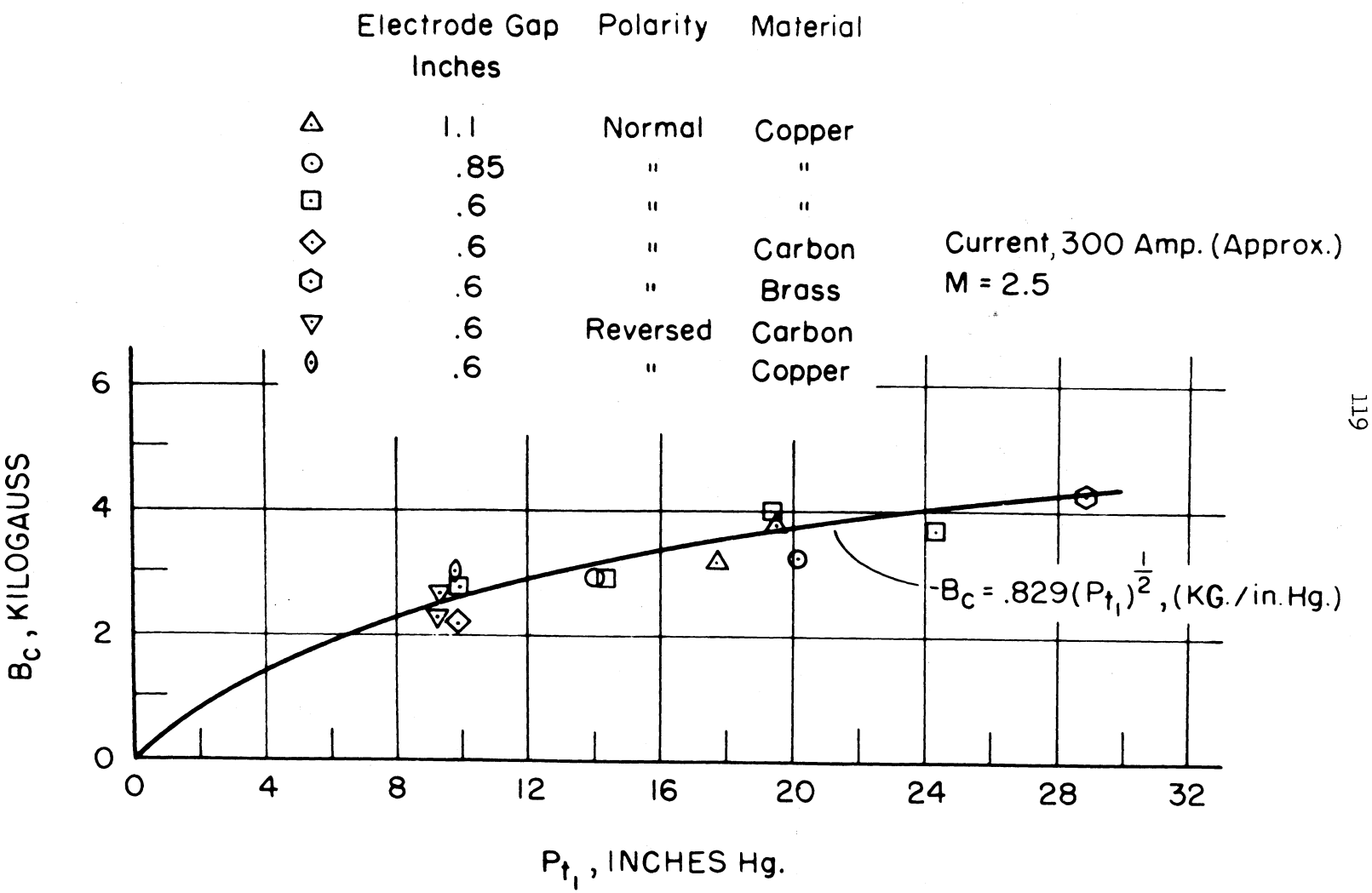

Fig. 66 Variation of Cathode Root Induction with Free-Stream Stagnation Pressure

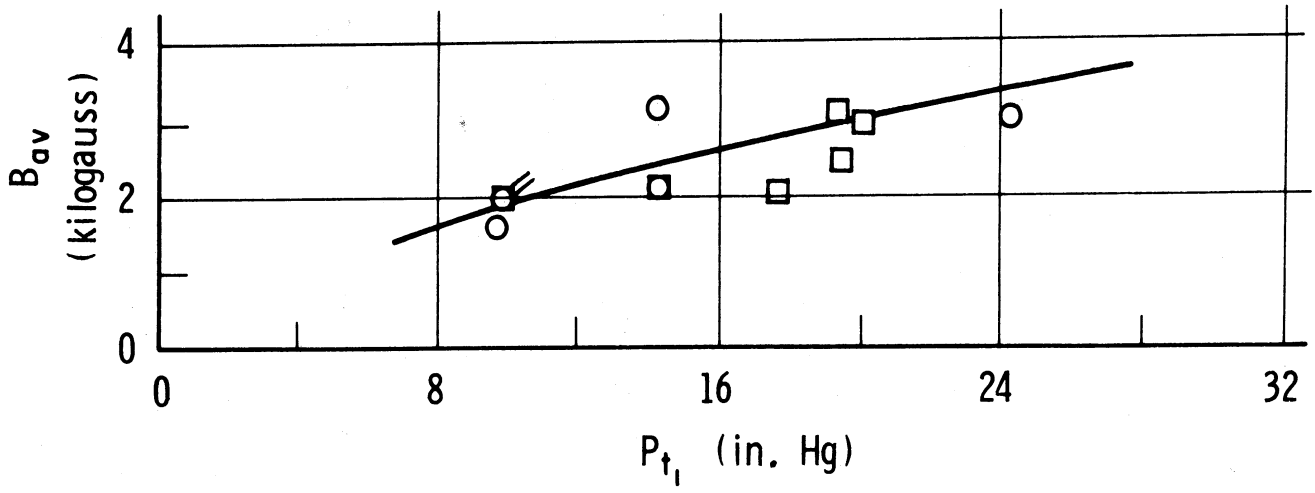

Fig. 67 Variation of Average Column Induction with Free-Stream Stagnation Pressure

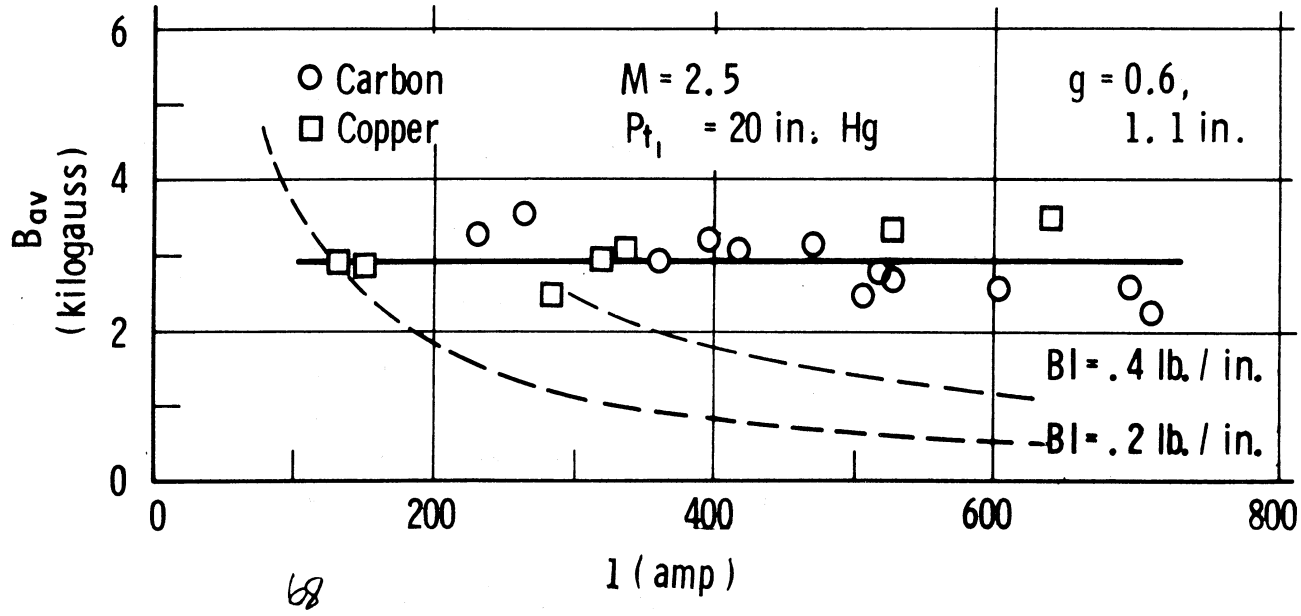

Fig. 68 Variation of Average Column Induction with Arc Current

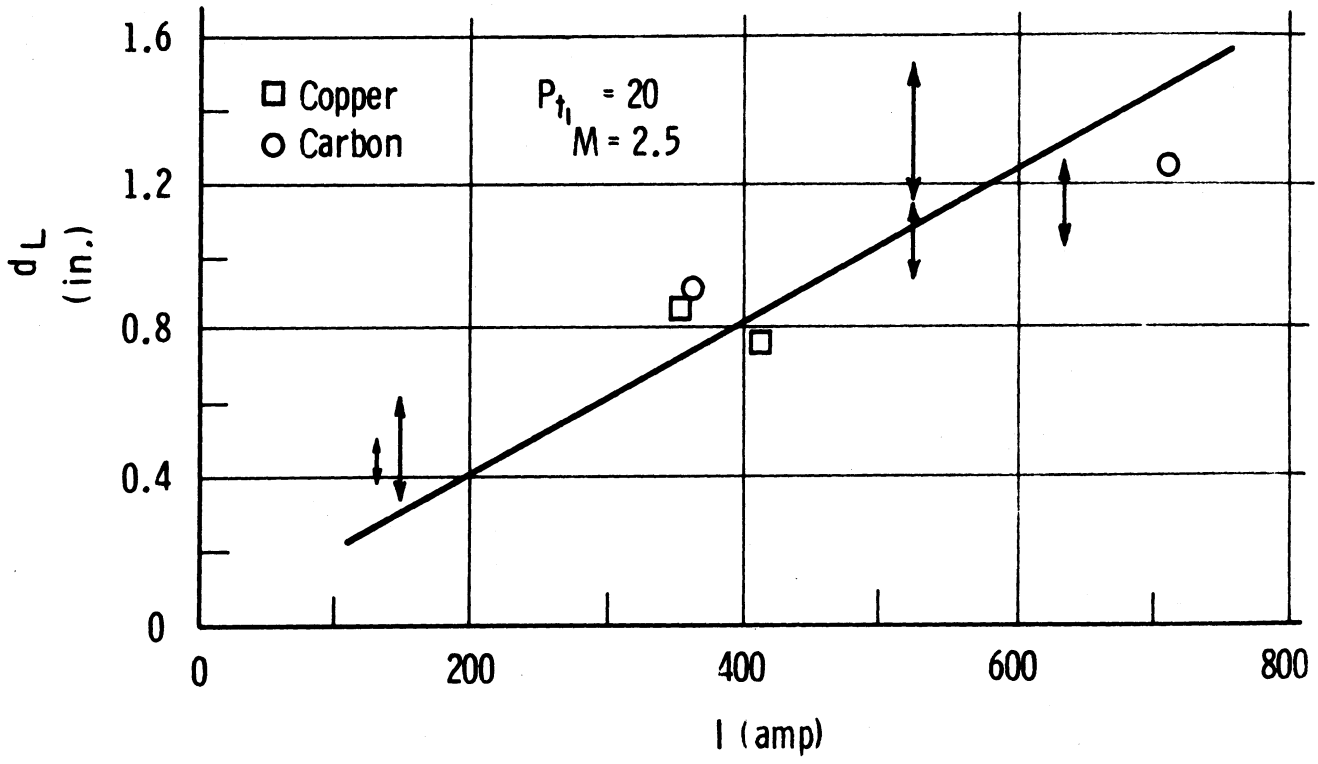

Fig. 69. Variation of Arc Luminosity-Width with Current.

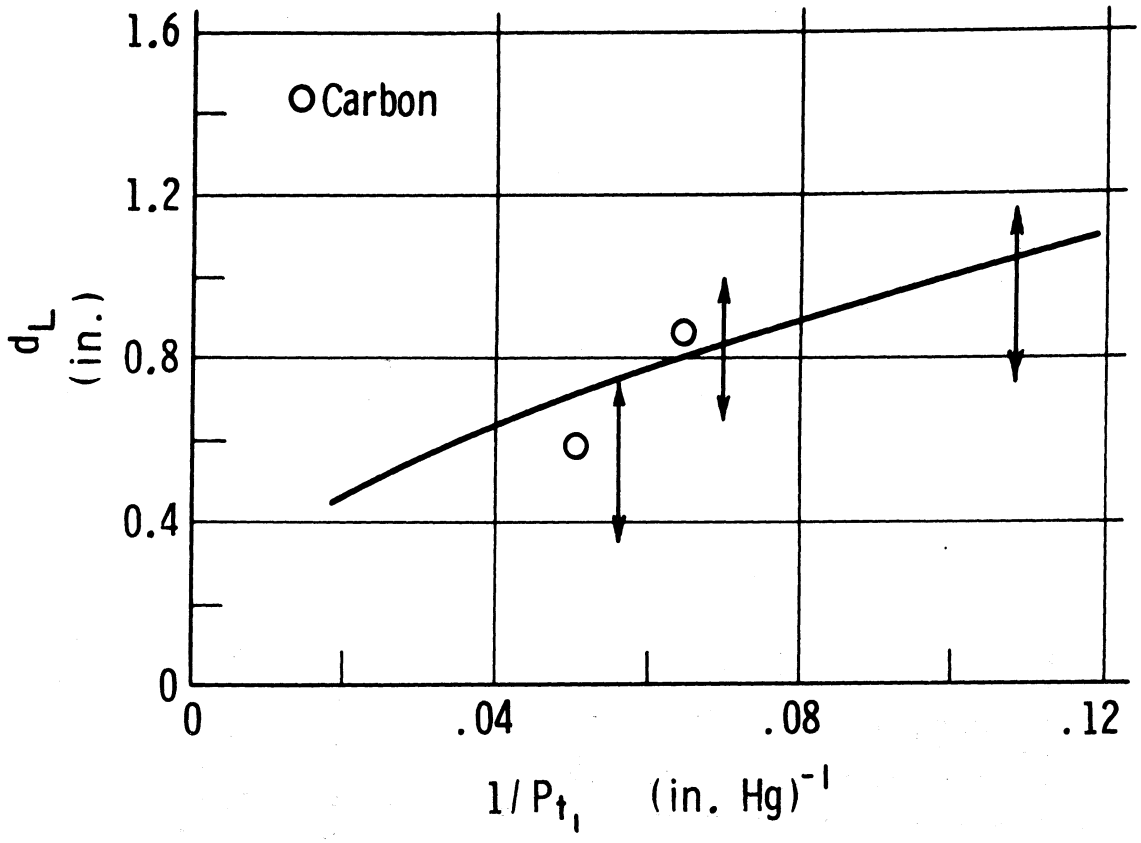

Fig. 70 Variation of Arc Luminosity-Width with Free-Stream Stagnation Pressure

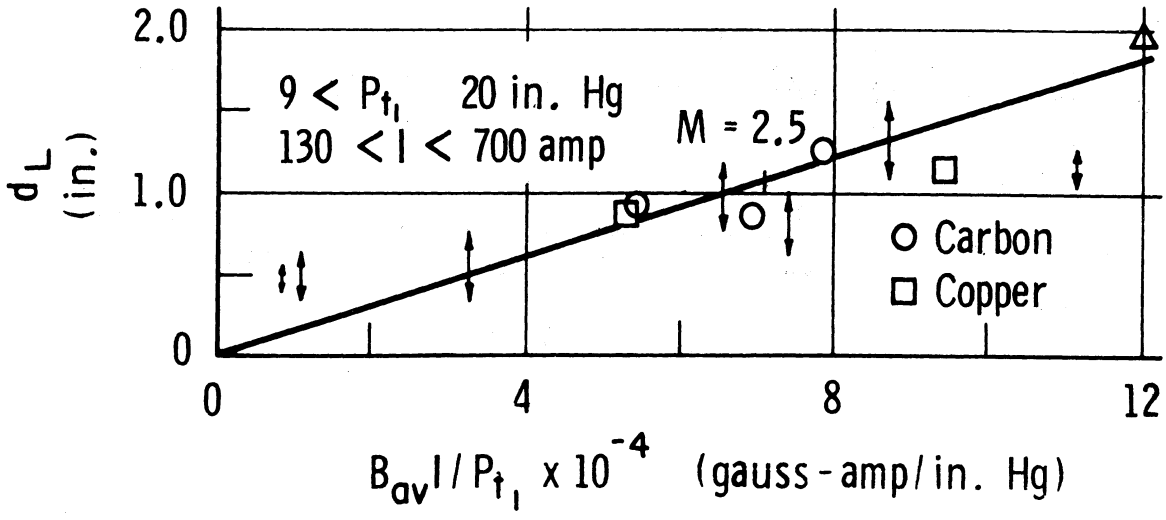

Fig. 71 Variation of Arc Luminosity-Width with $B_{AV}I/P_{t_1}$

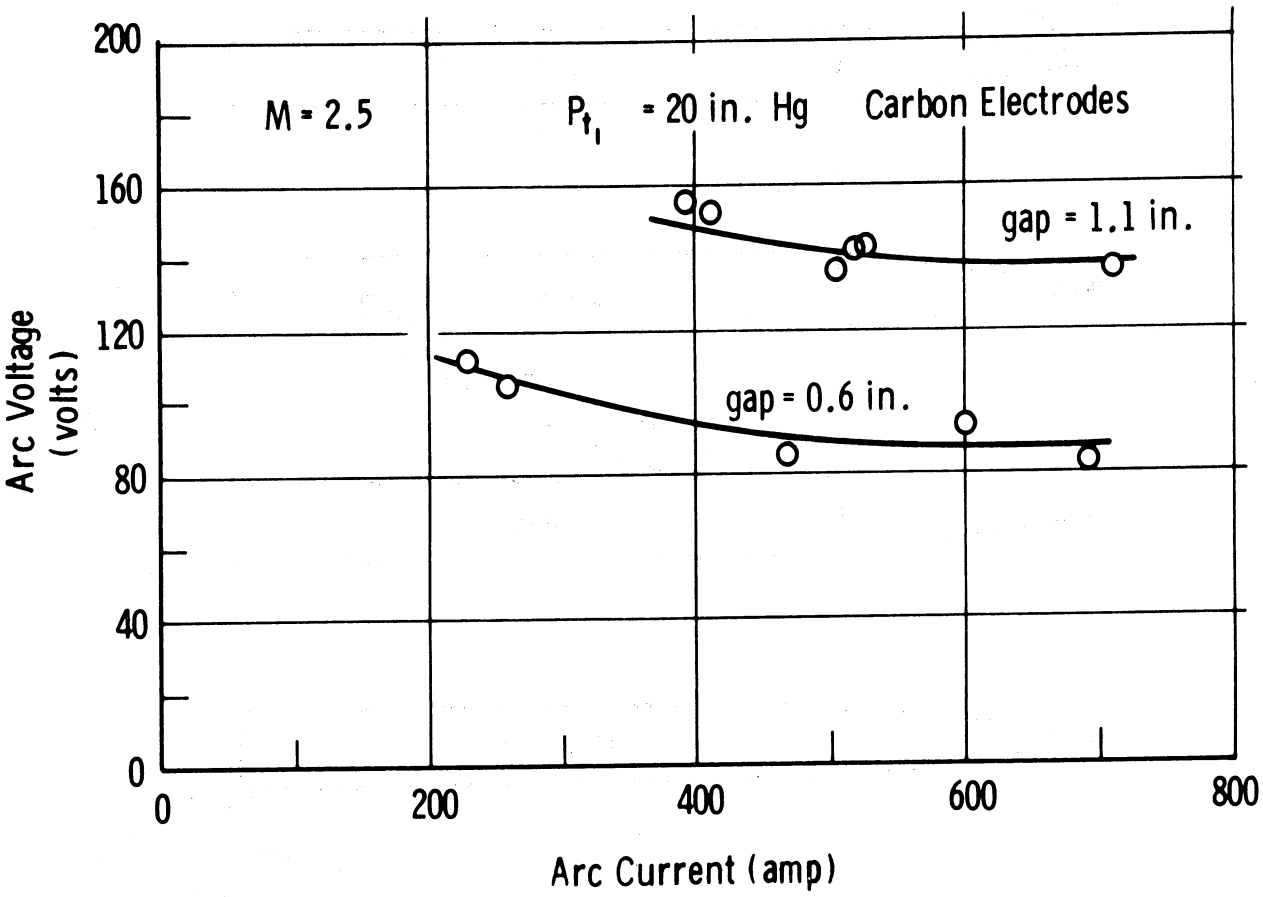

Fig. 72 Voltage-Current Characteristics for the Stable Arc

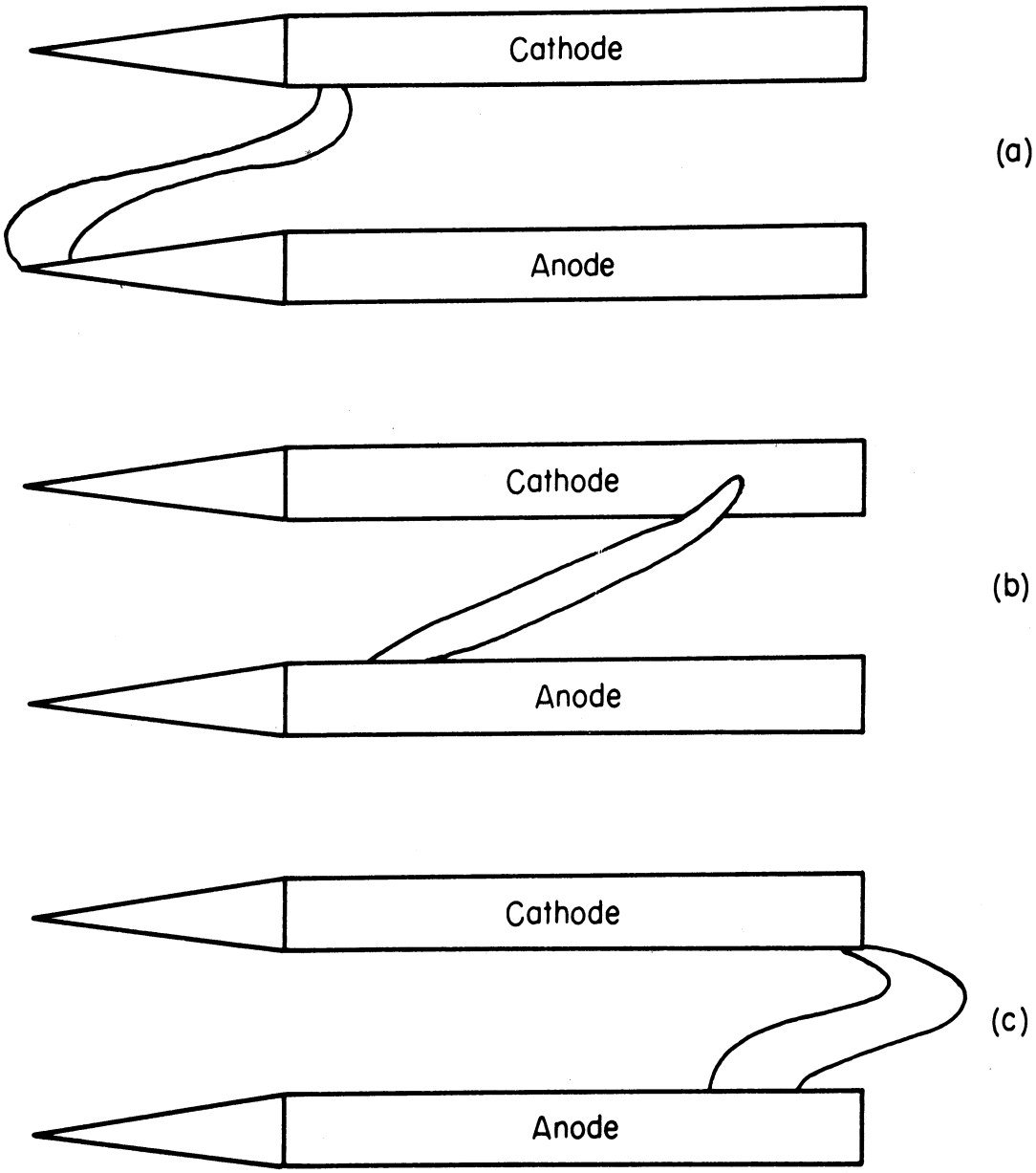

Fig. 73. Schematic Illustration of Changes in Arc Configuration with Field Coil Location or Pressure.

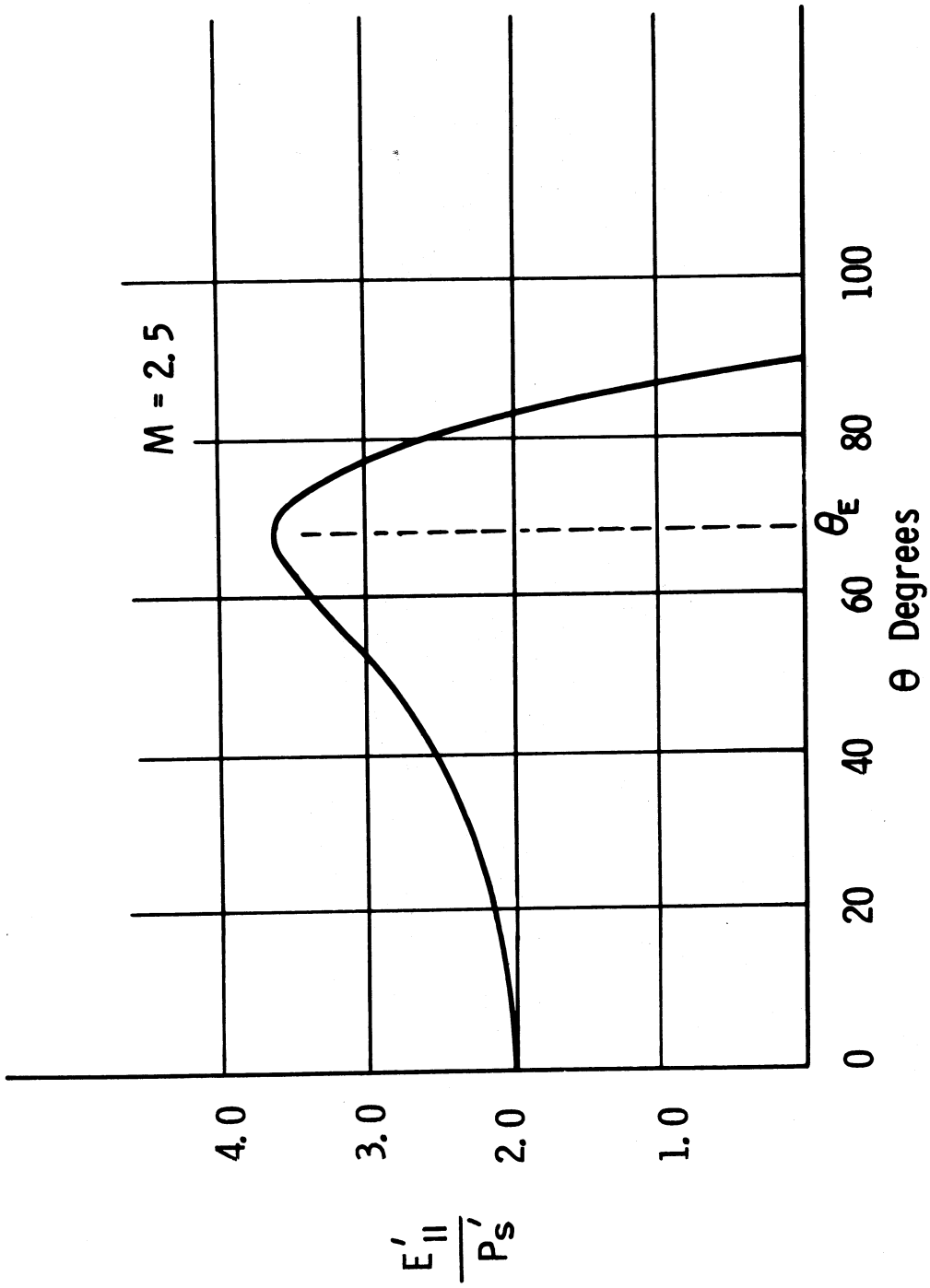

Fig. 74 Variation of Discharge Parameter with Slant Angle

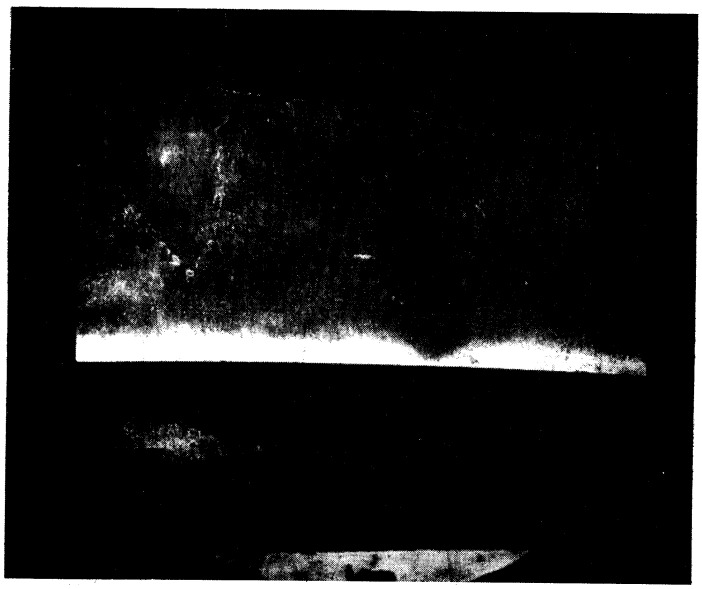

(a) Flow without Arc

(b) Flow with Arc, $W/P_{t_1} = .014$

Fig. 75 Schlieren Photographs Showing Flow Separation Caused by Excessive Arc Power; M = 2.35, P_{t_1} = 18.1 in. Hg

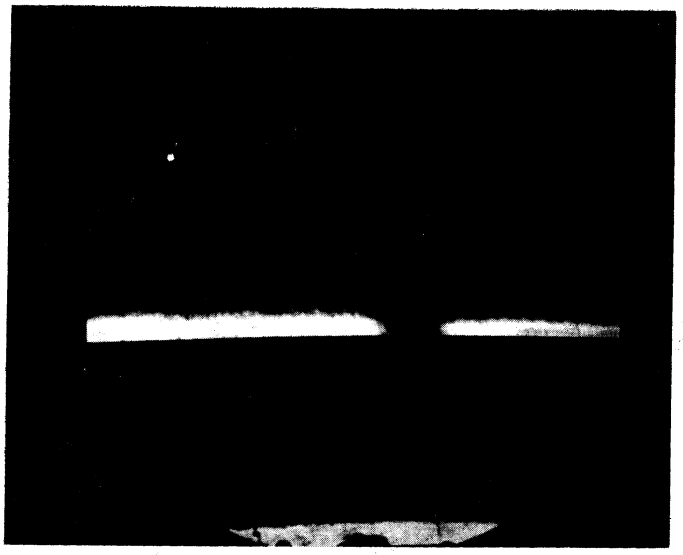

(a) Flow without Arc

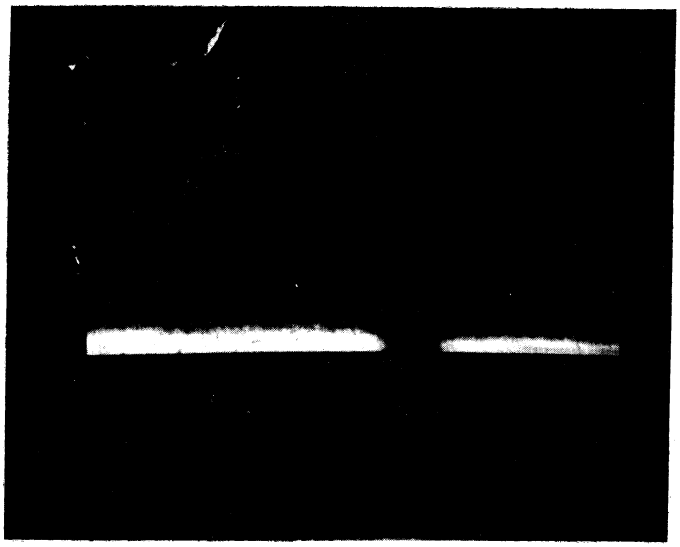

(b) Flow with Arc, $W/P_{t_1} = .006$

Fig. 76 Schlieren Photographs of Flow Along Lower Tunnel Wall Just Upstream of Electrodes; M = 2.65, P_{t_1} = 29.3 in. Hg.

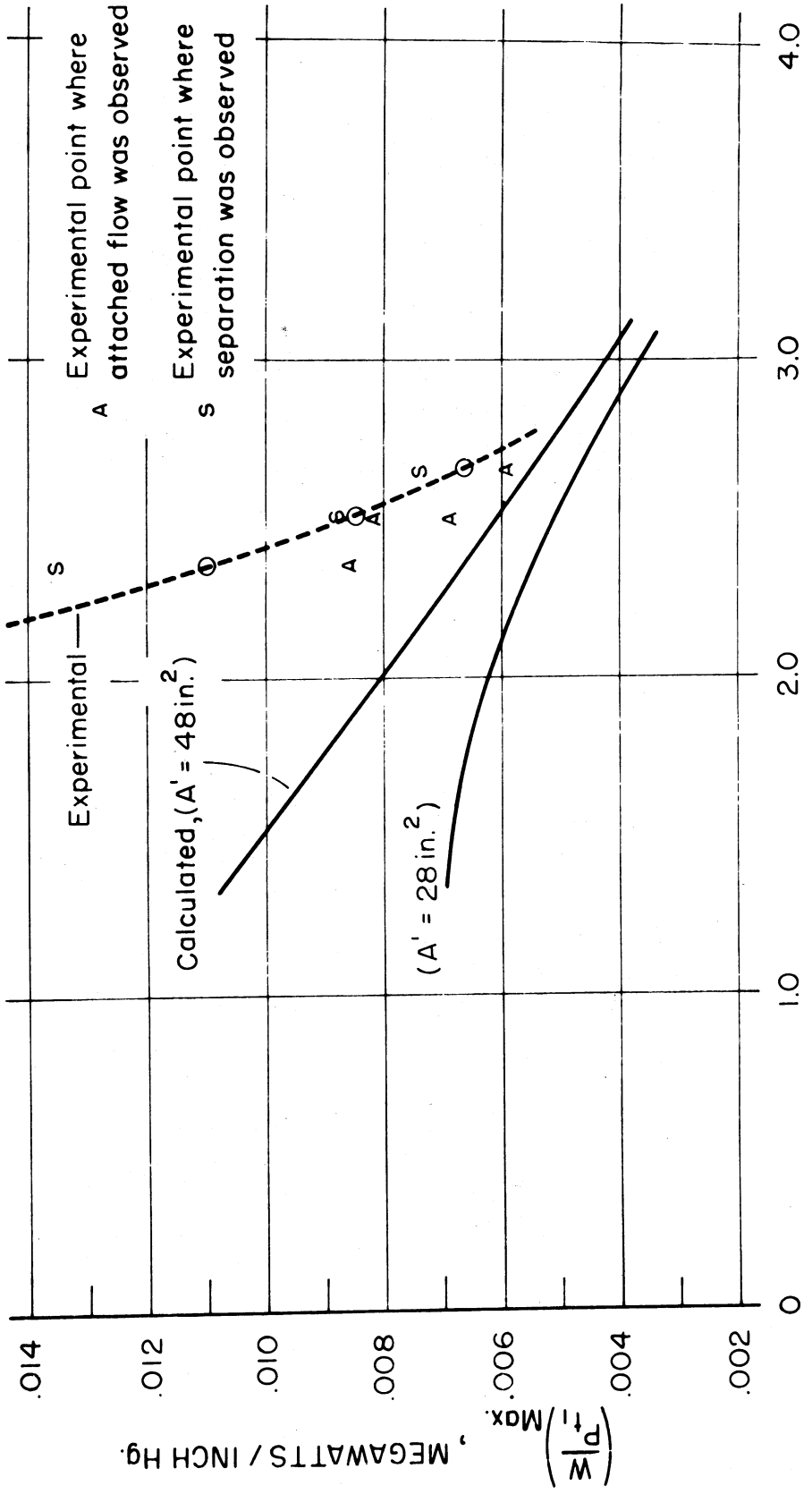

Fig. 77 Limits on Experimental Conditions Due to Thermal Blocking

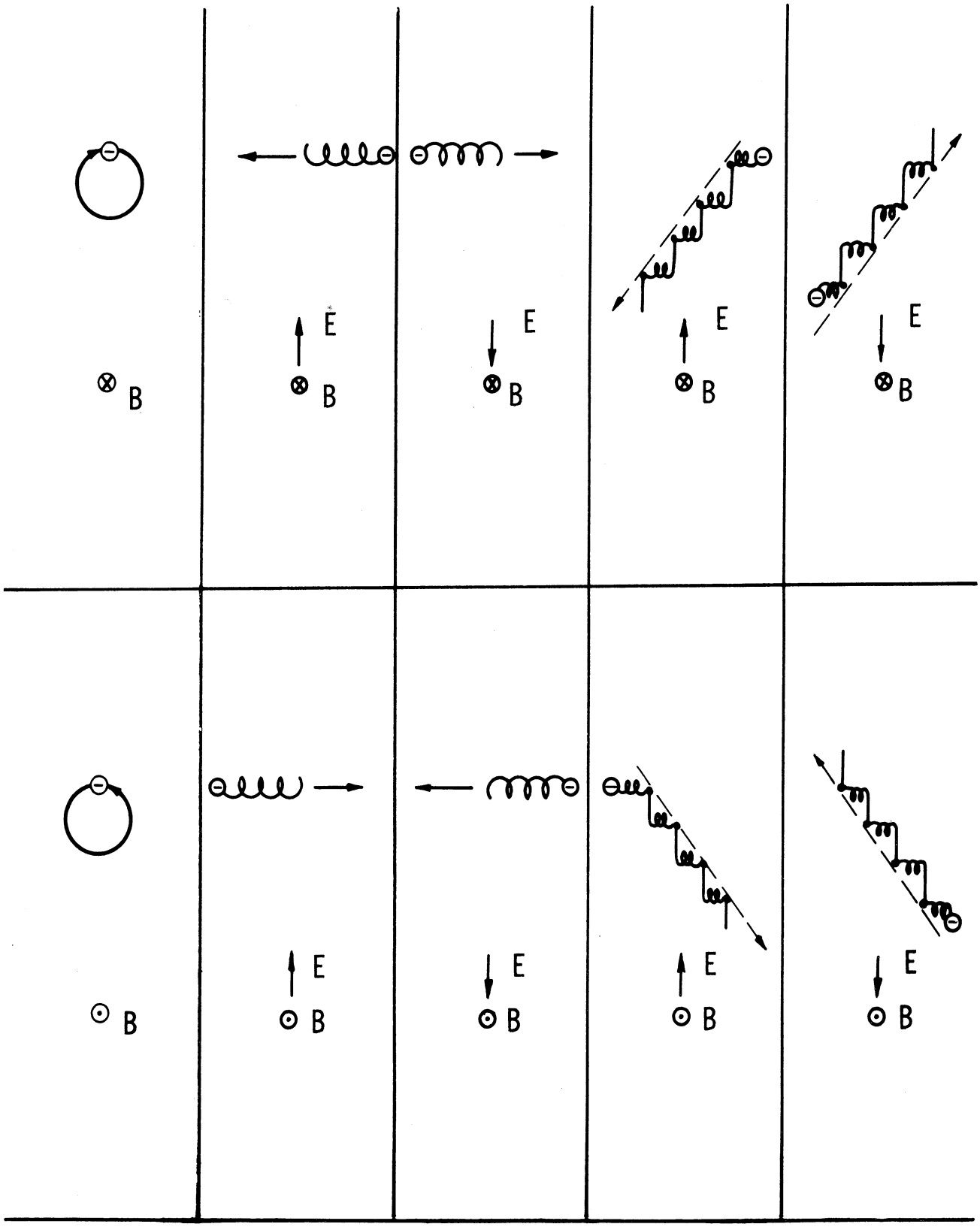

Fig. 78 Schematic Illustration of Hall Direction

Unclassified

Security Classification

DOCUMENT CONTROL DATA - R&D

(Security classification of title, body of abstract and indexing annotation must be entered when the overall report is classified)

1. ORIGINATING ACTIVITY *(Corporate author)*
The University of Michigan
Ann Arbor, Michigan

2a. REPORT SECURITY CLASSIFICATION
Unclassified

2b. GROUP

3. REPORT TITLE
The Magnetic Stabilization of an Electric Arc in Transverse Supersonic Flow

4. DESCRIPTIVE NOTES *(Type of report and inclusive dates)*
Scientific Report

5. AUTHOR(S) *(Last name, first name, initial)*
Bond, Charles E.

6. REPORT DATE	7a. TOTAL NO. OF PAGES	7b. NO. OF REFS
October 1965	89	101

8a. CONTRACT OR GRANT NO.	9a. ORIGINATOR'S REPORT NUMBER(S)
AF33(657)-8819	
b. PROJECT NO. 7063-03	
c. 61445014	9b. OTHER REPORT NO(S) *(Any other numbers that may be assigned this report)*
d. 681307	ARL 65-185

10. AVAILABILITY/LIMITATION NOTICES
Qualified requesters may obtain copies of this report from DDC.
Released to OTS.

11. SUPPLEMENTARY NOTES	12. SPONSORING MILITARY ACTIVITY
N/A	Aerospace Research Laboratories(ARN) Thermo-Mechanics Research Laboratory Wright-Patterson AFB, Ohio

13. ABSTRACT

A method is presented for the magnetic confinement and stabilization of a d-c electric arc in an unheated supersonic airstream directed normal to the electric field. It is shown that stable confinement is governed by dynamic processes in the positive column, and is independent of material and flow conditions at the surface of the cathode.

The experimental results demonstrate the possibility of stable conduction of electricity through transverse supersonic flow, and suggest that such conduction is governed by a convective interaction mechanism which is not entirely Hall-effect.

A general review of the convective arc is given, and results of the present investigation are compared with those of previous investigations.

DD FORM 1 JAN 64 1473

Unclassified

Security Classification

Security Classification

14. KEY WORDS	LINK A		LINK B		LINK C	
	ROLE	WT	ROLE	WT	ROLE	WT
Magnetic stabilization						
Transverse supersonic flow						
Convective arc						
Magnetic confinement						
Magnetic permeability						
Axial induction						

INSTRUCTIONS

1. ORIGINATING ACTIVITY: Enter the name and address of the contractor, subcontractor, grantee, Department of Defense activity or other organization *(corporate author)* issuing the report.

2a. REPORT SECURITY CLASSIFICATION: Enter the overall security classification of the report. Indicate whether "Restricted Data" is included. Marking is to be in accordance with appropriate security regulations.

2b. GROUP: Automatic downgrading is specified in DoD Directive 5200.10 and Armed Forces Industrial Manual. Enter the group number. Also, when applicable, show that optional markings have been used for Group 3 and Group 4 as authorized.

3. REPORT TITLE: Enter the complete report title in all capital letters. Titles in all cases should be unclassified. If a meaningful title cannot be selected without classification, show title classification in all capitals in parenthesis immediately following the title.

4. DESCRIPTIVE NOTES: If appropriate, enter the type of report, e.g., interim, progress, summary, annual, or final. Give the inclusive dates when a specific reporting period is covered.

5. AUTHOR(S): Enter the name(s) of author(s) as shown on or in the report. Enter last name, first name, middle initial. If military, show rank and branch of service. The name of the principal author is an absolute minimum requirement.

6. REPORT DATE: Enter the date of the report as day, month, year; or month, year. If more than one date appears on the report, use date of publication.

7a. TOTAL NUMBER OF PAGES: The total page count should follow normal pagination procedures, i.e., enter the number of pages containing information.

7b. NUMBER OF REFERENCES: Enter the total number of references cited in the report.

8a. CONTRACT OR GRANT NUMBER: If appropriate, enter the applicable number of the contract or grant under which the report was written.

8b, 8c, & 8d. PROJECT NUMBER: Enter the appropriate military department identification, such as project number, subproject number, system numbers, task number, etc.

9a. ORIGINATOR'S REPORT NUMBER(S): Enter the official report number by which the document will be identified and controlled by the originating activity. This number must be unique to this report.

9b. OTHER REPORT NUMBER(S): If the report has been assigned any other report numbers *(either by the originator or by the sponsor)*, also enter this number(s).

10. AVAILABILITY/LIMITATION NOTICES: Enter any limitations on further dissemination of the report, other than those imposed by security classification, using standard statements such as:

(1) "Qualified requesters may obtain copies of this report from DDC."

(2) "Foreign announcement and dissemination of this report by DDC is not authorized."

(3) "U. S. Government agencies may obtain copies of this report directly from DDC. Other qualified DDC users shall request through _____."

(4) "U. S. military agencies may obtain copies of this report directly from DDC. Other qualified users shall request through _____."

(5) "All distribution of this report is controlled. Qualified DDC users shall request through _____."

If the report has been furnished to the Office of Technical Services, Department of Commerce, for sale to the public, indicate this fact and enter the price, if known.

11. SUPPLEMENTARY NOTES: Use for additional explanatory notes.

12. SPONSORING MILITARY ACTIVITY: Enter the name of the departmental project office or laboratory sponsoring *(paying for)* the research and development. Include address.

13. ABSTRACT: Enter an abstract giving a brief and factual summary of the document indicative of the report, even though it may also appear elsewhere in the body of the technical report. If additional space is required, a continuation sheet shall be attached.

It is highly desirable that the abstract of classified reports be unclassified. Each paragraph of the abstract shall end with an indication of the military security classification of the information in the paragraph, represented as *(TS), (S), (C), or (U)*.

There is no limitation on the length of the abstract. However, the suggested length is from 150 to 225 words.

14. KEY WORDS: Key words are technically meaningful terms or short phrases that characterize a report and may be used as index entries for cataloging the report. Key words must be selected so that no security classification is required. Identifiers, such as equipment model designation, trade name, military project code name, geographic location, may be used as key words but will be followed by an indication of technical context. The assignment of links, rules, and weights is optional.